Report No. FHWA-KS-12-6 ▪ FINAL REPORT ▪ September 2012

Response of No-Name Creek FRP Bridge to Local Weather

Wenjie Liu
Eric Zhou
Youqi Wang
Kansas State University Transportation Center

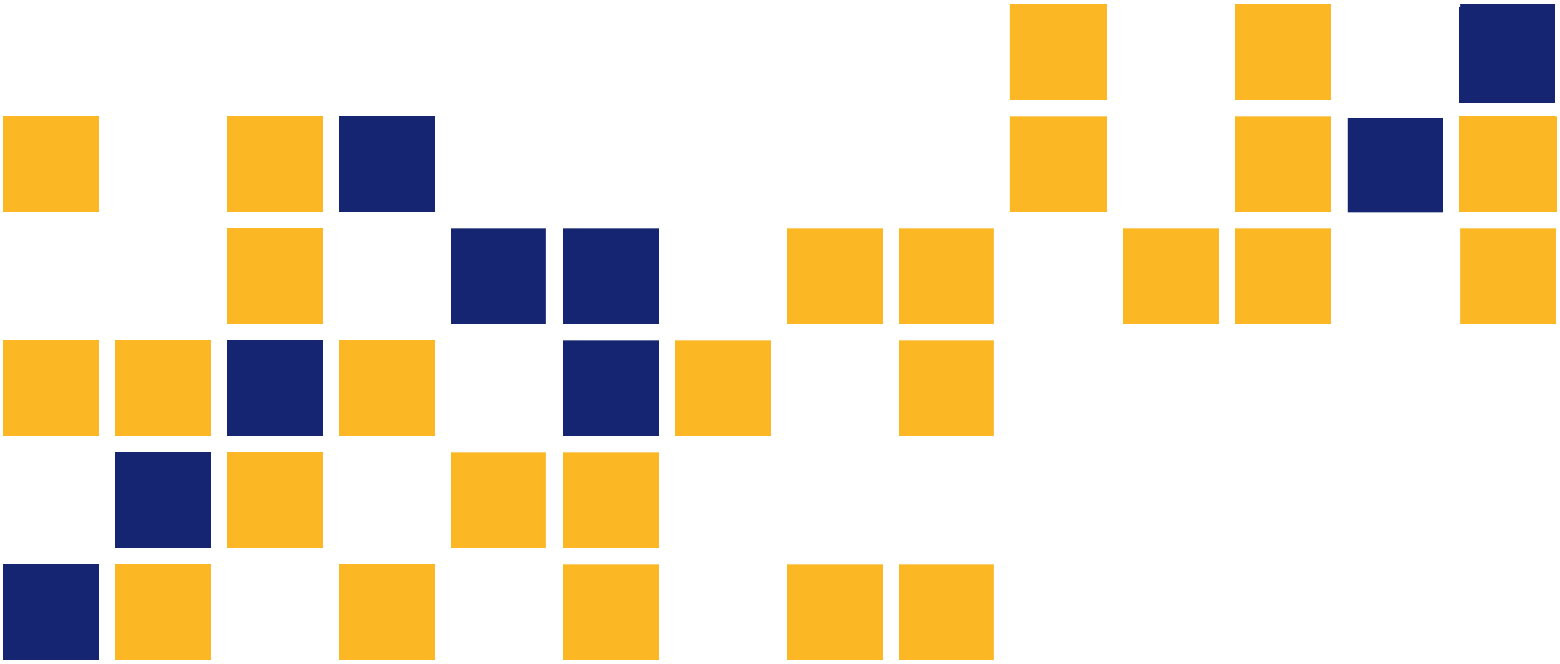

Kansas Department of Transportation

This page intentionally left blank.

1 Report No. FHWA-KS-12-6	**2 Government Accession No.**	**3 Recipient Catalog No.**
4 Title and Subtitle Response of No-Name Creek FRP Bridge to Local Weather		**5 Report Date** September 2012 **6 Performing Organization Code**
7 Author(s) Wenjie Liu, Eric Zhou, and Youqi Wang		**8 Performing Organization Report No.**
9 Performing Organization Name and Address Department of Civil Engineering Kansas State University Transportation Center 2118 Fiedler Hall Manhattan, Kansas 66506		**10 Work Unit No. (TRAIS)** **11 Contract or Grant No.** C1644
12 Sponsoring Agency Name and Address Kansas Department of Transportation Bureau of Materials and Research 700 SW Harrison Street Topeka, Kansas 66603-3745		**13 Type of Report and Period Covered** Final Report July 2006–June 2012 **14 Sponsoring Agency Code** IBRC-R045(201) RE-0452-01
15 Supplementary Notes		

16 Abstract

Since 1996, over 30 Fiber Reinforced Polymer (FRP) composite bridges have been installed in the United States. Bridge locations are in Kansas, Missouri, New York, Iowa, Colorado, West Virginia, Ohio, California, Idaho, Washington, Pennsylvania, Illinois, Maryland, Oregon, North Carolina and South Carolina.

Compared to traditional steel and concrete bridge structures, the FRP panel shows several significant advantages: reduced weight, higher strength, better corrosion resistance and quicker installation. However, FRP materials exhibit different physical properties. As such, a composite bridge would demonstrate different deformation and failure patterns than a traditional bridge. During the past years, much experimental research has been conducted to investigate FRP bridge deck performance. Most experiments divide into two types: 1) static and fatigue tests in the laboratory and 2) real traffic load tests in the field. These experimental results, as well as FEM analytical results, have served as baseline data for FRP bridge deck design.

A long-term remote monitoring system was designed to investigate the response of the No-Name Creek composite bridge to the local weather. The characteristics of the bridge temperatures, the temperature differences of the two panel surfaces and the relationship between the temperature difference and the deflection were investigated with respect to the different weather patterns. Twelve thermal sensors were embedded into the FRP bridge panels. In addition, 3 laser sensors were installed to measure bridge thermal deflection. Between October 2004 and September 2005, bridge temperature and deflection were measured at 20 minute intervals. Relations between weather condition, temperature distribution and bridge thermal deflection for that bridge were analyzed.

From the analysis of the experimental and FE methods, the responses of the composite bridge to weather are summarized as follows:

(1) The temperatures of the upper and bottom panel surfaces and their differences greatly change with time of day and season. The extreme temp usually appears in the early afternoon and the minimum temp usually appears in the early morning or in the night. The bottom surface temperature is near the climatic temperature.

(2) The bridge deflections are approximately proportional to the temperature differences.

(3) The bridge had a significant upward deflection on a sunny day during the summer with the maximum often occurring between 3:00-5:00PM. The bridge has a downward deflection during the night with it being the most severe in the winter.

(4) Comparing climate induced deflection to traffic load induced deflection, the climate induced deflection is at least on the same order of deflection as allowable traffic load. Therefore, it should be considered in the FRP bridge design process.

(5) Thermal load and deflection usually are larger on clear days than on unclear, rainy, and snowy days.

(6) Distributions of thermal load in the panel can form a larger amount of deflection in the hot season than in the cold season.

17 Key Words FRP, Fiber Reinforced Polymer, Bridge		**18 Distribution Statement** No restrictions. This document is available to the public through the National Technical Information Service www.ntis.gov.	
19 Security Classification (of this report) Unclassified	**20 Security Classification (of this page)** Unclassified	**21 No. of pages** 86	**22 Price**

Form DOT F 1700.7 (8-72)

Response of No-Name Creek FRP Bridge to Local Weather

Final Report

Prepared by

Wenjie Liu
Eric Zhou
Youqi Wang

A Report on Research Sponsored by

THE KANSAS DEPARTMENT OF TRANSPORTATION
TOPEKA, KANSAS

September 2012

PREFACE

The Kansas Department of Transportation's (KDOT) Kansas Transportation Research and New-Developments (K-TRAN) Research Program funded this research project. It is an ongoing, cooperative and comprehensive research program addressing transportation needs of the state of Kansas utilizing academic and research resources from KDOT, Kansas State University and the University of Kansas. Transportation professionals in KDOT and the universities jointly develop the projects included in the research program.

NOTICE

The authors and the state of Kansas do not endorse products or manufacturers. Trade and manufacturers names appear herein solely because they are considered essential to the object of this report.

This information is available in alternative accessible formats. To obtain an alternative format, contact the Office of Transportation Information, Kansas Department of Transportation, 700 SW Harrison, Topeka, Kansas 66603-3754 or phone (785) 296-3585 (Voice) (TDD).

DISCLAIMER

The contents of this report reflect the views of the authors who are responsible for the facts and accuracy of the data presented herein. The contents do not necessarily reflect the views or the policies of the state of Kansas. This report does not constitute a standard, specification or regulation.

Abstract

Since 1996, over 30 Fiber Reinforced Polymer (FRP) composite bridges have been installed in the United States. Bridge locations are in Kansas, Missouri, New York, Iowa, Colorado, West Virginia, Ohio, California, Idaho, Washington, Pennsylvania, Illinois, Maryland, Oregon, North Carolina and South Carolina.

Compared to traditional steel and concrete bridge structures, the FRP panel shows several significant advantages: reduced weight, higher strength, better corrosion resistance and quicker installation. However, FRP materials exhibit different physical properties. As such, a composite bridge would demonstrate different deformation and failure patterns than a traditional bridge. During the past years, much experimental research has been conducted to investigate FRP bridge deck performance. Most experiments divide into two types: 1) static and fatigue tests in the laboratory and 2) real traffic load tests in the field. These experimental results, as well as FEM analytical results, have served as baseline data for FRP bridge deck design.

A long-term remote monitoring system was designed to investigate the response of the No-Name Creek composite bridge to the local weather. The characteristics of the bridge temperatures, the temperature differences of the two panel surfaces and the relationship between the temperature difference and the deflection were investigated with respect to the different weather patterns. Twelve thermal sensors were embedded into the FRP bridge panels. In addition, 3 laser sensors were installed to measure bridge thermal deflection. Between October 2004 and September 2005, bridge temperature and deflection were measured at 20 minute intervals. Relations between weather condition, temperature distribution and bridge thermal deflection for that bridge were analyzed.

From the analysis of the experimental and FE methods, the responses of the composite bridge to weather are summarized as follows:

(1) The temperatures of the upper and bottom panel surfaces and their differences greatly change with time of day and season. The extreme temp usually appears in the early afternoon and the minimum temp usually appears in the early morning or in the night. The bottom surface temperature is near the climatic temperature.

(2) The bridge deflections are approximately proportional to the temperature differences.

(3) The bridge had a significant upward deflection on a sunny day during the summer with the maximum often occurring between 3:00-5:00PM. The bridge has a downward deflection during the night with it being the most severe in the winter.

(4) Comparing climate induced deflection to traffic load induced deflection, the climate induced deflection is at least on the same order of deflection as allowable traffic load. Therefore, it should be considered in the FRP bridge design process.

(5) Thermal load and deflection usually are larger on clear days than on unclear, rainy, and snowy days.

(6) Distributions of thermal load in the panel can form a larger amount of deflection in the hot season than in the cold season.

Table of Contents

List of Tables

List of Figures

Chapter 1: Introduction

1.1 Background

Since 1996, over 30 fiber reinforced polymer (FRP) composite bridges have been installed in the United States. Bridge locations are in Kansas, Missouri, New York, Iowa, Colorado, West Virginia, Ohio, California, Idaho, Washington, Pennsylvania, Illinois, Maryland, Oregon, North Carolina and South Carolina.

Compared to traditional steel and concrete bridge structures, the FRP panel shows several significant advantages: reduced weight, higher strength, better corrosion resistance and quicker installation. However, FRP materials exhibit different physical properties. As such, a composite bridge would demonstrate different deformation and failure patterns than a traditional bridge. During the past years, much experimental research has been conducted to investigate FRP bridge deck performance. Most experiments divide into two types: 1) static and fatigue tests in the laboratory and 2) real traffic load tests in the field. These experimental results, as well as FEM analytical results, have served as baseline data for FRP bridge deck design.

In September of 2004, a Kansas State University began a remote monitoring project for the first composite bridge built in the US: No-Name Creek FRP bridge. Twelve thermal sensors were embedded into the FRP bridge panels. In addition, 3 laser sensors were installed to measure bridge thermal deflection. Between October 2004 and September 2005, bridge temperature and deflection were measured at 20 minute intervals. The data were transferred to a computer in the composite laboratory at Kansas State University through a wireless connection. Relations between weather condition, temperature distribution and bridge thermal deflection for that bridge were analyzed.

1.2 Necessity of Monitoring Composite Bridge

FRP materials exhibit different properties than traditional materials. These properties include thermal transfer coefficients and thermal expansion coefficients. Most FRP used in bridge deck construction is made of glass fibers and various polymers. These are insulators, so do not conduct heat well. As a consequence, top surface temperature would be significantly

higher than bottom surface temperature under the summer sun. In contrast, the opposite would occur during the night in the winter. This temperature difference would induce bridge thermal deflection. Experimental results show that temperature induced deflection is on the same order or greater than that induced by traffic loads. Therefore, temperature induced deflection must be considered in FRP bridge deck design. The experimental results also show that a systematic research is necessary in order to establish thermal deflection guidelines in a wide geographic location for FRP bridge deck design.

1.2.1 Material Thermal Properties

The composite materials have very low thermal conductivity and diffusivity compared with those of the structural steels. Table 1 lists the material thermal properties of the composite bridge components and the structural steel. The conductivities of composites are about 1% of the steel and the diffusivities of composites are about 4% of the steel. Since the temperatures on the upper and bottom surfaces are different with time and weather, greater temperature gradients and thermal loads will be produced between these two surfaces.

TABLE 1
Material Thermal Property of Composites and Structural Steel

	Conductivity (W/m. ºC)	Density (kg/m^3)	Specific heat (KJ/kg. ºC)	Diffusivity (m^2/s)
Steel	45.3	7833	502	1.15E-5
Glass-Composite	0.45	1800	1300	1.92E-7
Honey Core	0.08	176	1003	4.53E-7

1.2.2 Bridge Panel Structure

The composite bridge panel consists of the upper glass-fiber laminate, polymer the honeycomb core and the bottom glass-fiber laminate. The composite panel is thicker than the steel structure for support of the same traffic load. Since temperature gradient is proportional to

panel thickness, and since heat transfer time also increases with thickness, the thermal loads and deformations are further increased between the upper and bottom surfaces.

1.2.3 Weather Effects

Local weather conditions determine the thermal load applied to the bridge panels. For example, the top surface temperature of the bridge deck could be much higher than the bottom surface on a sunny day during the summer. This temperature difference would induce an upward thermal deflection. In contrast, the top surface temperature of the bridge deck could be significantly lower than the bottom surface temperature on a snowy day during the winter. This temperature difference would induce a downward thermal deflection. In Kansas, the temperature can rise above 100 ºF in a summer afternoon and fall below –5 ºF during a winter night. Figure 1 demonstrates the deflection tendency of the No-Name Creek bridge panel produced by a steady state thermal finite element (FE) simulation when the temperature difference between the two surfaces is 20 ºF. The strong solar incident in a clear day can produce a much higher temperature on the upper surface than that on the bottom surface, deforming the panel upward, as shown in Figure 1(a). The rapid descend of the climatic temperature with a strong wind can produce much lower temperatures on the upper surface than that on the bottom surface, deforming the panel downward, as shown in Figure 1(b). The impact of thermal loads may be aggregated in severe weather.

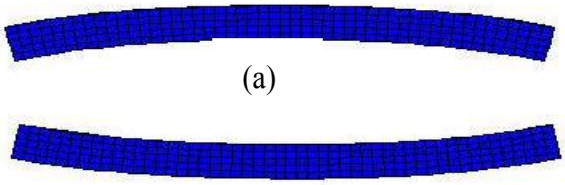

(a)

(b)

FIGURE 1
Deformation Tendency of Composite Bridge with Weather

1.3 Long Term Remote Monitoring of Bridge Deflection

A long-term remote monitoring system was designed to investigate the response of the No-Name Creek composite bridge to the local weather. The system simultaneously measured the temperatures of the upper and bottom panel surfaces and the panel displacements. The weather in Russell, Kansas generally varies seasonally and regularly, so one year of monitoring is a minimal period for assessing the effects of various kinds of weather patterns on the bridge. A one hour data acquisition interval matches the minimal interval of climatic data registered at the local weather station and substantially satisfies the characteristic description of the temperature-deflection relationship of the bridge in response to weather. Between October 2004 and September 2005, bridge temperature and deflection were measured at 20 minute intervals. The data were transferred to a computer in the composite laboratory at Kansas State University. The measured data were acquired and temporarily saved by the on site Datalogger, and then transferred daily into the host computer at the Composite Lab of Kansas State University, located about 160 miles from the bridge, through a wireless phone. The monitoring process and the post-process data analysis were done in the Lab.

The characteristics of the bridge temperatures, the temperature differences of the two panel surfaces and the relationship between the temperature difference and the deflection were investigated with respect to the different weather patterns. One of the statistical methods, the probability distribution method, was used to form 2% probability curves of extreme temperatures, extreme thermal loads and extreme deflections. The 2% probability curve matches the local 50 year climatic record curve well. This should be considered in composite bridge design in Kansas. The finite element (FE) simulations for typical weather patterns were completed to investigate both the temperature distributions in the cross-section of the panel and the variations of the thermal load-deflection ratio between seasons. Special weather (snow, rain) effects were also examined.

Chapter 2: Bridge Structure and Acquisition System

2.1 No-Name Creek FRP Bridge

No-Name Creek bridge was the first all composite highway bridge in the United States. Its speed limit is 55 miles/hour. Designed to support an AASHTO HS-25 load in both lanes, it is a single span, self-supporting glass fiber reinforced composite bridge, as shown in Figure 2. Length is 23'3"; width 27'9". It is composed of three composite sandwich panels, as shown in Figure 3-a. The micro-structure of the sandwich panel is shown in Figure 3-b. It has a 0.657" thick top structural plate, a 0.689" thick bottom structural plate and a sandwich core with a 20.5" depth. All panels are made of glass fiber reinforced polyester. In addition, the top structural plate is covered by a 0.75" thick layer of polyester concrete. Details of fiber orientation, fiber volume fraction and core geometry can be found in Ref.[1]. The bridge is located on a county road three miles east of Russell, Kansas. The accurate geographic location is 38º53'23"N and 98º51'26"W.

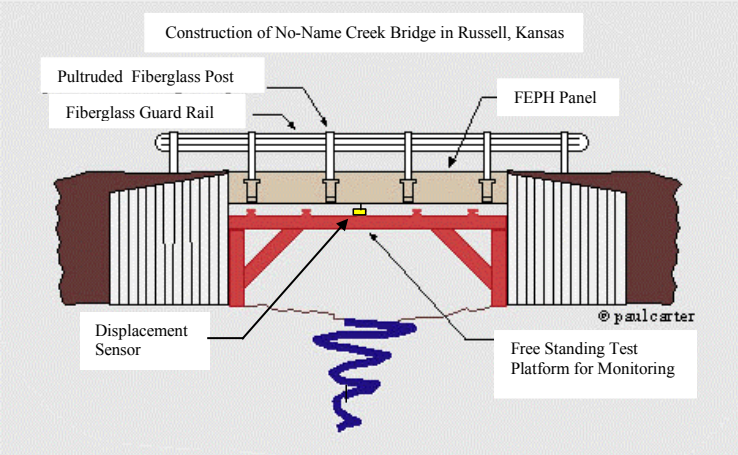

FIGURE 2
Structure of the Composite Bridge in Russell, KS

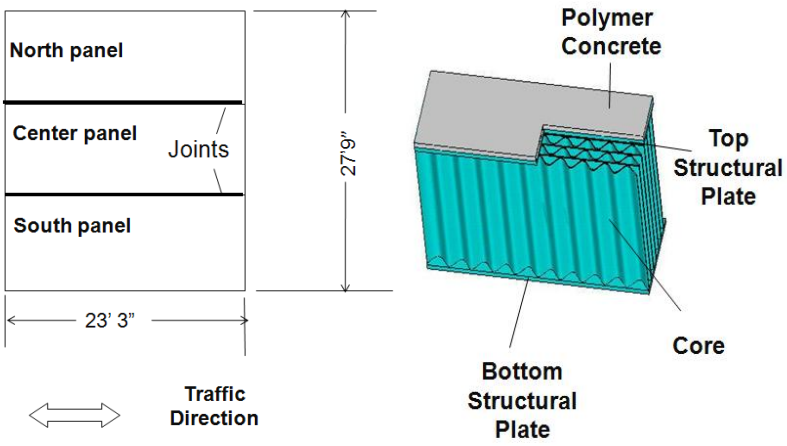

3-a Bridge panel dimensions 3-b Microstructure of the bridge panel

FIGURE 3
Dimension and Micro-Structure of Bridge Panel

2.2 Bridge Monitoring System and Experimental Set-up

The monitoring system is shown in Figure 4. A data acquisition system receives temperature data and deflection data from thermal sensors and laser sensors respectively. A solar panel powers the system. Data is automatically transmitted to a wireless modem and transfers to a computer through a dial-up modem. Refer to Figure 5. Twelve SAS-10 thermistor probe, thermo-sensors were embedded into the bridge to measure panel temperatures. The bottom sensors were fixed onto the bottom composite laminate using a polyester adhesive; the upper sensors were stuck onto the upper glass-fiber laminate and covered with polyester/rock mixtures. Four other sensors were installed to measure air temperature. Two were used to measure air temperature near the top and bottom surfaces, one to measure the air temperature below the bridge and one to measure the air temperature inside the equipment chamber. Three Acuity Research's AR200-25 triangulating laser displacement sensors were installed in a testing frame underneath the bridge to measure bridge deflection. Bridge temperature and deflection were recorded every 20 minutes and stored in the data logger. The data were sent back to a computer in Composite Laboratory at Kansas State University every evening through a wireless connection.

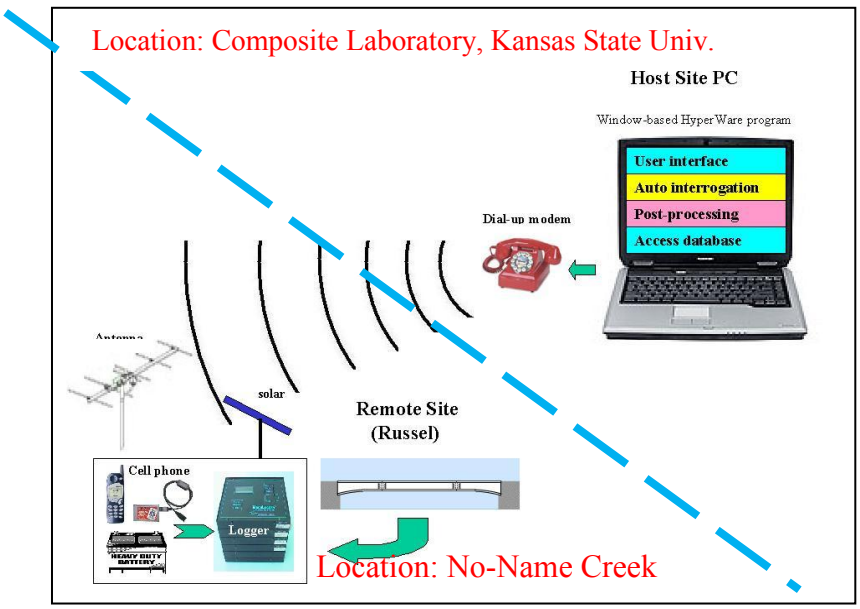

FIGURE 4
Monitoring System

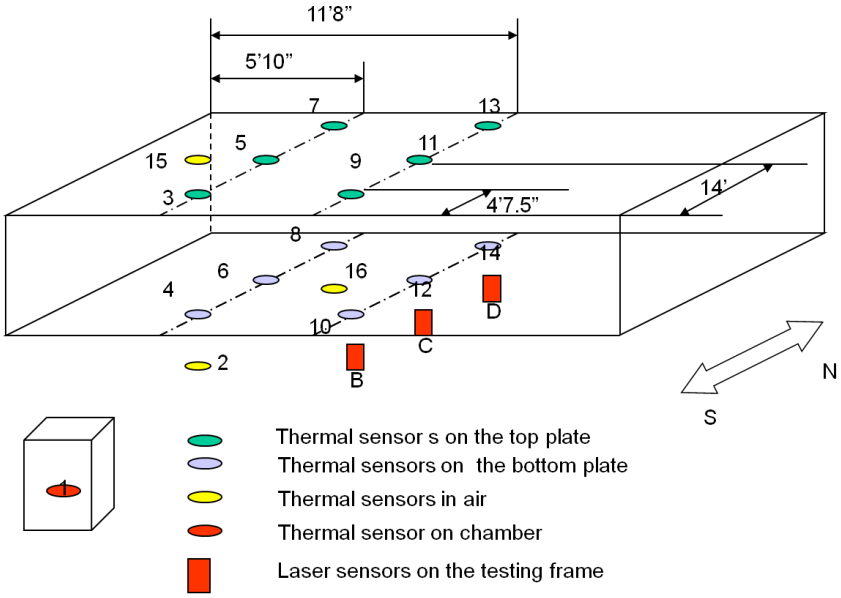

FIGURE 5
Sensor Layout

Chapter 3: Response of Bridge to the Typical Weather Patterns

3.1 General Description

The response of the composite bridge to weather mainly depends on the weather patterns (clearness, cloud, rain, and snow) and the temperature ascending or descending speeds. The responses of the bridge to weather are characterized by the thermal loads and deflections.

3.1.1 Thermal Loads

Figure 6 shows a typical temperature curve measured from a bridge panel, where T-upper is the temperature on the upper surface of the bridge panel; T-bottom is the temperature on the bottom surface; T-weather is the climatic temperature and dT is the temperature difference between the upper and bottom surfaces. dT_{max} and dT_{min} denote the daily maximum and minimum temperature differences. The thermal load applied to the bridge is characterized as:

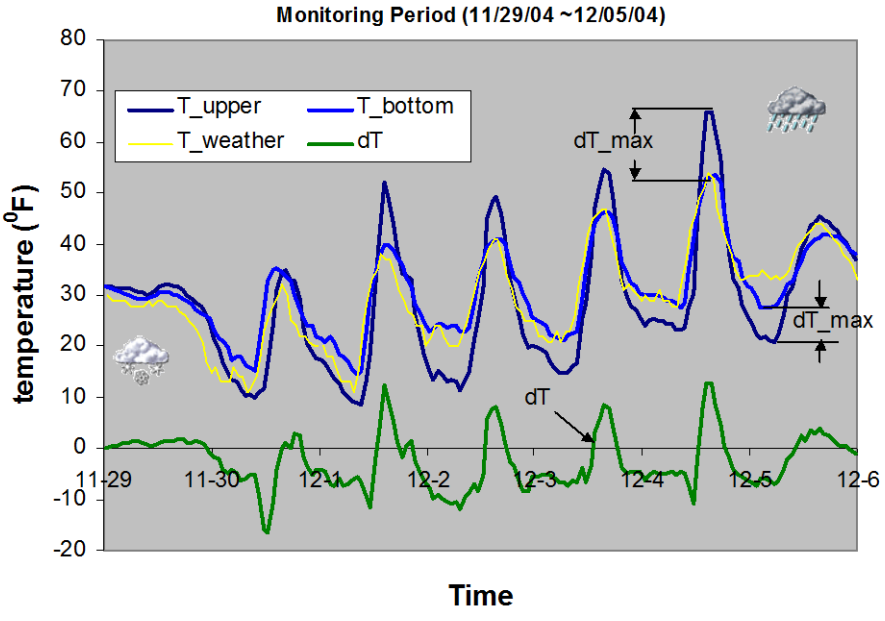

FIGURE 6
Measured Temperatures

The temperatures of the two panel surfaces varied with the climatic temperatures. The measured bottom temperature was almost equal to the climatic temperature. The daily dT_{max} usually appeared in the early afternoon and depended on the intensities of solar irradiation on the upper surface. dT_{max} was larger on a sunny day, medium on a cloudy day, and smaller on a rainy or snowy day.

The daily dT_{min} occured at night or in the early morning. dT_{min} was also related to weather conditions. The temperature of the bottom surface could be signifficantly lower than the upper surface if the climatic temperature decreased rapidly due to a strong wind.

3.1.2 Thermal Load Induced Deflection

The thermal deflection of the bridge panels were related to dT, as shown in Figure 7. The bridge deflections D were approximately proportional to the temperature differences dT. D_{max} and D_{min} appeared at T_{max} and T_{min}, respectively. The tendencies of the deflection of the three panels were similar, but the magnitude of the center panel were the largest.

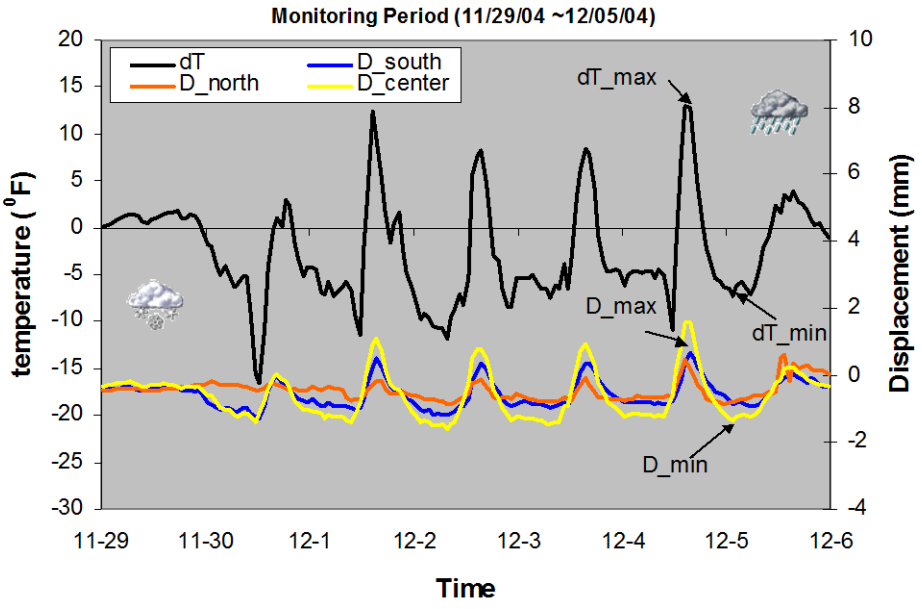

FIGURE 7
Thermal Deflections During the Monitoring Period

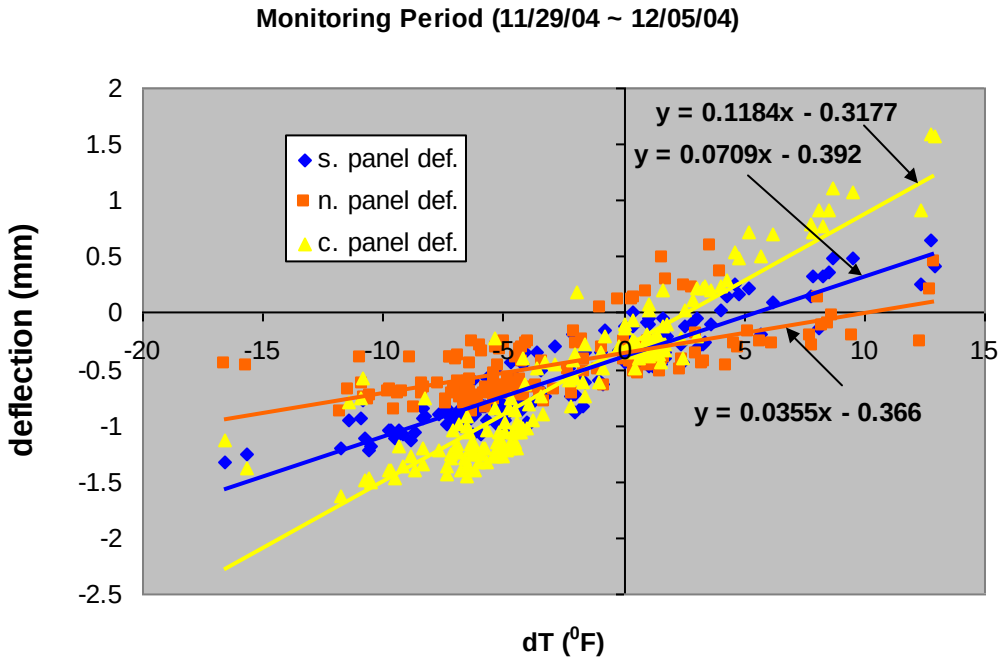

FIGURE 8
Relations of the Deflection and the Temperature Difference (dD/dT)

The gradient of the deflection to the temperature difference (dD/dT) represents the relation of the deflection and the thermal load. Generally speaking, a larger dT induces a larger deflection. However, deflection is also related to other weather conditions. For example, the upper surface and lower surface may have different moisture contents due to snow or rain. A rapid temperature drop would also affect the deflection and the temperature difference ratio. The daily, weekly and monthly average gradient can be obtained by the schematic method, as shown in Figure 8. In the trend line equation, the constant before the variable **x** of dT is the gradient and the constant of the second term is the offset relative to the zero point. Occasionally, with some complex weather conditions, the deviations of measured data to the trendline are too large to represent the gradient, so the gradient is obtained by the formula of $(D\_{max}-D\_{min})\_/(dT\_{max}-dT\_{min})$. The experimental results showed that the gradients change with the season, which will be discussed in the following section.

3.1.3 Critical Data

The upper surface of a panel is directly subjected to solar irradiation and climatic convection; as a result, maximum and daily minimum temperatures usually occur on this surface. During the monitoring period, the maximum value was 118 ºF, 12 ºF higher than the relative climatic temperature (106 ºF). The minimum temperature was –7.52 ºF, 3.48 ºF higher than the relative climatic temperature (-11 ºF). The annual dT_{max} was 35 ºF in the hot season; dT_{min} was –21 ºF in the cold season; the average gradient (dD/dT) was about 0.16 mm/ ºF.

For the center panel, the annual D_{max} was 6.9 mm and D_{min} –2.36 mm. In 2004, the response of the bridge to traffic load was measured. A truck of 70,340 lb was used. The measured middle panel deflection under the truck load was 3.93 mm. Weather related bridge thermal deflection was greater than traffic load induced deflection in this case. Therefore, weather induced thermal deflection cannot be neglected in composite bridge design.

3.1.4 Effects of Weather Patterns

The thermal loads and deflections of the composite bridge depend on the weather patterns. dT_{max} depends on the degree of weather clearness, i.e., the amount of direct solar energy received by the upper surface. dT_{min} depended on the temperature descending speed and the convection conditions. Snowy or rainy weather did not aggregate the thermal loads and deflections. Extremely high deflections appeared on very clear days after several cloudy or rainy days. Extremely low deflections appeared after several days of rapidly decending climatic temperature.

3.2 Analysis for Typical Weather Patterns

3.2.1 Normal Patterns

3.2.1.1 Direct Solar Irradiation

The solar energy incident was the major factor to determine the level of thermal loads and deflections of the bridge during normal weather (clear, unclear and cloudy days). Solar energy consists of direct and diffuse parts. The bridge upper surface absorbs the direct part of solar irradiation, increasing its temperature faster than the bottom surface. Diffuse solar irradiation is assumed to reach the earth's surface uniformly from all directions, so it would not induce a

significant temperature difference between the upper surface and the bottom surface. Variation of climatic temperatures is governed by the incident solar irradiation and the thermal inertia of the earth. Solar energy stored in the atmospheric air, the ground and the bridge during the day is slowly released at night.

On a clear day, direct solar irradiation is about 90% of total solar irradiation. On a cloudy day, direct solar irradiation is perhaps less than about 5% of total solar irradiation. Therefore, $dT_{\_max}$ and $D_{\_max}$ were much larger on a clear day than on an unclear day. As shown in Figures 6 and 7, December 4, 2004 was much clearer than other days.

3.2.1.2 Ambient Temperature and Convection

The ambient temperature and convection conditions also affected dT and bridge deflections. Ambient temperatures above the upper surface were usually higher in the day and lower at night than those below the bottom surface because convections above the upper surface were always larger than those below the bottom surface. The negative $T_{\_min}$ occured when $T_{\_weather}$ fell rapidly due to strong wind during cold seasons, as shown in Figures 6 and 7.

3.2.2 Rain Patterns

3.2.2.1 Rain Distribution

Heavy storms sometimes occurred at the bridge site. Figure 9 illustrates the rain distributions in Russell, Kansas during the monitoring period. 16% of the monitored year were rainy days, with frequent rainfall during summer, fall, and spring. The daily maximum precipitation was 3.8".

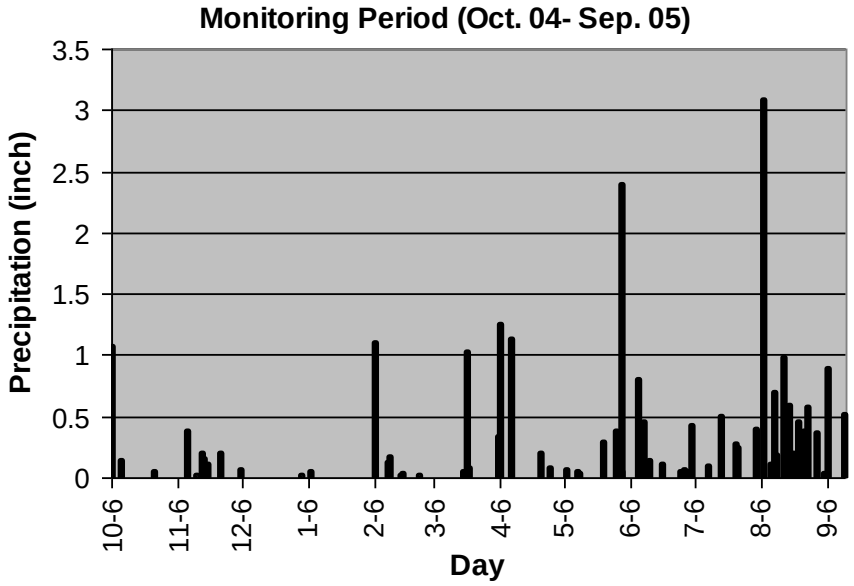

FIGURE 9
Rain Distributions During Monitoring Period

3.2.2.2 Rain Effects

The thermal loads and deflections of the bridge were usually smaller on rainy days than on clear days. Figure 10 shows the variation of average thermal loads and deflections due to precipitation. With precipitation, $dT_{\_max}$ and $D_{\_max}$ obviously decrease (Figure 10 (a)) and $dT_{\_min}$ and $D_{\_min}$ slightly increase (Figure 10 (b)) because of the cooling effect of rain on the upper surface.

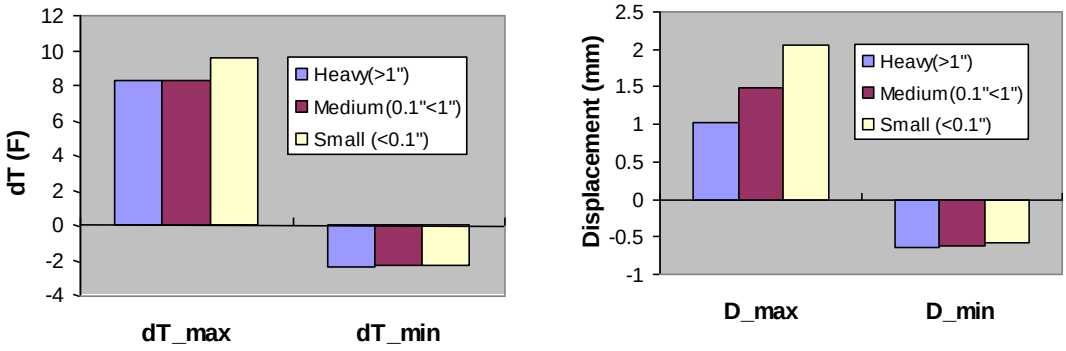

(a) Thermal loads (b) Deflections

FIGURE 10
Effects of Precipitation on the Bridge

Figure 11 shows the variation of thermal loads and deflections on a specific heavy rain day. During the duration of the rain, the sun does not produce direct irradiation to the upper surface, so the temperatures on the two surfaces of the bridge were similar to the climatic temperature. The small bridge deflection may be due to the higher moisture contents of the upper surface plate than the lower surface plate.

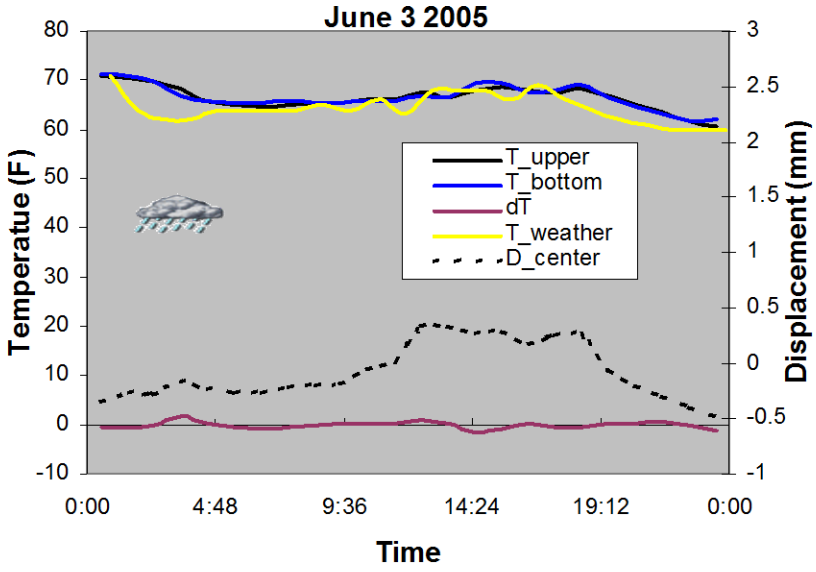

FIGURE 11
Variation of Thermal Loads and Deflection in a Heavy Rain Day

3.2.3 Snow Pattern

3.2.3.1 Snow Distribution

There were heavy snows during the winter at the bridge site. Figure 12 illustrates snow distribution in Russell, Kansas during the monitoring period. The number of snow days were about 5% of that year, concentrated within the winter, November through February. The maximum daily snowing time was about 23 hours.

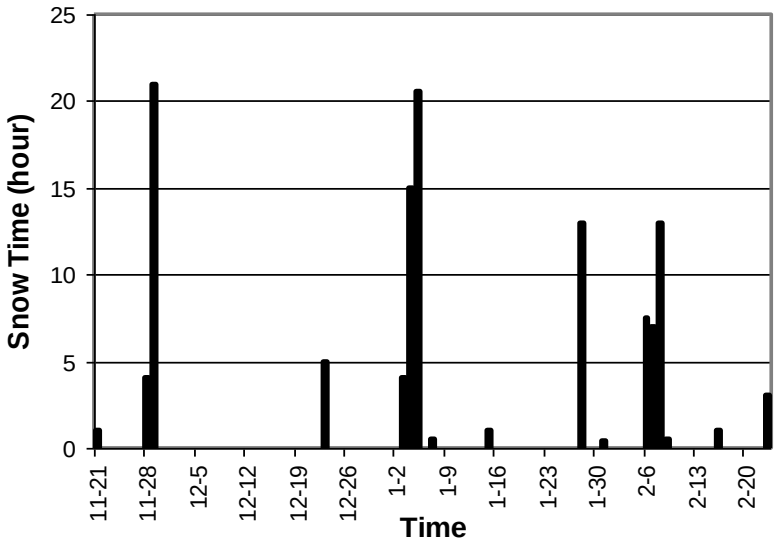

FIGURE 12
Snow Distributions in Russell, KS, During Monitoring Period

3.2.3.2 Snow Effects

The thermal loads and deflections of the bridge usually were smaller on snow days than on clear days. This would be expected for two reasons: 1) less sun exposure during a snow day and 2) prevention of the upper surface from being convected by the climatic conditions due to the snow. Figure 13 (a) and (b) statistically demonstrate that the average $dT_{\_max}$ and $D_{\_max}$ decrease with the snow time but have opposite signs due to the load of snow; the magnitude of $dT_{\_min}$ and $D_{\_min}$ also decreased with the snow time since climatic conditions would have more

influence on $dT_{\_min}$ and $D_{\_min}$ on a light snow day than the snow temperature and load would have on a heavy snow day.

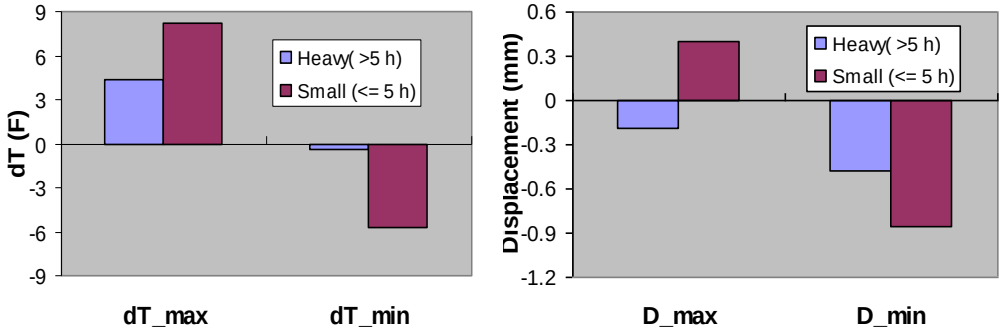

(a) Thermal loads (b) Deflections

FIGURE 13
Variations of Thermal Loads and Deflections with Snow

The thermal loads and deflections of the bridge were investigated for two kinds of snow patterns: climatic temperature falls quickly or falls slowly. Figure 14 illustrates the variations of thermal loads and deflections during snow days when the climatic temperatures fell quickly: climatic temperature was always much lower than the two surface temperatures. At first, the large convection on the upper surface, induced by the strong wind, made the upper surface temperature lower than the bottom surface temperature. With an increased thickness of the snow layer on the upper surface, however, the snow protects the upper surface from the strong convection induced by low climatic temperatures, causing the upper surface temperature to become higher than the bottom surface tempurature. Although the dT curve steepened, the corresponding panel deflection did not follow the trend because of the protection from the thick snow layer.

Figure 15 shows the variations of thermal loads and deflections of the bridge during the snow days when the climatic temperatures changed slowly. The thermal load dT and deflection D are smaller in this case than those when temperatures changed quickly.

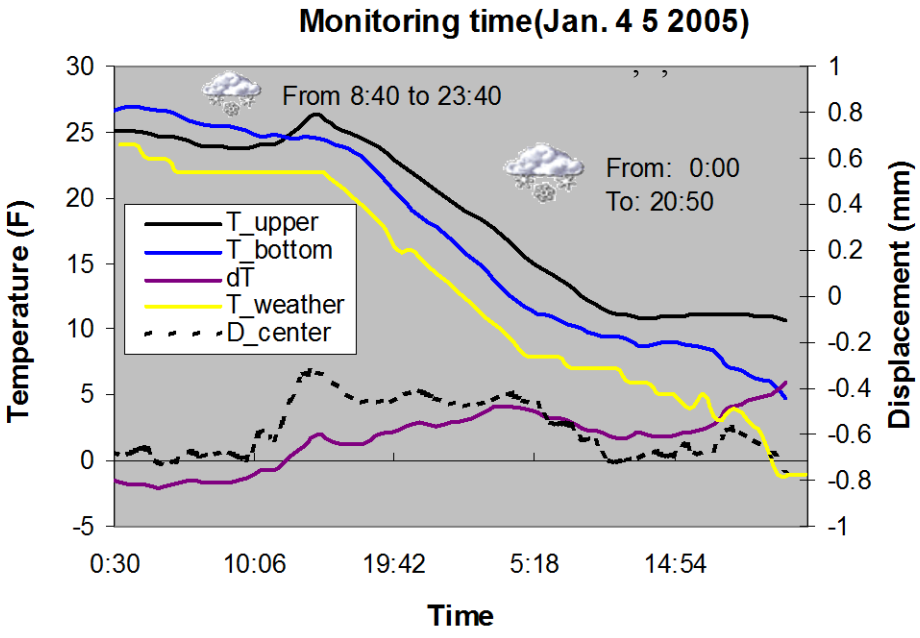

FIGURE 14
Thermal Loads and Deflections with Quick Temperature Descent on Snow Days

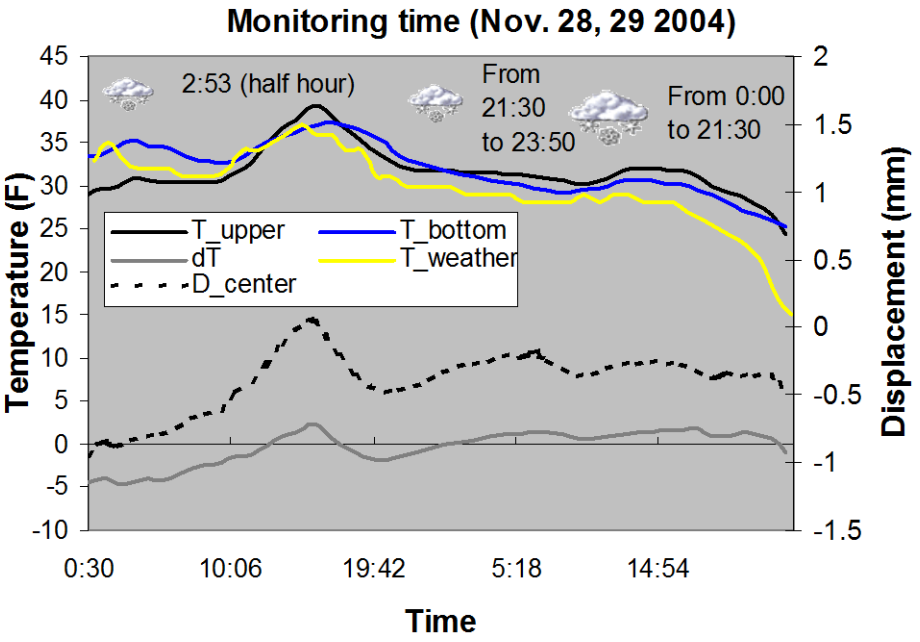

FIGURE 15
Thermal Loads and Deflections with Slow Temperature Descent on Snow Days

3.3 Annual Extreme Deflections

The weather patterns that form extreme deflections of the bridge were investigated by selecting two sets of maximum and minimum deflections during the monitoring period.

3.3.1 Annual Maximum Deflection

The annual maximum deflections were usually produced on very clear days, i.e. strong solar irradiation days, after several cloudy or rainy days. Figure 16 shows the weather pattern that caused that year's penultimate loads and deflections. Those values occurred on a clear day that came after four unclear days in which it had rained the final two.

Figure 17 shows the weather pattern that caused that year's largest thermal loads and deflections. Similar to the weather pattern yielding the penultimate values, the largest values happened during a clear day after four days of rainy and unclear weather.

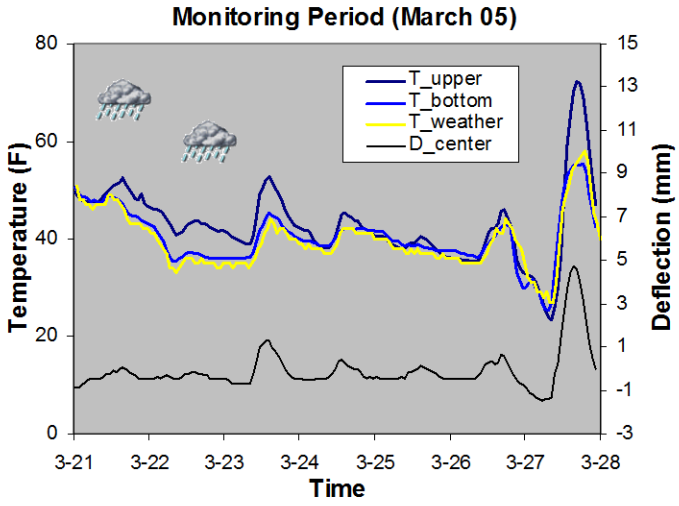

FIGURE 16
The Penultimate Largest Thermal Loads and Deflections

Three factors induced this phenomenea. Firstly, there was a large thermal load (dT), as was recorded on the clear days. Secondly, with such climatic conditions, the temperature in the cross-section of the panel along the thickness direction was distributed in such a way to produce

thermal forces that generated larger deflections than would be generated under usual climatic conditions. During several, consecutive unclear or rainy days, the temperature differences dT become very small, as shown in Figure 16 and 17, so a thermal steady state with small temperature gradients were formed in the cross-section. When the day turned clear, the strong solar irradiation produced large gradients in the outer portions of the two surface plates and a large dT. This temperature distribution resulted in more deformation. Thirdly, the upper surface contained more moisture than the lower surface. A small portion of the bridge deflection was due to this hygroload.

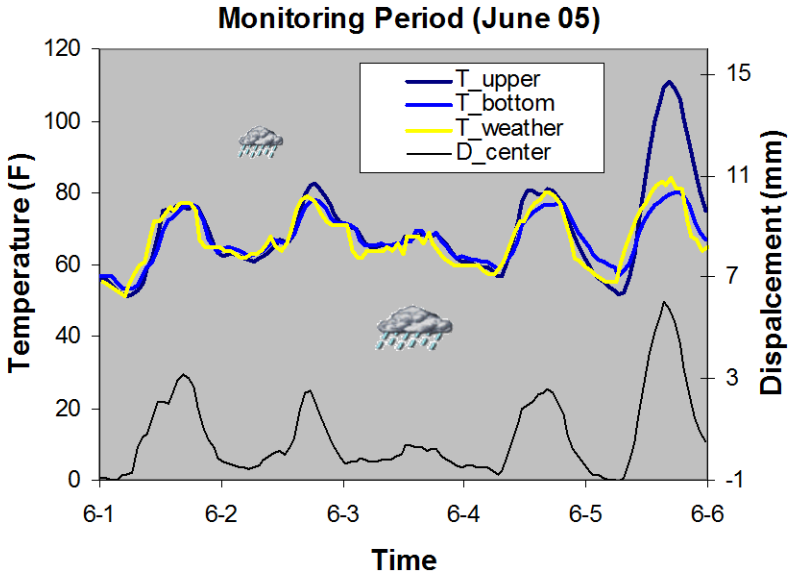

FIGURE 17
Variations of the Maximum Thermal Loads and Deflections

3.3.2 Annual Minimum Deflection

The annual minimum thermal deflections were usually produced during several days of rapid, continuous temperature decent in the cold season. Figure 18 shows the weather pattern that caused the second largest downward deflection during the monitored year. The daily $T_{\_min}$ and $D_{\_min}$ continually decrease with the climatic temperature in all four days. Figure 19 shows the weather pattern that caused the largest downward deflection during the monitored year. Similar

to the climatic conditions that produced the second largest downward deflection, the largest downward deflection occured after one day of rapid temperature decline following two days of extremely low climatic temperature.

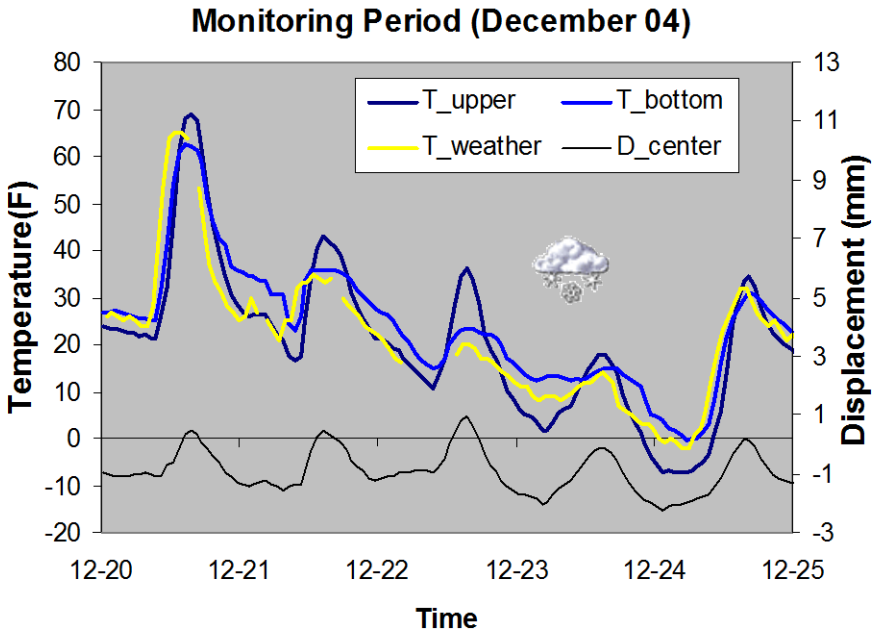

FIGURE 18
Weather Pattern for the Second Minimum Thermal Loads and Deflections

The annual minimum deflections were induced by two factors. First, these deflections happened when the negative thermal load dT was very large. Second, the temperature distributions in the panel cross-section along the vertical direction form the thermal forces were larger than in usual climatic conditions. With the continuous temperature decent, the upper panel surface was subjected to larger temperature changes than the bottom surface due to convection. As such, the temperatures of the upper portion of the panel became significantly lower than the bottom portion, producing larger thermal forces between the two surface plates, which, in tern, generated the largest and the second largest downward deflections, as shown in Figure 18 and 19.

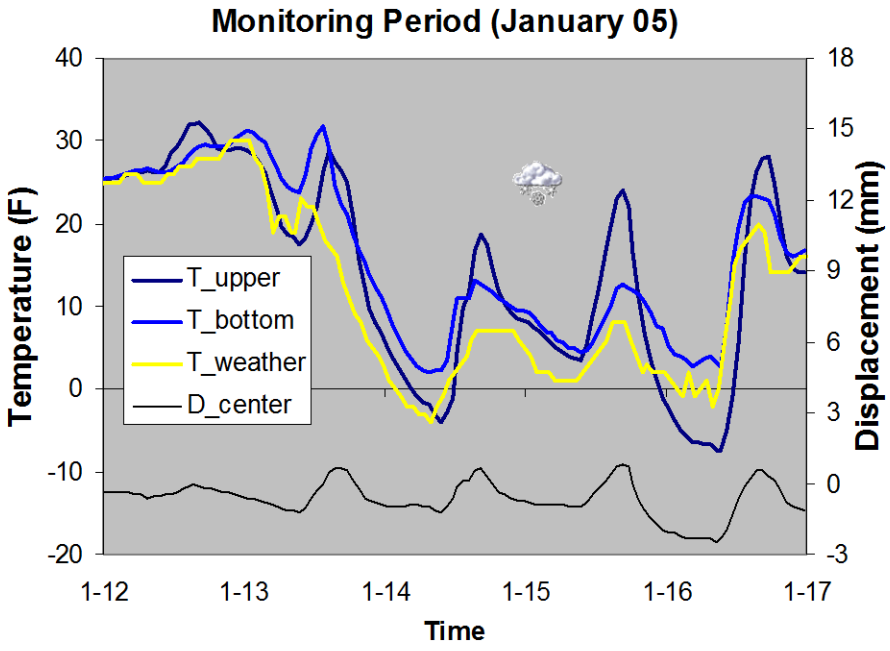

FIGURE 19
Weather Pattern for the Minimum Thermal Loads and Deflection

Chapter 4: Statistical Analysis of the Bridge Responses to Weather

In this section, the annual variations of the thermal loads and deflections induced by local weather are investigated. The probability distribution method is used to evaluate the extreme states of thermal loads and deflections for a 50 year period. Annual variations of the gradient of the deflection to the temperature (dD/dT) were examined and the zero-deflection position were derived.

4.1 Determination of 2% Probability Distributions

Composite bridge designers want to know the possible maximum weather-induced thermal lads and deflections during the life of the bridge. The acquisition data merely reflected a single year of variations of the thermal loads and deflections with respect to local weather; however, by employing a statistical method, the acquired data can predict the possible extreme states of the bridge using the historical climatic record.

The probability distribution method is used to realize the prediction. Figure 20 illustrates the various climatic temperatures at the bridge site over time. $T_{\_hour,}$ obtained from the NCDC website [9], represents the hourly climatic temperatures in the monitoring period. The average climatic maximum, mean and minimum temperatures are denoted by $T_{\_max}$, $T_{\_mean}$, and $T_{\_min}$, respectively. $T_{\_hmean}$, $T_{\_hmax}$, and $T_{\_hmin,}$ obtained from AOL National Weather [10], represent the mean, maximum, and minimum temperatures from the past 50 years. The climate was warmer in the monitoring period since the temperatures $T_{\_mean}$ are much high in the winter compared with $T_{\_hmean}$. According to the probability distribution principle, the possibility of the occurrence of $T_{\_hmax}$ and $T_{\_hmin}$ should be 2% (1 time/50 year); the daily maximum and minimum temperatures should exceed by 7.3 times the (or equal to) $T_{\_hmax}$ or $T_{\_hmin}$ in the monitoring period. In Figure 20, there are 7 days in which temperatures exceeded the historic extreme values and 3 days in which the temperatures equaled these values. The possibility of this occurrence is 2.7 %, so the discrepancy is small.

As shown in Figure 20, the bounds of 2% probability for temperature are derived from the average $T_{\_max}$ and $T_{\_min}$ using the probability distribution method. Assuming that the daily average extreme temperatures have Gaussian distributions, the upper-bound $T_{\_ub2\%}$ and lower-bound $T_{\_lb2\%}$ are obtained by moving the curves of $T_{\_max}$ and $T_{\_min}$ by 2.04 units of the standard deviation (2% of occurrence), respectively. These new curves have a good fit with the historical extreme temperatures, as shown in Figure 20.

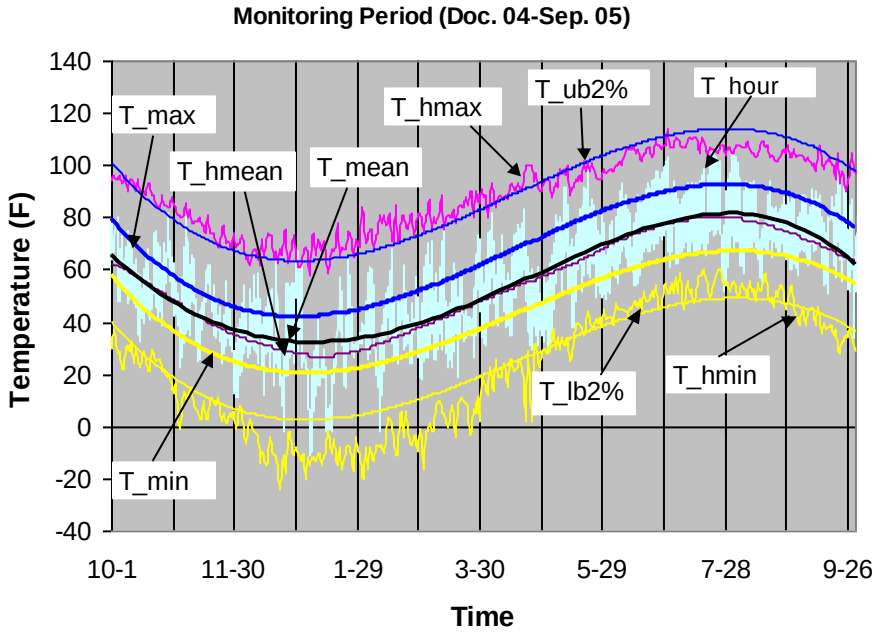

FIGURE 20
Comparison of the Historical and Monitored Temperatures

The discrepancy of the fit between the 2% probability bounds and the historical extreme curves for temperatures is investigated by subtracting the bound values from the historical values with a different unit of standard deviation (percentage of probability). The results in Figure 21 demonstrate that the minimum discrepancies are near 2% for both bounds. This further proves that the assumption of a 2% probability distribution is correct for our cases.

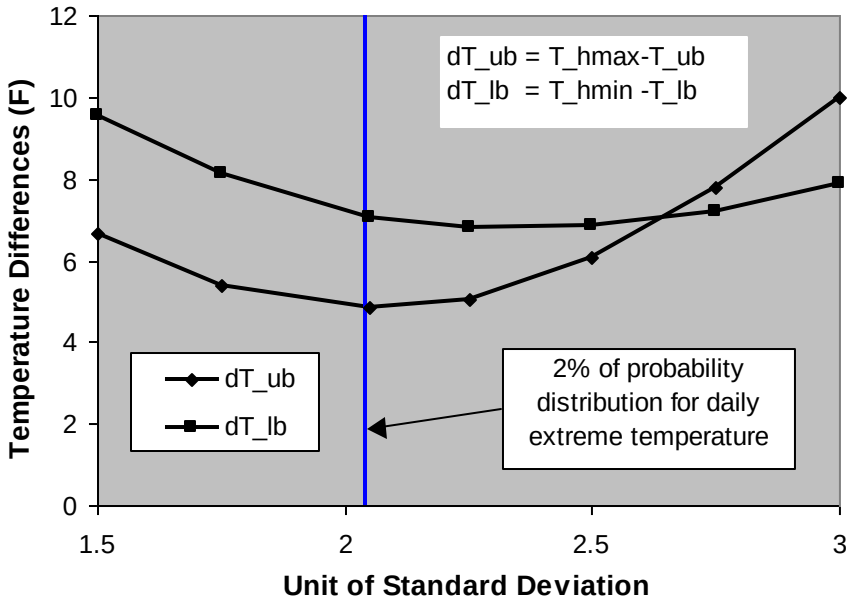

FIGURE 21
Temperature Differences between the Extreme Curves and the Bound Curves with Percentage of Probability

4.2 Bridge Temperatures

Appendix I presents the bridge upper and lower surface temperature curves and the climatic temperature curves within the 52 week monitoring period. The upper surface temperature is the average temperature derived from 6 thermal sensors located on the upper surface and the lower surface temperature is the average temperature derived from 6 thermal sensors located on the bottom surface. The climatic temperature is from the local weather station.

4.2.1 Upper Surface

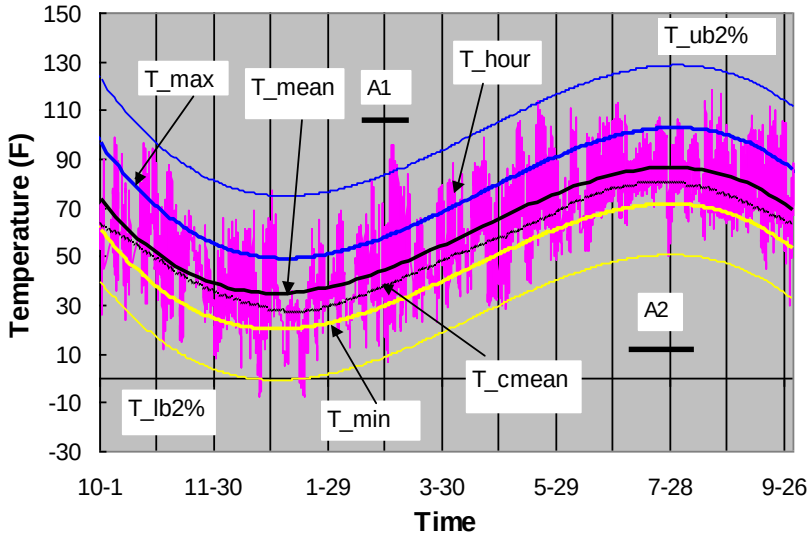

FIGURE 22
Temperatures on the Upper Surface During Monitoring Period

Figure 22 illustrates the variations of temperatures on the panel upper surface. These temperatures have the same tendencies as the climatic temperatures. However, the measured mean $T_{\_mean}$ is much higher than the climatic mean $T_{\_cmean}$ due to solar irradiation. Similarly, the measured $T_{\_max}$ and $T_{\_min}$ are higher than the relative climatic temperatures. The standard deviation of $T_{\_max}$ is 13.1 ºF and is larger than that of $T_{\_min}$ (9.95 ºF). The extreme temperatures with 2% of occurrence are 126 ºF and –4 ºF, obtained from the curves of $T_{\_ub2\%}$ and $T_{\_lb2\%}$. The measured temperatures are 114.28 ºF and –7.526 ºF.

4.2.2 Bottom Surface

Figure 23 illustrates the temperatures of the panels bottom surface. The measured mean temperature $T_{\_mean}$ is approximately equal to the climatic temperatures $T_{\_cmean}$. Their differences become large in January and February, which may be caused by the rapid climatic temperature change and snowy weather. The standard deviations of $T_{\_max}$ and $T_{\_min}$ are 10.3 ºF and 8.73 ºF,

which are smaller than those on the upper surface. The maximum extreme temperatures with 2% of occurrence are 108 ºF and 8 ºF. The measured temperatures are 103 ºF and –3.712 ºF.

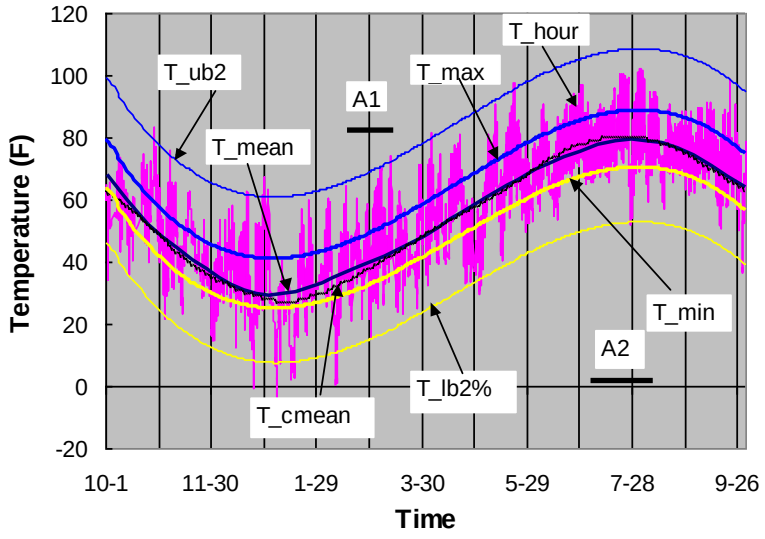

FIGURE 23
Temperatures on the Panel Bottom Surface

4.2.3 Temperature Difference dT between the Upper and Lower Surfaces

The weekly temperature difference curves between the upper and lower surfaces are shown in Appedix II. Figure 24 illustrates the variations of the temperature differences between the upper and bottom surfaces during the whole monitoring period. The fluctuations are much larger at $dT_{\_max}$ than at $dT_{\_min}$. The average $dT_{\_max}$ varies with climatic temperatures, but the tendency is interrupted by Zone A1 and A2. In Zone A1, $dT_{\_max}$ is very large, but $D_{\_max}$ is modest, since the continuous temperatures increase rapidly in a short period of several days. In Zone A2, large positive $dT_{\_max}$ and negative $dT_{\_min}$ are caused by the thermal lag between the upper and bottom surfaces, which will be analyzed using FE simulation. The maximum extreme dT with a 2% possible occurrence is 33 ºF and –15 ºF.

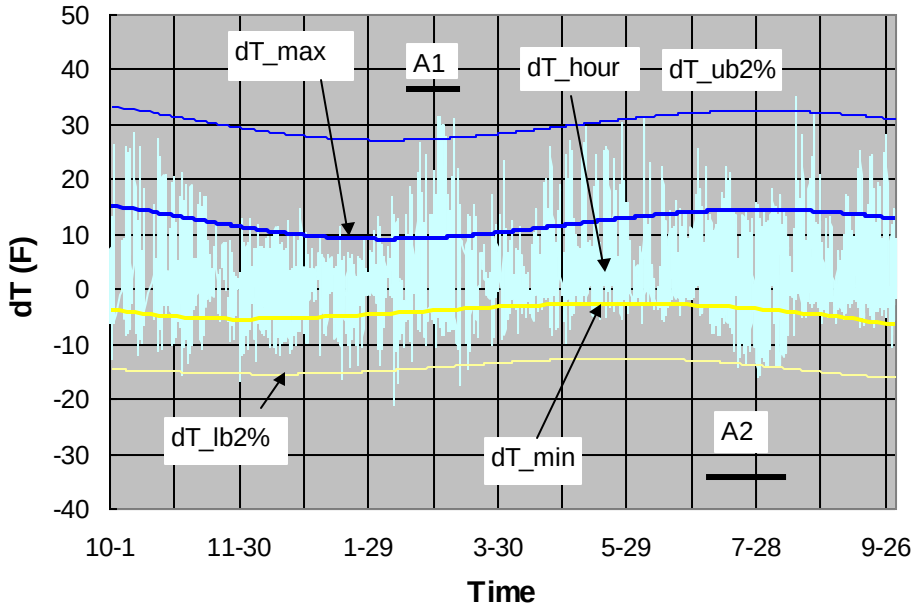

FIGURE 24
Temperature Difference between the Upper and Bottom Surfaces

4.3 Bridge Deflection

The weekly bridge panel deflection curves are shown in Appendix II. Figure 25 shows the various deflections of the bridge's center panel. The maximum daily deflections greatly change with the season, but the minimum daily deflections have small changes. The characteristics of the bridge deflections can be described as follows: (1) The standard deviation of $D_{\_max}$ is 1.12 mm and much larger than that of $D_{\_min}$ (0.38 mm). (2) The deflections of bridge $D_{\_max}$ are proportional to the seasonal temperatures. (3) The actual maximum deflection (6.90 mm) occured in June and the maximum $D_{\_ub2\%}$, that appeared in both June and July was 6.14 mm. Their difference was small. (4) The actual $D_{\_min}$ was -2.36 mm. It occurred in January. The minimum $D_{\_lb2\%}$, was –1.83 mm.

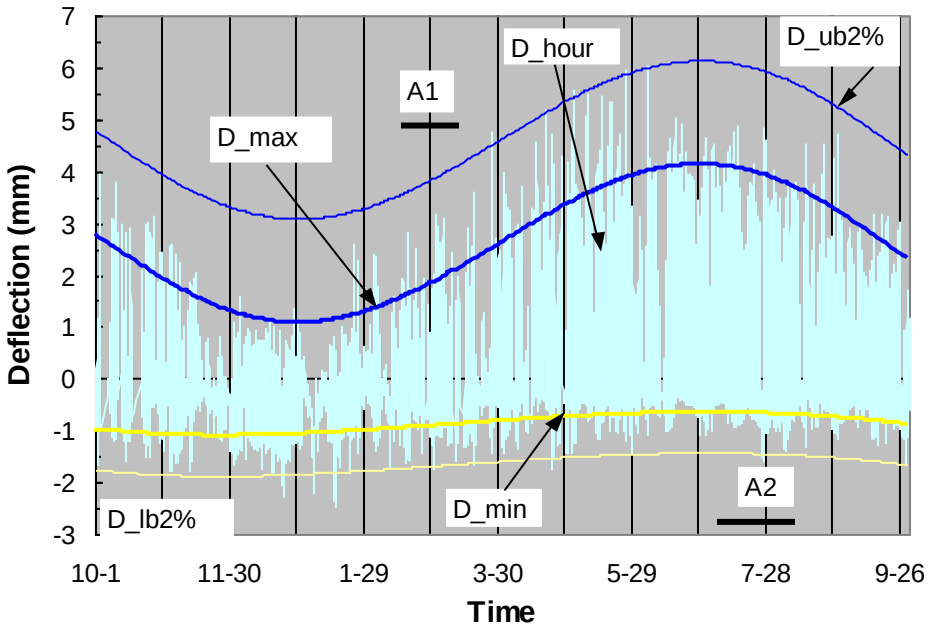

FIGURE 25
Deflections of the Bridge Center Panel During the Monitoring Period

4.4 Bridge Position with Zero Thermal Load

Figure 26 shows the variations of the bridge position when the daily temperature differences between the two surfaces dT are equal to zero. The actual zero thermal load points flutter near the horizontal line (D = 0), so this line is regarded as the zero thermal load line. All deflections in this report took this line as the baseline. Hence, the values of **these** deflections reflect the actual position of the bridge.

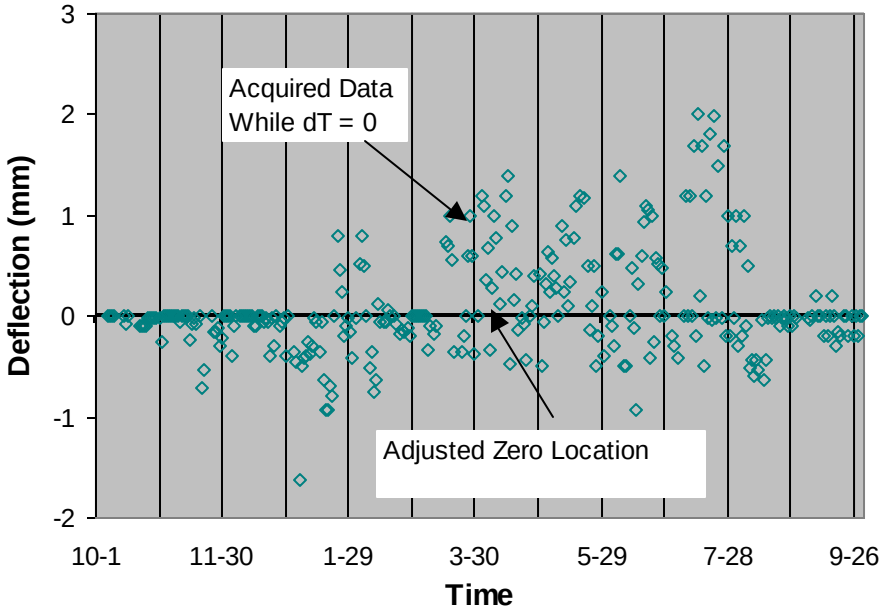

FIGURE 26
Bridge Panel Vertical Positions while dT = 0

Most of the deflections produced by the zero thermal loads match the baseline well, particularly from August to March, except for a few modest deviation points. There are some big deviation points from April to July, which may be caused by steep temperature changes at dT=0, thermal lag, storm, and so on.

4.5 Relations of Deflection and dT

Appedix II shows the relations between the bridge deflection and the temperature difference between the bridge upper bottom surfaces. Figure 27 shows the variations of the weekly gradient (dD/dT) in the monitoring period. The gradients slightly vary with time and are proportional to the seasonal temperature. The reason may be that the gradient of solar irradiation and climatic temperature are larger in the cold season than in the hot season, so the interior composite plates have less volumes and less thermal forces in the cold season than in the hot season when the dT are equal.

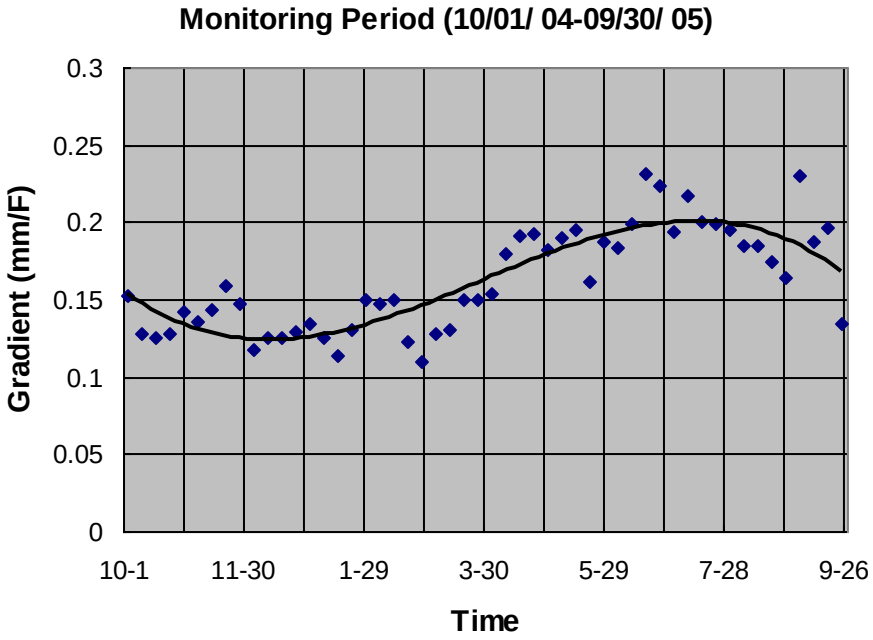

FIGURE 27
Variation of Gradient (dD/dT) During the Monitor Period

4.6 General Characteristics

Based upon the recorded data, the method of 2% probability Gaussian distribution can be used to predict the annually extreme states that occurred at a probability rate of 2% for local climatic temperature, temperature diferrence between the upper and lower panel surfaces, and the bridge deflection.

The climatic T_{cmean} was much lower than the measured T_{mean} of the panel upper surface, but was almost equal to the T_{mean} of the panel bottom surface. The annual extreme temperatures with a 2% occurrence was 126 ºF and –4 ºF for the upper surface and 108 ºF and 8 ºF for the bottom surface. The fluctuations were much larger at dT_{max} than at dT_{min}. The daily average maximum dT varied with climatic temperatures; however, it was not the case in zones A1 and A2, in which irregular thermal states were observed. The deflections of bridge D_{max} were obviously

proportional to the seasonal temperatures. The actual measured maximum deflection was 6.90 mm; the maximum $D_{\_ub2\%}$, was 6.14 mm. The actual measured $D_{\_min}$ was -2.36 mm; the minimum $D_{\_lb2\%}$, was –1.83 mm.

Chapter 5: FE Heat Transfer Simulation of the Composite Bridge

In this section, FE simulation was conducted to derive the distribution of temperatures of the bridge panel with respect to weather and to investigate the effects of thermal boundary conditions during different seasons. This would provide insight into temperature distribution within the interior panel and into the thermal lag phenomenon (Zone A2).

5.1 FE Experiment

5.1.1 FE Model

A 15" long segment of the bridge panel is used to build a 2D symmetric FE model, as shown in Figure 28. The right side of the model is the symmetric surface. The red region is filled with polyester and stone, within which a thermal sensor is embedded. In the FE model, a high conductivity and diffusivity thin plate is added to the top of the soil that covers the bridge panel. The thin plate absorbs the heat flux from the sun. The test verified that the error induced by the special plate can be neglected. There are 4200 Plane55 elements with a side length of 0.04".

5.1.2 Material Thermal Properties

The material thermal properties of the composite bridge are listed in Table 2. The upper and bottom Glass-fiber composite plates have very low conductivity and diffusivity properties. The mixture that covers the thermal sensors consists of polymer (adhesive), rock and air, so its thermal property is assumed by the volume fraction of these three materials.

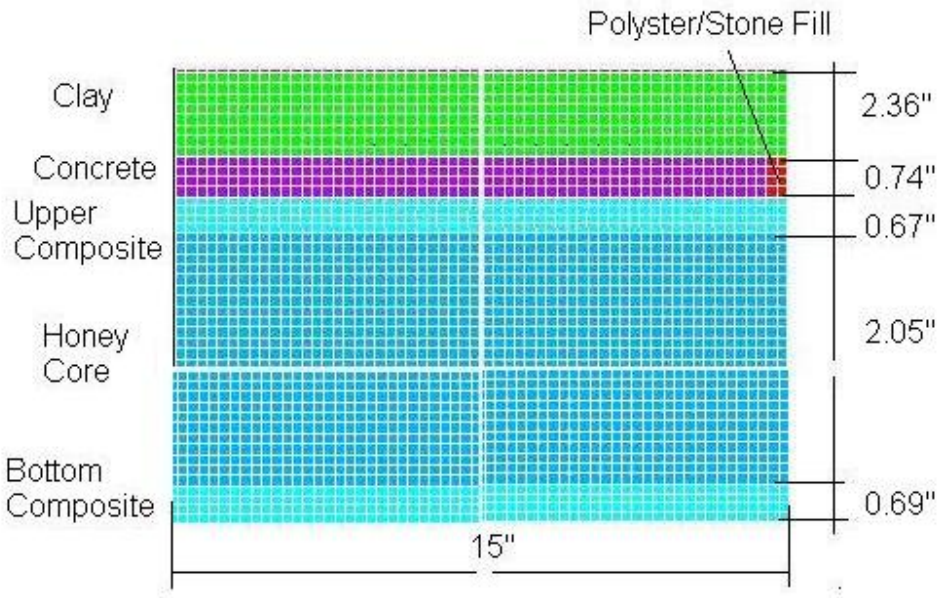

FIGURE 28
A 2D FE Model of the Composite Bridge Panel

TABLE 2
Material Thermal Properties of the Bridge Composite

Name	Conductivity (W/m·F)	Density (kg/m^3)	Specific Heat (J/kg·F)
Clay	0.6	1649	1800
Concrete	0.79	1600	840
Glass Composite	0.45	1800	1300
Air	0.0181	1.766	1003
Honey Core	0.083	13.5	1003
Polyester/Rock	0.23	1200	1800

The honeycomb core consists of flat and sinusoidal plates constructed from short fibers oriented randomly, known as Choop Strand Mat (ChopSM). The core contains most of the bridge's internal volume, so its thermal properties has a large effect on its response to weather. Figure 29 illustrates the 2D geometry of the honeycomb core. The volume fraction of the composite is about 15%. Hence, the conductivity, specific heat, and density of the core are determined by rule of mixtures based on volume fractions. These values are listed in Table 2.

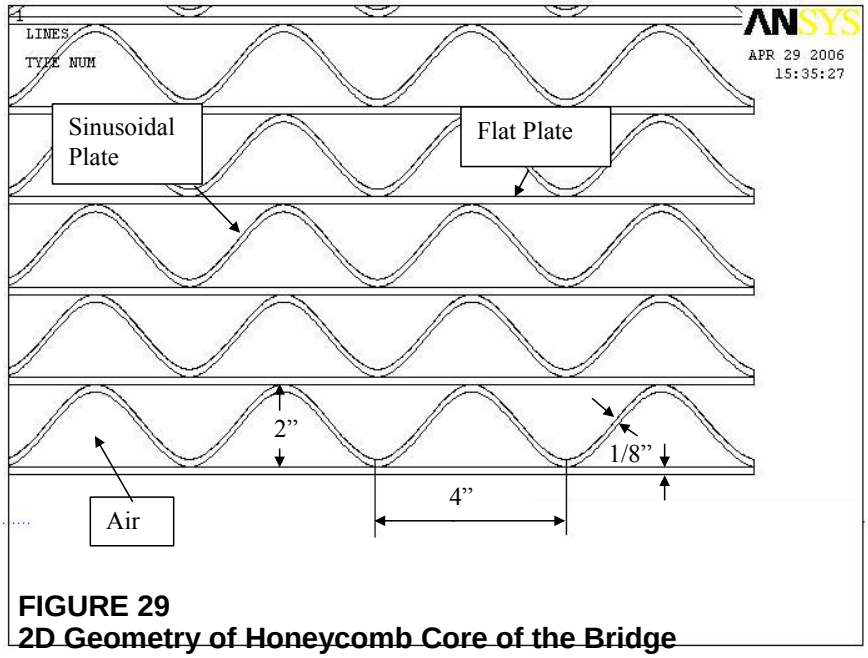

FIGURE 29
2D Geometry of Honeycomb Core of the Bridge Panel

5.1.3 Boundary Conditions

The right end of the FE model is a symmetrical surface and the left end is an insulated surface. The thermal loads consist of convection and solar irradiation. The time-dependent convection is applied to the upper and bottom panel surfaces, while the time-dependent solar irradiation is only applied to the upper surface.

(1) Solar irradiation: Daily solar energy and intensity in Russell, KS (Lat. 38.86º N, Lon. 98.83º) can be interpolated by the data listed in the solar manual received from the nearest stations, Goodland, KS (Lat. 39.37º N, Lon. 101.70º W) and Dodge, KS (Lat. 37.77º N, Lon. 99.97º W) [7] [8]. Figure 30 illustrates the distributions of daily solar energy intensity in three typical months. The absorptivity of the soil surface on the bridge from solar irradiation was about

0.75 [10]. The curves of the daily solar intensity had obvious differences in accordance with the season. The shape became tall and narrow in the hot season, short and wide in the cold season. This kind of distribution resulted in large gradients of heat flux on the upper surface in the winter and small gradients in the summer. The daily solar energy at the bridge site varyed with respect to the month and was derived according to the data obtained from the nearest city's solar station records [7][8], as shown in Figure 32.

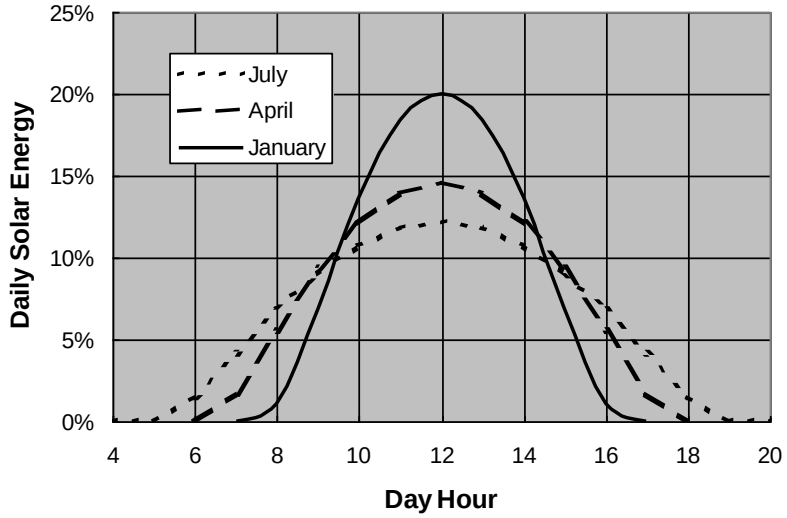

FIGURE 30
Daily Solar Distributions During Three Seasons in Russell, KS

(2) Ambient Temperatures: The ambient temperatures measured near the upper surface and near the lower surface were similar and close to the climatic temperatures. Therefore, the climatic temperature was taken as the ambient temperature for both the upper surface and the lower surface.

(3) Convection heat transfer: Convection coefficient strongly depends on fluid material properties, velocity, solid surface geometry and roughness. ASHRAE [10] suggests that the outside surface of a building convection coefficient $h_{0,winter}$ =34.0 W/m2 and wind speed = 15mph; $h_{0,\ summer}$ =22.7 W/m2 and wind speed = 7.5 mph. The employed coefficients are interpolated

according to the actual wind speeds shown in Figure 32. The convection coefficient on the bottom surface is usually much smaller than that on the upper surface. The ratio is assumed to be 1:2.

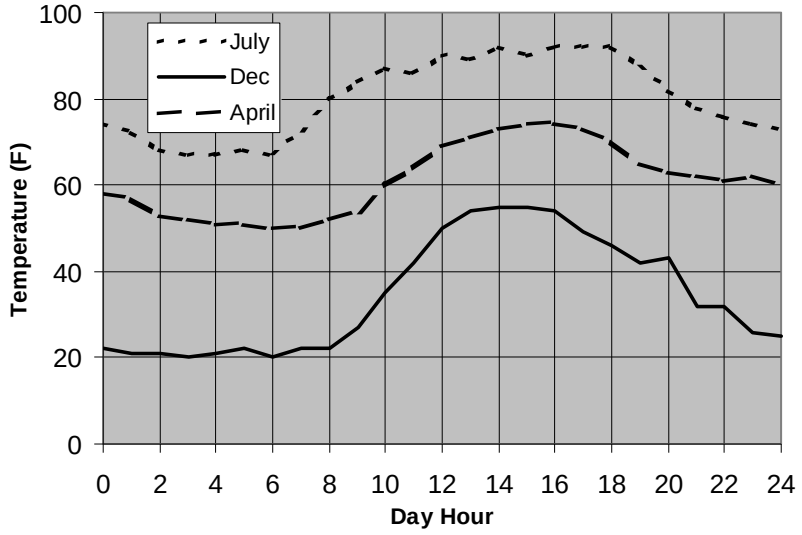

FIGURE 31
Typical Ambient Temperatures of Three Seasons in Russell, KS

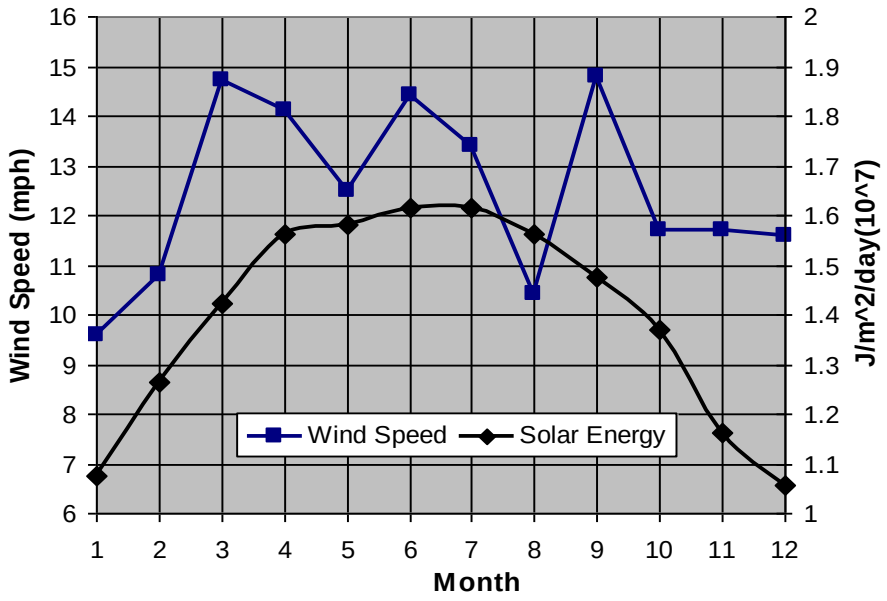

FIGURE 32
Monthly Average Wind Speeds and Solar Energy in Russell, KS

5.1.4 FE Program

The simulations run automatically on ANSYS using the APDL program. The heat steady state at the initial time was obtained according to the measured surface temperatures. Then the loading curves of solar irradiation, ambient temperatures, and convection coefficients were applied to the relevant surfaces of the panel at a one hour interval.

5.2 Simulated Results

5.2.1 Typical Weathers

The two clear days from the hottest and coldest seasons are selected to make a comparison of the results obtained from both the experimental and numerical methods. By including solar irradiations, ambient temperatures and convection coefficients in boundary conditions, as shown in Figures 30–32, the results of FE simulations are generally in good agreement with the experimental results.

(1) Cold Weather

The temperatures of the panel surfaces obtained from FEM are compared with the experimental results in the coldest season, shown in Figure 33. The measured daily minimum temperature of the upper surface $T_{\_upper}$ in the morning were lower than the daily minimum climatic temperature that was assumed to be the ambient temperature. This phenomenon demostrates the actual ambient temperatures of the upper surface were lower than the climatic temperature $T_{\_weather}$. Therefore, the temperatrues of the upper surface derived from numerical simulation, $T_{\_upp\_FEM,}$ are generally higher than the relevant measured temperatures.

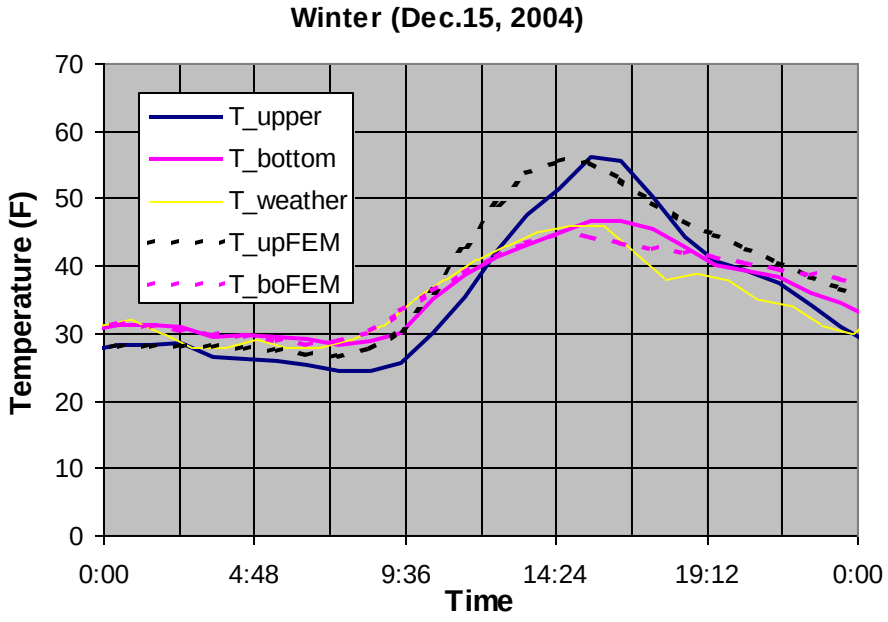

FIGURE 33
Variations of Temperatures on the Panel Surfaces in the Coldest Season

(2) Hot Weather

Figure 34 shows the comparison of temperatures of the panel surfaces obtained from the measured and FEM methods. The measured temperatures of the bottom surface $T_{\_bottom}$ were slightly lower than climatic temperature $T_{\_weather}$ in the day time, which may have been caused by 1) the big discrepancy between the actual ambient temperatures near the bottom and the

climatic temperature and 2) the low convection under the bridge. Generally speaking, numerical results and experimental results are in good agreement with the measured results.

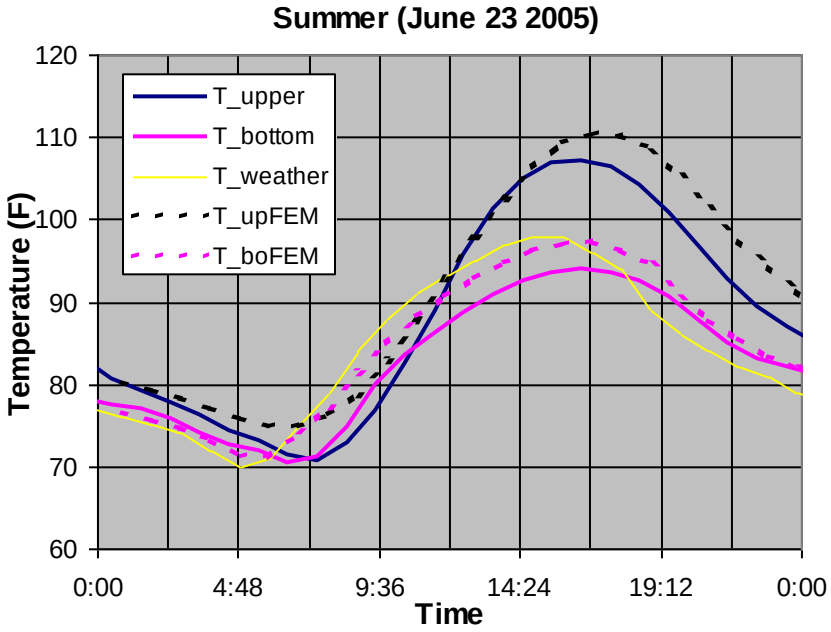

FIGURE 34
Variations of Temperatures on the Panel Surfaces in the Hottest Season

(3) Thermal Lag

In the statistic analysis section, the large thermal lag between the upper and bottom surfaces (Zone A2) appeared from July 5 through August 15. Refer to Appendix II. In this period, the thermal deflection changes lag the thermal load changes applied to the bridge. Figure 35 shows the results obtained from both the measured method and the FEM. FE simulation demonstrates that the large thermal lag is produced from the solar irradiation and convection characteristics, ambient temperature distribution, and the soil humidity on the bridge surface.

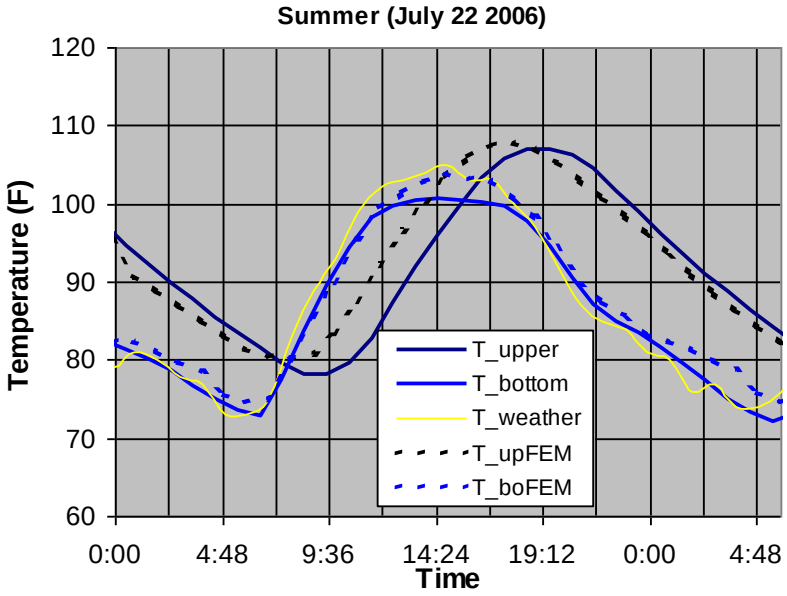

FIGURE 35
Variations of Temperatures on the Panel Surfaces in the Hottest Season

5.2.2 Internal Temperature Distribution

Figure 36 shows the temperature distributions along the cross-section of the bridge panel at dT_{max} for both the hot and cold seasons. As shown in Figure 33 and 34, dT_{max} was about 13 ºF for both cases. The minimum temperatures appeared in the middle of honeycomb core. Both curves in the three segments have similar shapes.

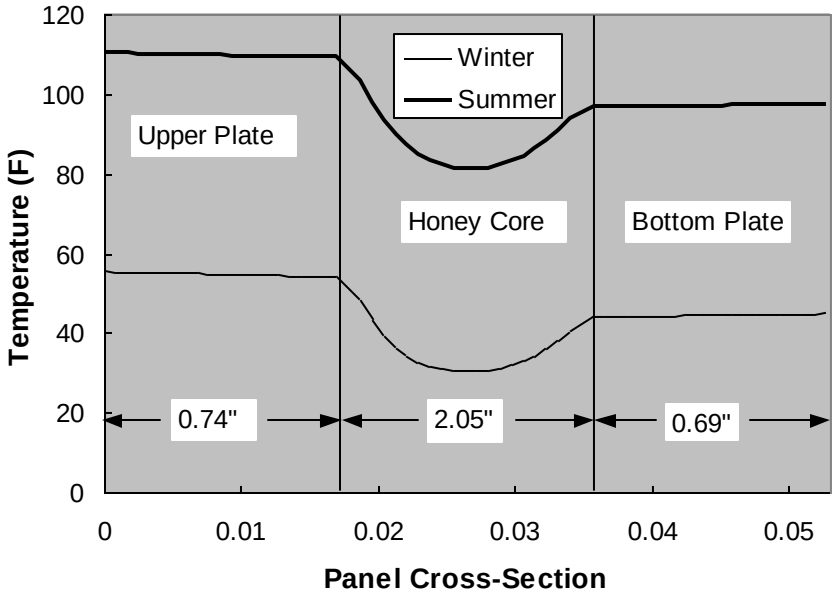

FIGURE 36
Internal Temperature Distributions in the Hot and Cold Seasons

The temperature slope of the two surface plates were slightly steeper in the cold season than in the hot season, which could be due to the difference in the daily solar irradiation and ambient temperature patterns. At the moment of dT_{max}, the temperature gradient was slightly lower in the outer portion of the two surface plates in the hot season than in the cold season, so the average temperature differences between two surface plates were larger in the hot season than in cold season. Therefore, the distributions of thermal load in the panel can form larger deflections in the hot season than in the cold season.

Chapter 6: Conclusions

From the analysis of the experimental and FE methods, the responses of the composite bridge to weather are summarized as follows:

(1) The temperatures of the upper and bottom panel surfaces and their differences dT greatly change with time of day and season. The extreme dT_{max} usually appears in the early afternoon and dT_{min} usually appears in the early morning or in the night. The bottom surface temperature is near the climatic temperature.

(2) The bridge deflections D are approximately proportional to the temperature differences dT; and, D_{max} and D_{min} appear at T_{max} and T_{min}, respectively.

(3) The annual dT_{max} (35 ºF) and D_{max} (6.90 mm) occurred in the hot season. The annual dT_{min} (–21 ºF)and D_{min} (–2.36 mm) happened in the cold season. The average gradient (dD/dT) is about 0.16 mm/ ºF. The bridge has a significant upward deflection on a sunny day during the summer with the maximum often occurring between 3:00-5:00PM. The bridge has a downward deflection during the night with it being the most severe in the winter.

(4) No-Name Creek FRP bridge is designed to support an AASHTO HS-25 load in both lanes. In 2004, the response of the bridge to a truck of 70,340 lb was measured. The middle panel deflection under the truck load was 3.93 mm. Comparing climate induced deflection to traffic load induced deflection, the climate induced deflection is at least on the same order of deflection as allowable traffic load. Therefore, it should be considered in the FRP bridge design process.

(5) Thermal load dT and deflection D usually are larger on clear days than on unclear, rainy, and snowy days. The gradients (dD/dT) slightly vary with the seasons.

(6) 2% probability Gaussian distribution slightly underestimated the annual extreme states occur at a probable rate of 2% at local climatic temperatures and thermal loads for the two panel surfaces and bridge deflections. Maximum $D_{ub2\%}$, is 6.14 mm and $D_{lb2\%}$, is –1.83 mm.

(7) The results of FE simulation generally are in good agreement with the experimental results if the simulation is loaded with the dynamic boundary conditions obtained from the authorized station and manuals. The variations of thermal loads and deflections with respect to

time are mainly caused by the distribution pattern of daily solar intensity, daily solar energy, ambient temperature, and convection coefficient.

(8) The variations of gradients (dD/dT) are caused by small changes in thermal load distribution inside panels. From the FEM analysis, at the moment of dT_{max}, one finds that the temperature gradient in the outer portion of the two surface plates in the hot season is slightly lower than in the cold season, so the differences of the average temperatures between the two surface plates are larger in the hot season than in cold season. Therefore, the distributions of thermal load in the panel can form a larger amount of deflection in the hot season than in the cold season.

References

[1] http://www.ksci.com
[2] http://www.cemr.wvu.edu/~wwwcfc/frp/frpbri.html
[3] http://vt.edu/10021/eng/esm/jlesko/tcb/tcb.html
[4] http://www.bceo.org/technology.html
[5] http://cemr.wvu.edu/~wwwcfc/frp/wickwire.htm
[6] William Marion and Stephen Wilcox, 1995, Solar Radiation Data Manual for Flate-Plate and Concentrating Collectors, National Renewable Energy Laboratory.
[7] Solar Radiation Data Manual, WBAN NO. 13985
[8] Solar Radiation Data Manual for Flat-Plate and Concentrating Collectors, National Renewable Energy Laboratory
[8] Bradshaw, Vaughn, 1993, Building Control Systems, John Wiley & Sons, Inc.
[9] http://cdo.ncdc.noaa.gov/ulcd/ULCD
[10] CenGel, Y. A., 1998, Heat Transfer: A Practical Approch, McGraw-Hill

Appendix I: Measured Bridge Penal Temperatures and Climatic Temperatures

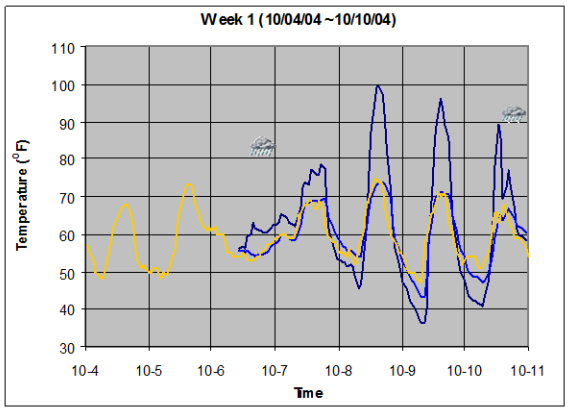

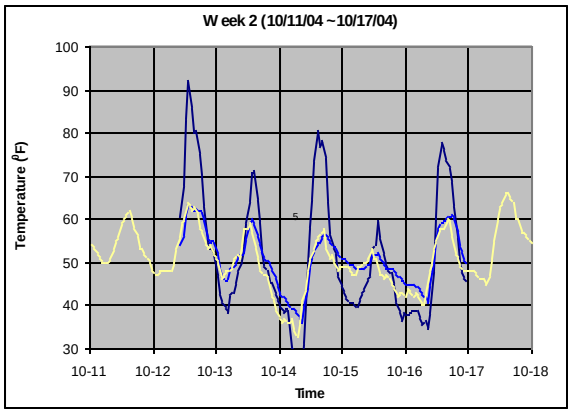

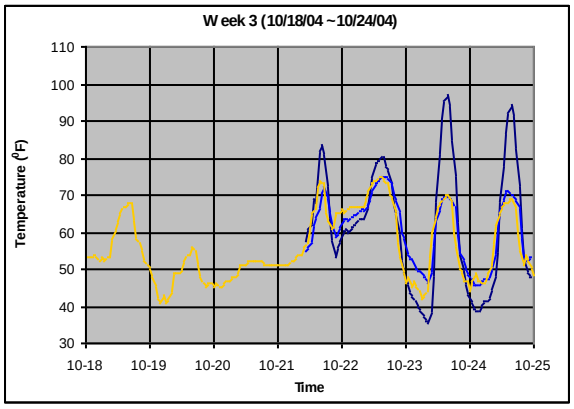

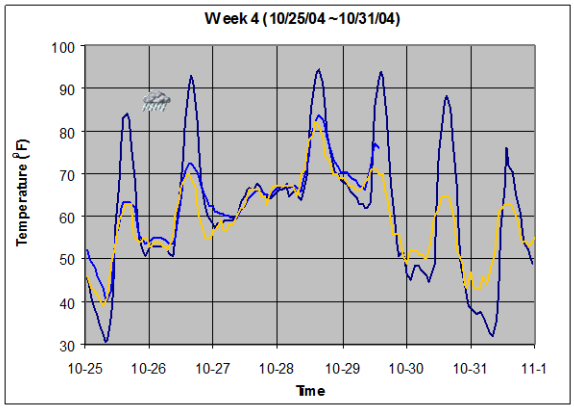

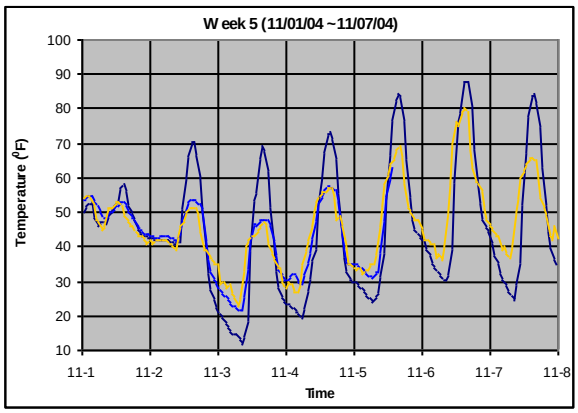

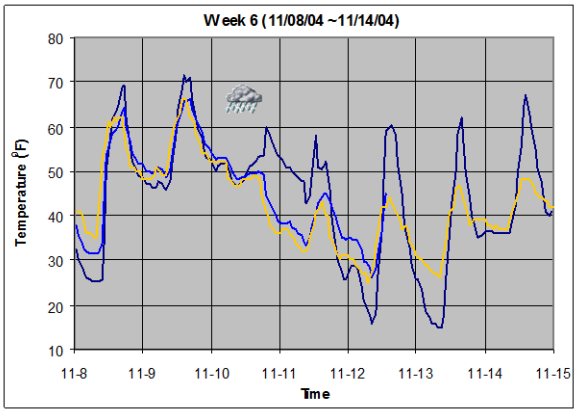

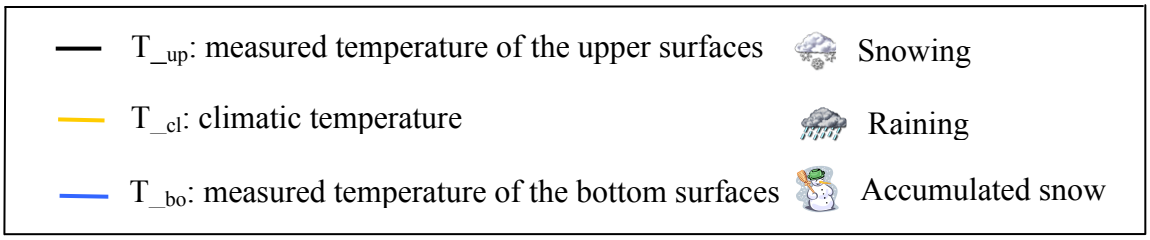

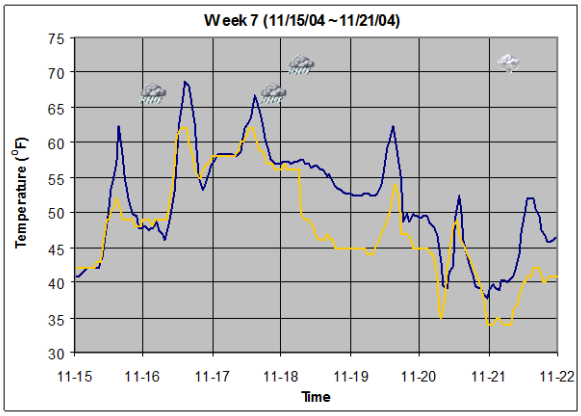
Week 7 (11/15/04 ~11/21/04)
Temperature (°F)
75
70
65
60
55
50
45
40
35
30
11-15
11-16
11-17
11-18
11-19
11-20
11-21
11-22
Time

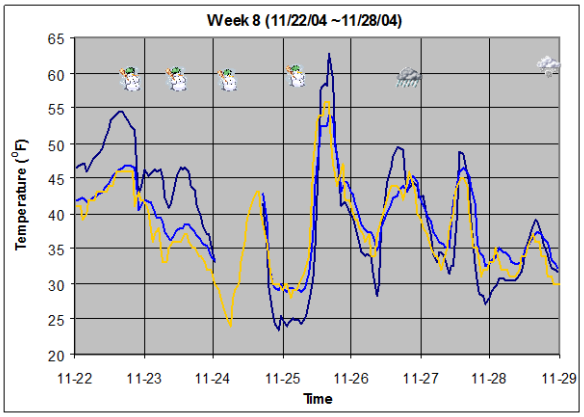
Week 8 (11/22/04 ~11/28/04)
Temperature (°F)
65
60
55
50
45
40
35
30
25
20
11-22
11-23
11-24
11-25
11-26
11-27
11-28
11-29
Time

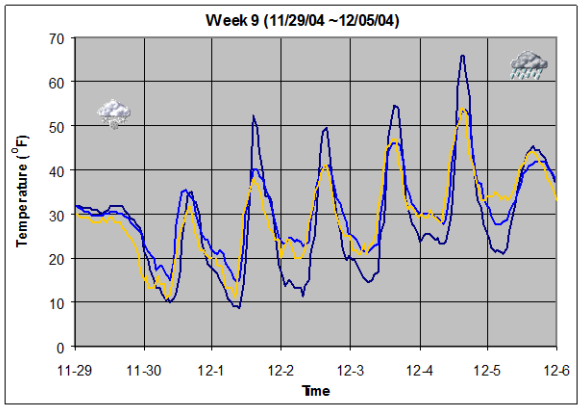
Week 9 (11/29/04 ~12/05/04)
Temperature (°F)
70
60
50
40
30
20
10
0
11-29
11-30
12-1
12-2
12-3
12-4
12-5
12-6
Time

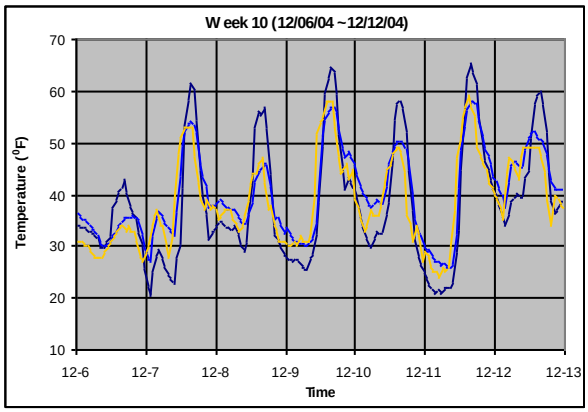
Week 10 (12/06/04 ~12/12/04)
Temperature (°F)
70
60
50
40
30
20
10
12-6
12-7
12-8
12-9
12-10
12-11
12-12
12-13
Time

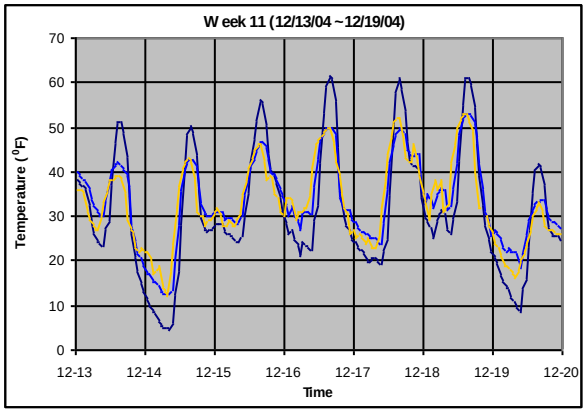
Week 11 (12/13/04 ~12/19/04)
Temperature (°F)
70
60
50
40
30
20
10
0
12-13
12-14
12-15
12-16
12-17
12-18
12-19
12-20
Time

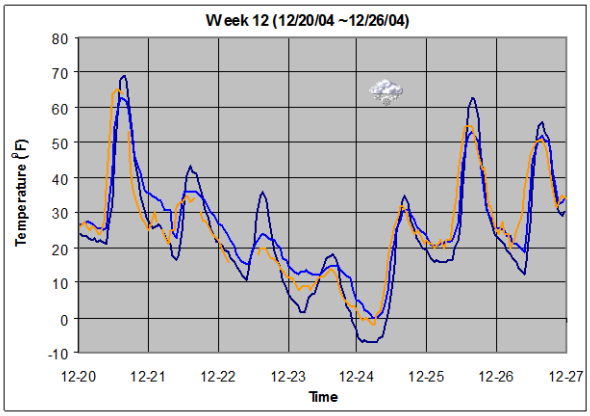
Week 12 (12/20/04 ~12/26/04)
Temperature (°F)
80
70
60
50
40
30
20
10
0
-10
12-20
12-21
12-22
12-23
12-24
12-25
12-26
12-27
Time

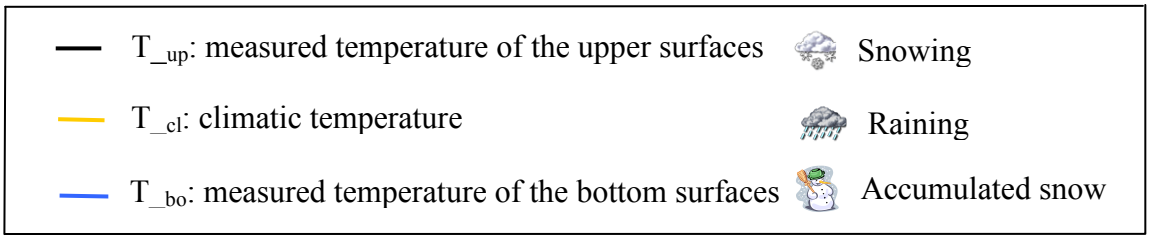
T_up: measured temperature of the upper surfaces
T_cl: climatic temperature
T_bo: measured temperature of the bottom surfaces
Snowing
Raining
Accumulated snow

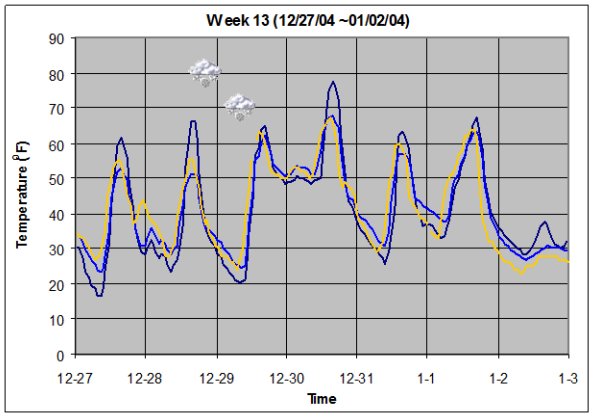
Week 13 (12/27/04 ~01/02/04)
Temperature (°F)
90
80
70
60
50
40
30
20
10
0
12-27
12-28
12-29
12-30
12-31
1-1
1-2
1-3
Time

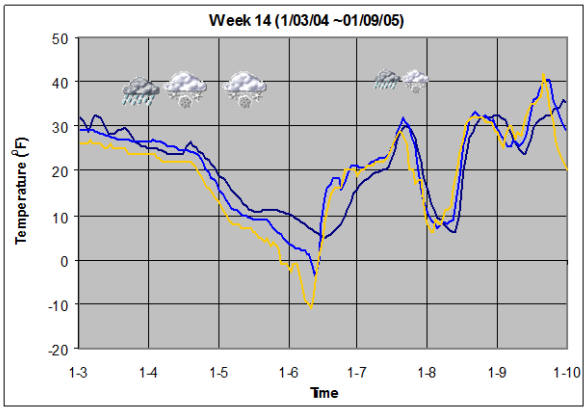
Week 14 (1/03/04 ~01/09/05)
Temperature (°F)
50
40
30
20
10
0
-10
-20
1-3
1-4
1-5
1-6
1-7
1-8
1-9
1-10
Time

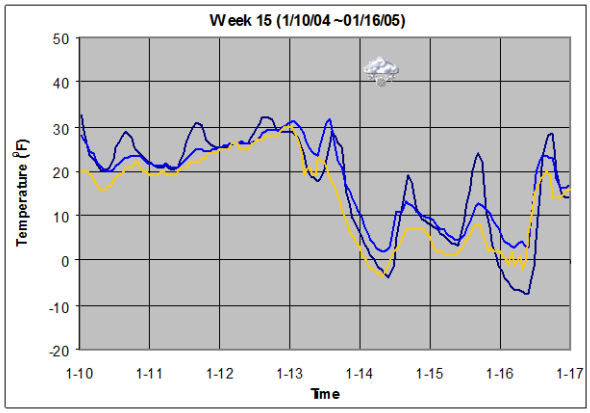
Week 15 (1/10/04 ~01/16/05)
Temperature (°F)
50
40
30
20
10
0
-10
-20
1-10
1-11
1-12
1-13
1-14
1-15
1-16
1-17
Time

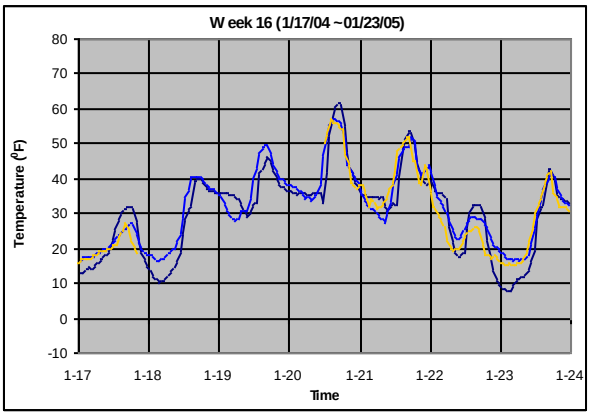
Week 16 (1/17/04 ~01/23/05)
Temperature (°F)
80
70
60
50
40
30
20
10
0
-10
1-17
1-18
1-19
1-20
1-21
1-22
1-23
1-24
Time

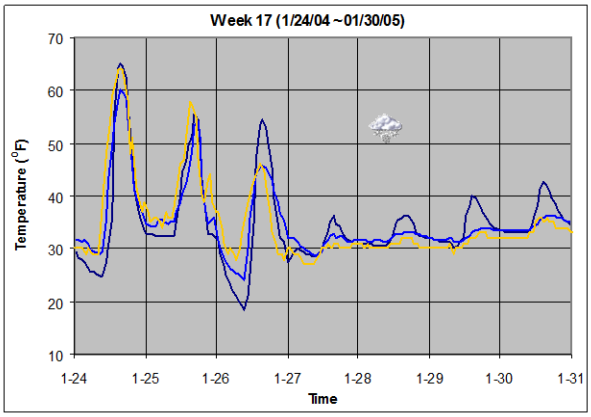
Week 17 (1/24/04 ~01/30/05)
Temperature (°F)
70
60
50
40
30
20
10
1-24
1-25
1-26
1-27
1-28
1-29
1-30
1-31
Time

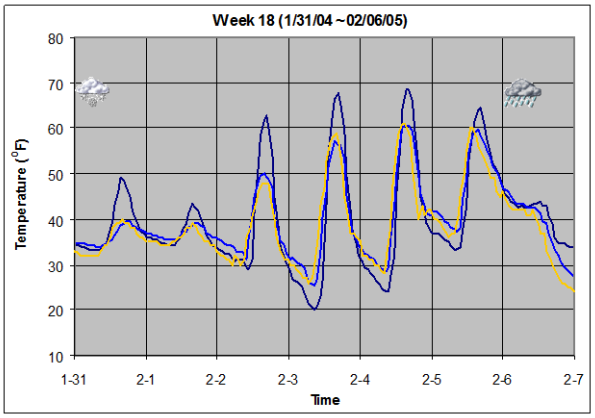
Week 18 (1/31/04 ~02/06/05)
Temperature (°F)
80
70
60
50
40
30
20
10
1-31
2-1
2-2
2-3
2-4
2-5
2-6
2-7
Time

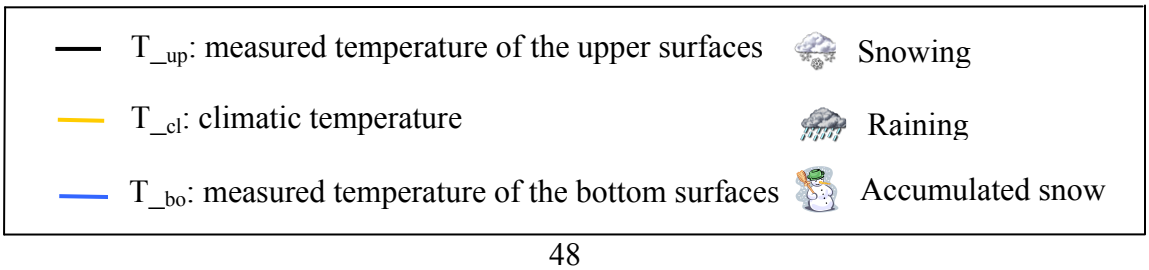
T_up: measured temperature of the upper surfaces
T_cl: climatic temperature
T_bo: measured temperature of the bottom surfaces
Snowing
Raining
Accumulated snow

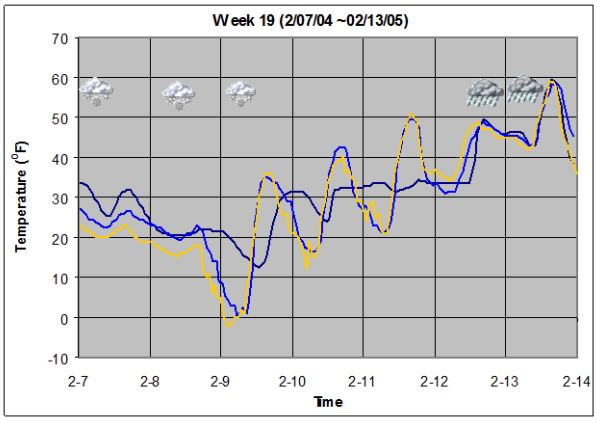
Week 19 (2/07/04 ~02/13/05)
Temperature (°F)
70
60
50
40
30
20
10
0
-10
2-7
2-8
2-9
2-10
2-11
2-12
2-13
2-14
Time

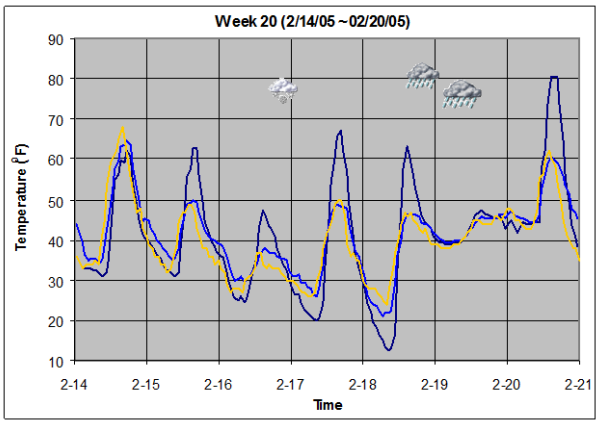
Week 20 (2/14/05 ~02/20/05)
Temperature (°F)
90
80
70
60
50
40
30
20
10
2-14
2-15
2-16
2-17
2-18
2-19
2-20
2-21
Time

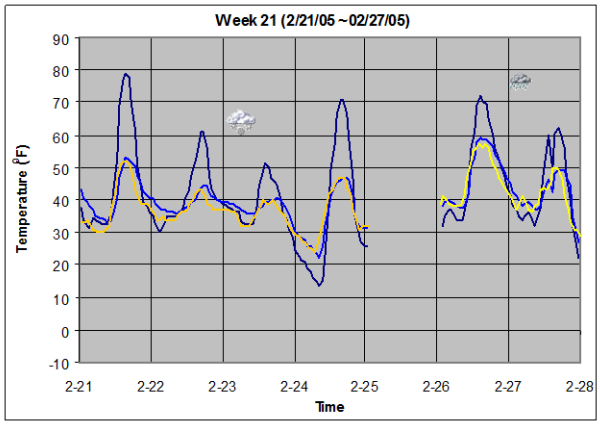
Week 21 (2/21/05 ~02/27/05)
Temperature (°F)
90
80
70
60
50
40
30
20
10
0
-10
2-21
2-22
2-23
2-24
2-25
2-26
2-27
2-28
Time

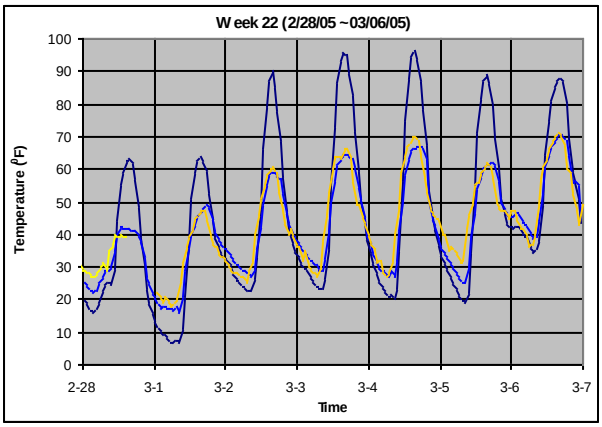
Week 22 (2/28/05 ~03/06/05)
Temperature (°F)
100
90
80
70
60
50
40
30
20
10
0
2-28
3-1
3-2
3-3
3-4
3-5
3-6
3-7
Time

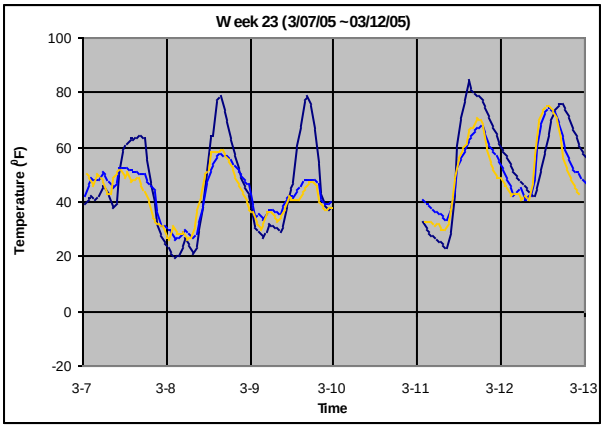
Week 23 (3/07/05 ~03/12/05)
Temperature (°F)
100
80
60
40
20
0
-20
3-7
3-8
3-9
3-10
3-11
3-12
3-13
Time

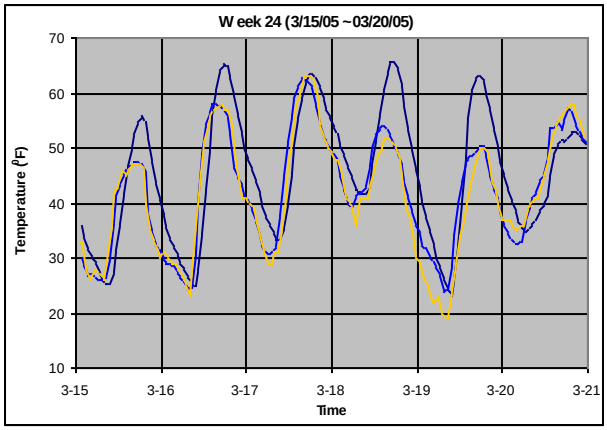
Week 24 (3/15/05 ~03/20/05)
Temperature (°F)
70
60
50
40
30
20
10
3-15
3-16
3-17
3-18
3-19
3-20
3-21
Time

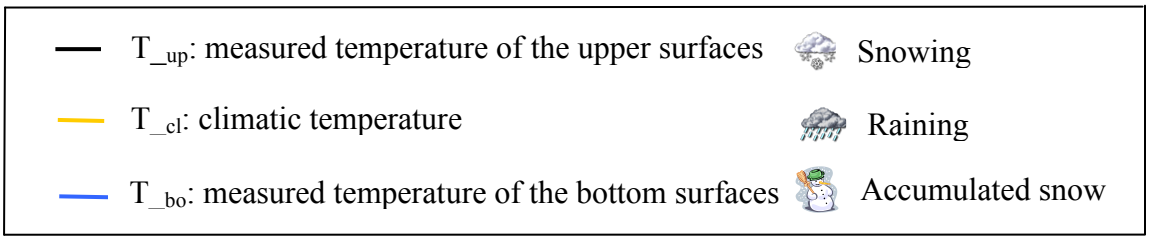
T_up: measured temperature of the upper surfaces
T_cl: climatic temperature
T_bo: measured temperature of the bottom surfaces
Snowing
Raining
Accumulated snow

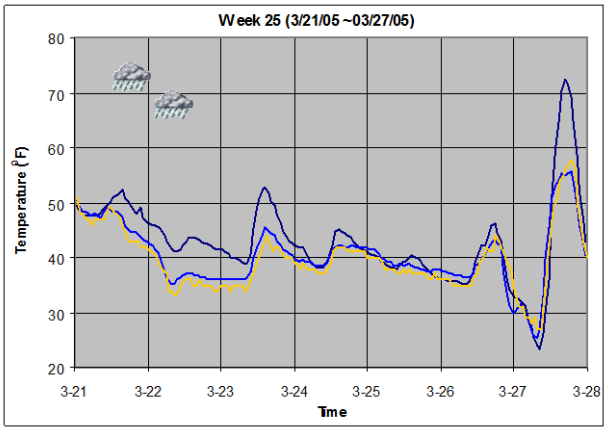

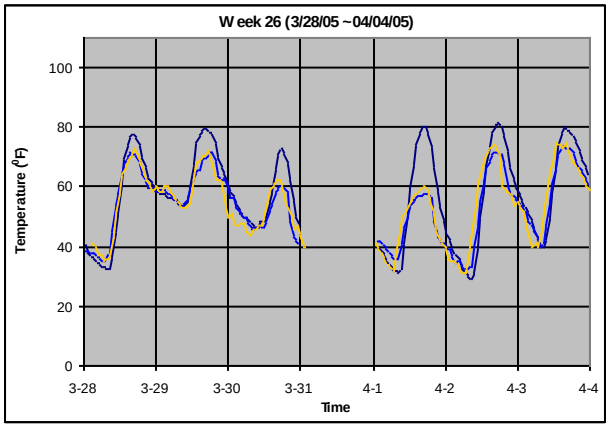

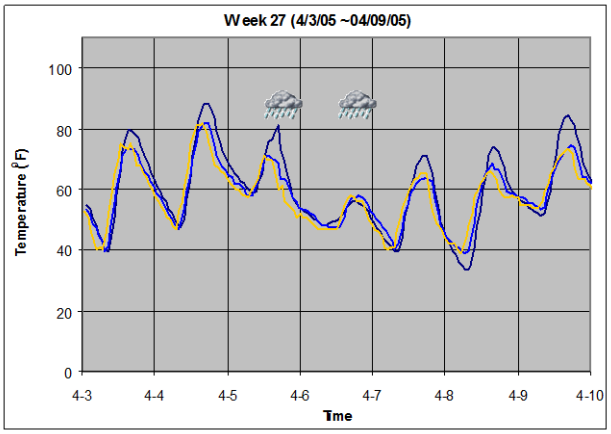

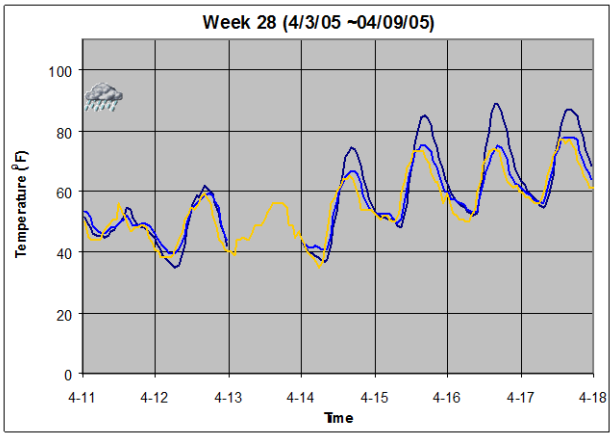

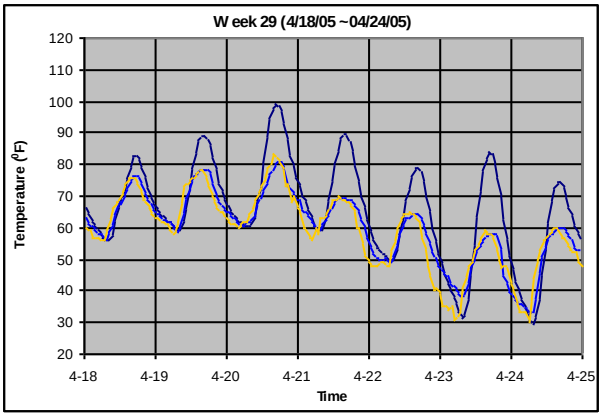

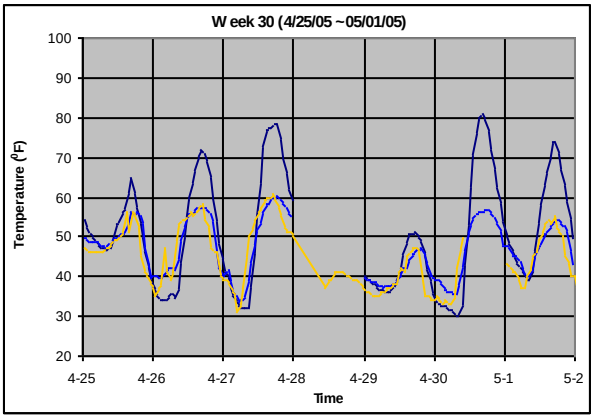

T_up: measured temperature of the upper surfaces

T_cl: climatic temperature

T bo: measured temperature of the bottom surfaces

Snowing

Raining

Accumulated snow

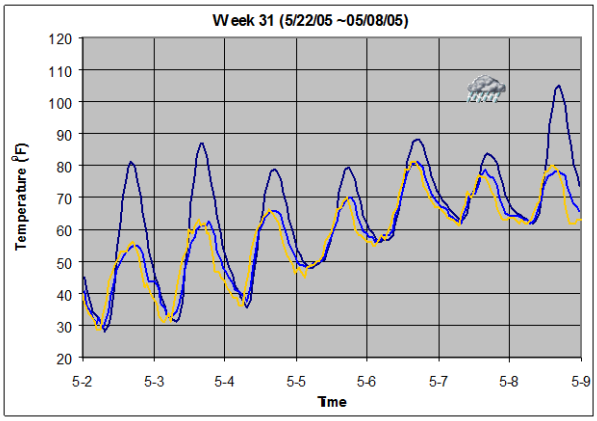
Week 31 (5/22/05 ~05/08/05)
Temperature (°F)
120
110
100
90
80
70
60
50
40
30
20
5-2
5-3
5-4
5-5
5-6
5-7
5-8
5-9
Time

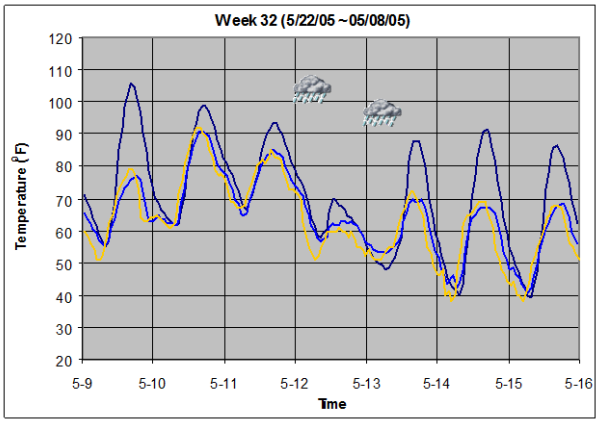
Week 32 (5/22/05 ~05/08/05)
Temperature (°F)
120
110
100
90
80
70
60
50
40
30
20
5-9
5-10
5-11
5-12
5-13
5-14
5-15
5-16
Time

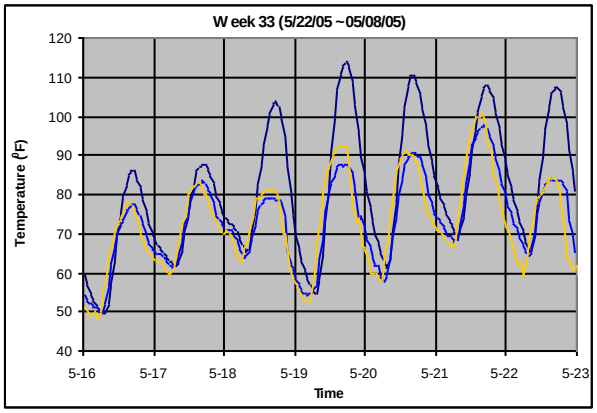
Week 33 (5/22/05 ~05/08/05)
Temperature (°F)
120
110
100
90
80
70
60
50
40
5-16
5-17
5-18
5-19
5-20
5-21
5-22
5-23
Time

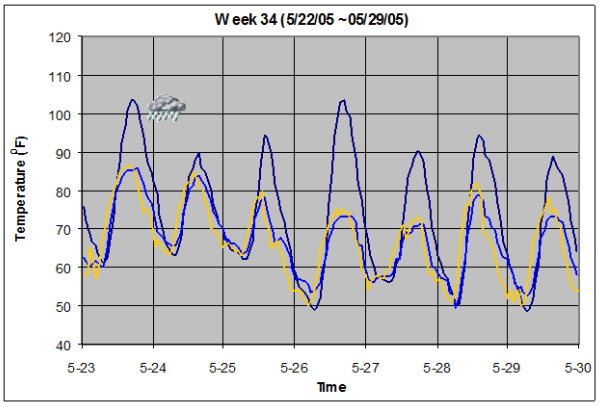
Week 34 (5/22/05 ~05/29/05)
Temperature (°F)
120
110
100
90
80
70
60
50
40
5-23
5-24
5-25
5-26
5-27
5-28
5-29
5-30
Time

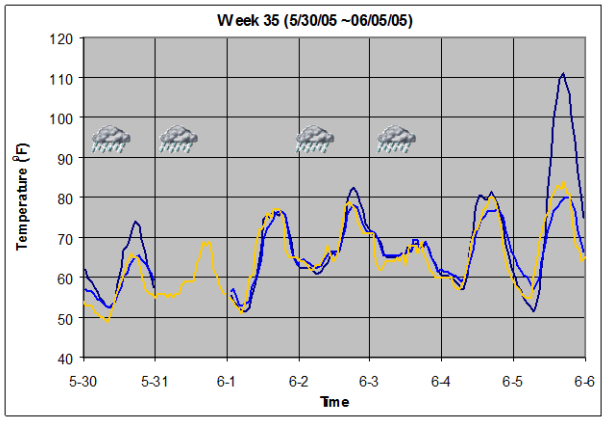
Week 35 (5/30/05 ~06/05/05)
Temperature (°F)
120
110
100
90
80
70
60
50
40
5-30
5-31
6-1
6-2
6-3
6-4
6-5
6-6
Time

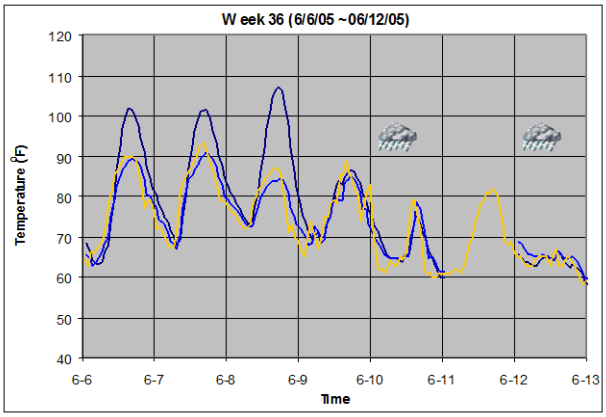
Week 36 (6/6/05 ~06/12/05)
Temperature (°F)
120
110
100
90
80
70
60
50
40
6-6
6-7
6-8
6-9
6-10
6-11
6-12
6-13
Time

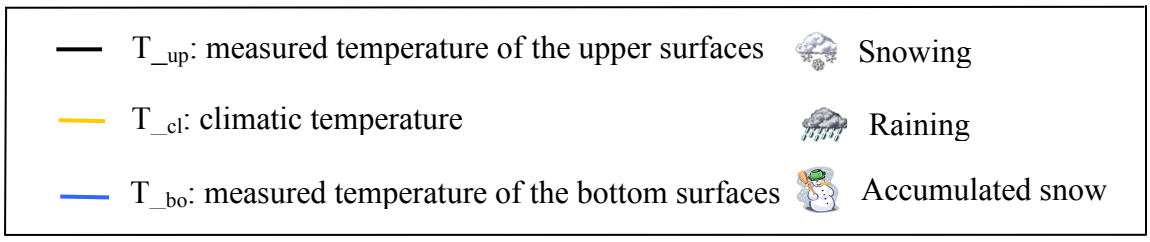
T_up: measured temperature of the upper surfaces
T_cl: climatic temperature
T_bo: measured temperature of the bottom surfaces
Snowing
Raining
Accumulated snow

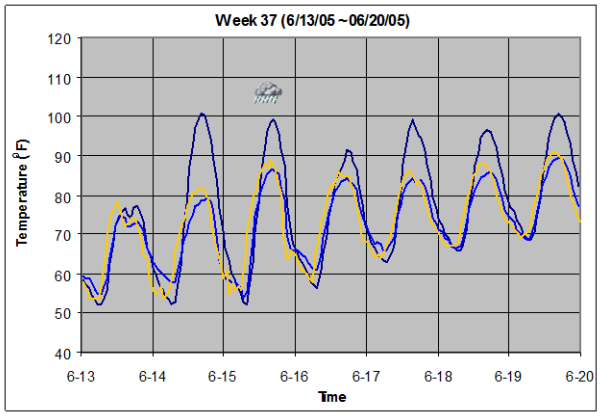
Week 37 (6/13/05 ~06/20/05)
Temperature (°F)
120
110
100
90
80
70
60
50
40
6-13
6-14
6-15
6-16
6-17
6-18
6-19
6-20
Time

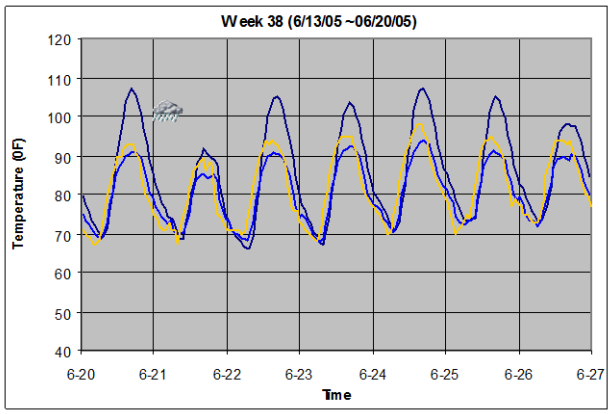
Week 38 (6/13/05 ~06/20/05)
Temperature (0F)
120
110
100
90
80
70
60
50
40
6-20
6-21
6-22
6-23
6-24
6-25
6-26
6-27
Time

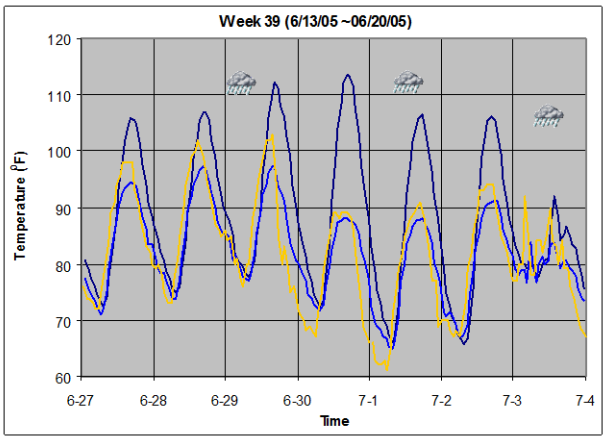
Week 39 (6/13/05 ~06/20/05)
Temperature (°F)
120
110
100
90
80
70
60
6-27
6-28
6-29
6-30
7-1
7-2
7-3
7-4
Time

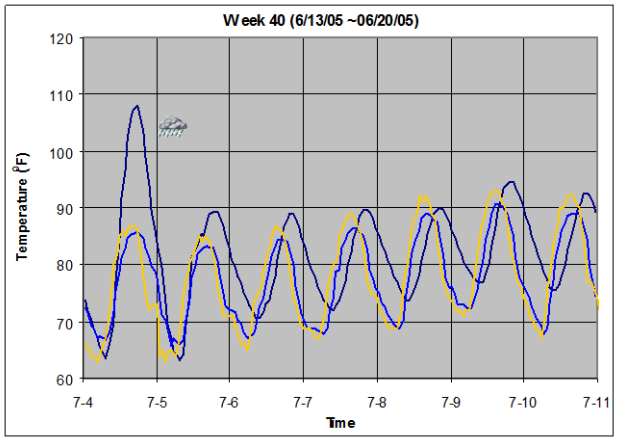
Week 40 (6/13/05 ~06/20/05)
Temperature (°F)
120
110
100
90
80
70
60
7-4
7-5
7-6
7-7
7-8
7-9
7-10
7-11
Time

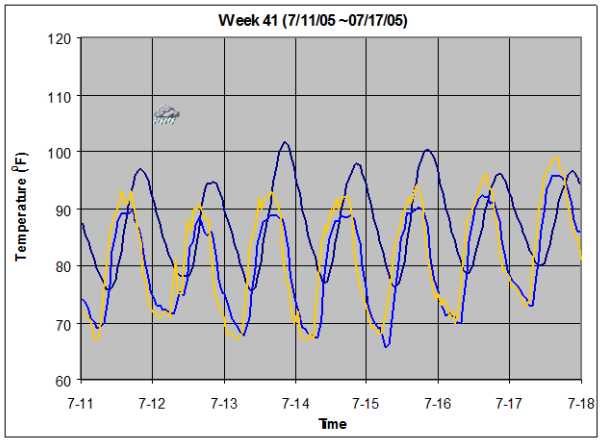
Week 41 (7/11/05 ~07/17/05)
Temperature (°F)
120
110
100
90
80
70
60
7-11
7-12
7-13
7-14
7-15
7-16
7-17
7-18
Time

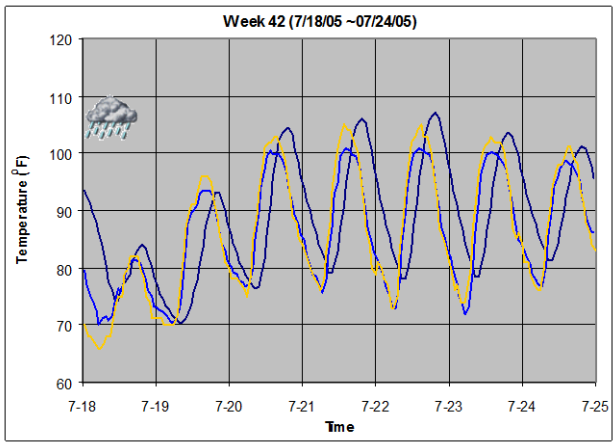
Week 42 (7/18/05 ~07/24/05)
Temperature (°F)
120
110
100
90
80
70
60
7-18
7-19
7-20
7-21
7-22
7-23
7-24
7-25
Time

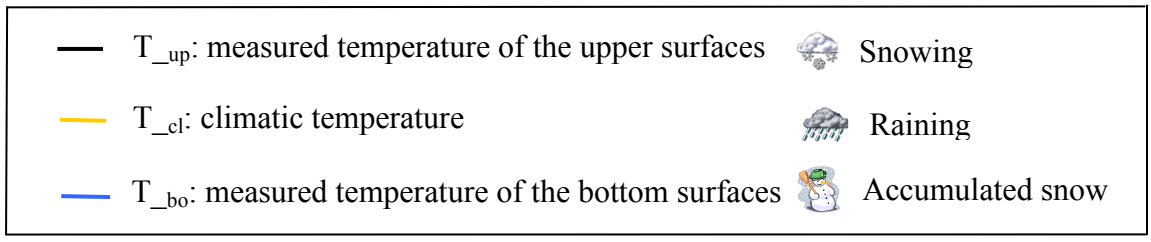
T_up: measured temperature of the upper surfaces
T_cl: climatic temperature
T_bo: measured temperature of the bottom surfaces
Snowing
Raining
Accumulated snow

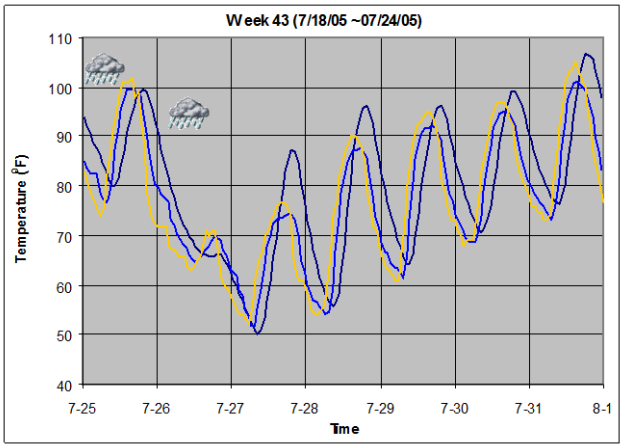
Week 43 (7/18/05 ~07/24/05)
Temperature (°F)
110
100
90
80
70
60
50
40
7-25
7-26
7-27
7-28
7-29
7-30
7-31
8-1
Time

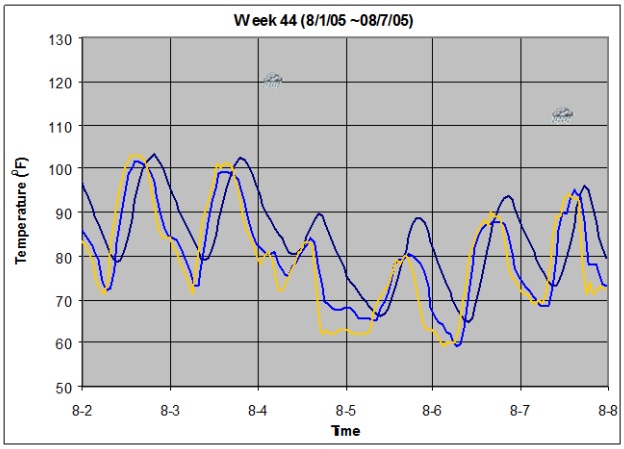
Week 44 (8/1/05 ~08/7/05)
Temperature (°F)
130
120
110
100
90
80
70
60
50
8-2
8-3
8-4
8-5
8-6
8-7
8-8
Time

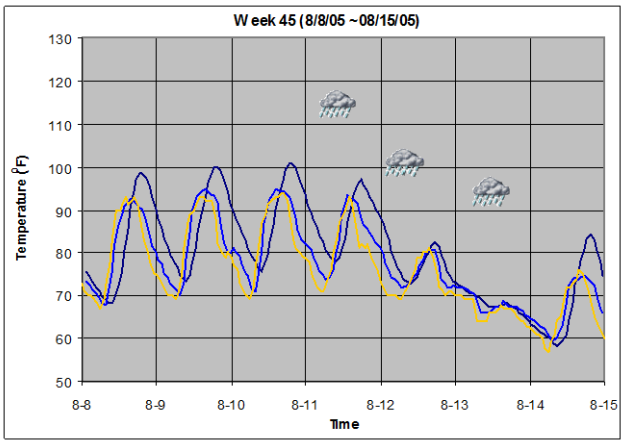
Week 45 (8/8/05 ~08/15/05)
Temperature (°F)
130
120
110
100
90
80
70
60
50
8-8
8-9
8-10
8-11
8-12
8-13
8-14
8-15
Time

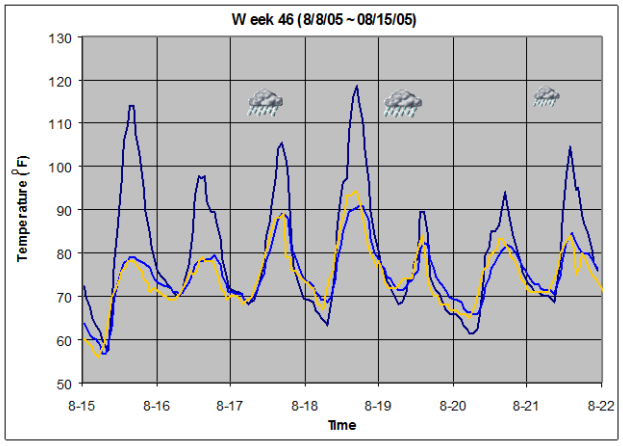
Week 46 (8/8/05 ~08/15/05)
Temperature (°F)
130
120
110
100
90
80
70
60
50
8-15
8-16
8-17
8-18
8-19
8-20
8-21
8-22
Time

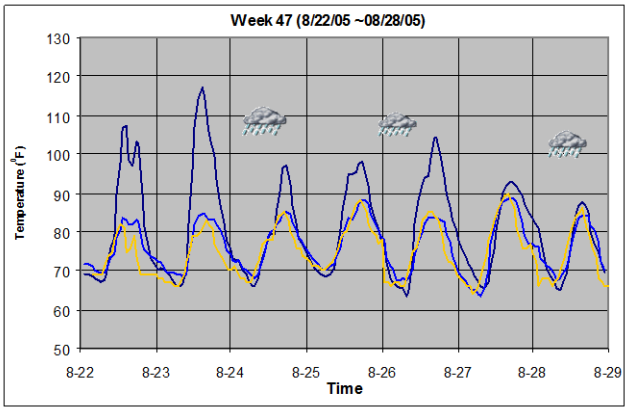
Week 47 (8/22/05 ~08/28/05)
Temperature (°F)
130
120
110
100
90
80
70
60
50
8-22
8-23
8-24
8-25
8-26
8-27
8-28
8-29
Time

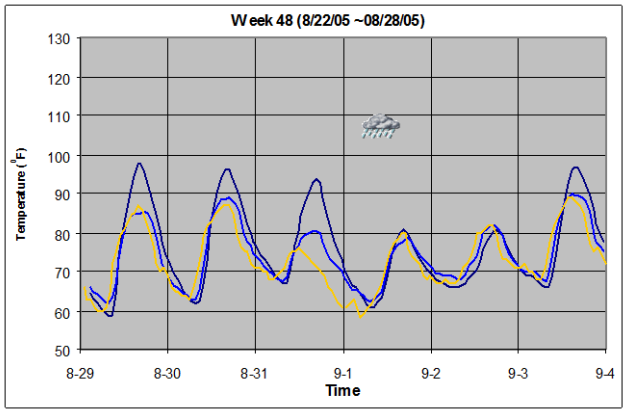
Week 48 (8/22/05 ~08/28/05)
Temperature (°F)
130
120
110
100
90
80
70
60
50
8-29
8-30
8-31
9-1
9-2
9-3
9-4
Time

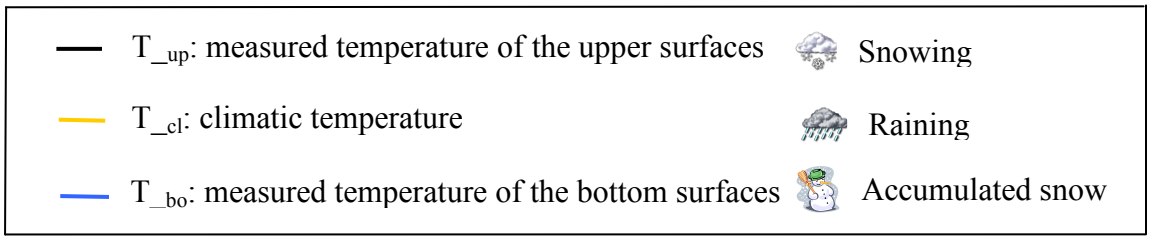
T_up: measured temperature of the upper surfaces
T_cl: climatic temperature
T_bo: measured temperature of the bottom surfaces
Snowing
Raining
Accumulated snow

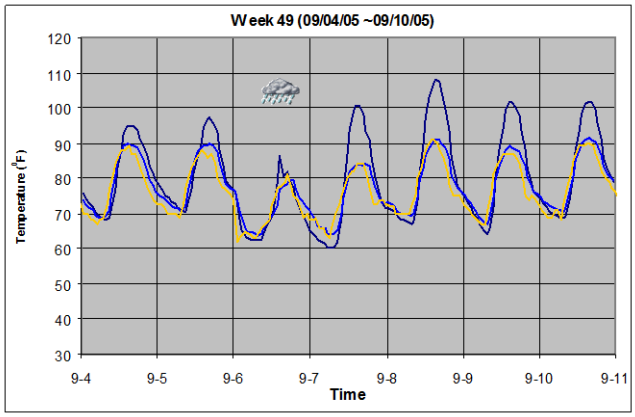
Week 49 (09/04/05 ~09/10/05)
Temperature (°F)
120
110
100
90
80
70
60
50
40
30
9-4
9-5
9-6
9-7
9-8
9-9
9-10
9-11
Time

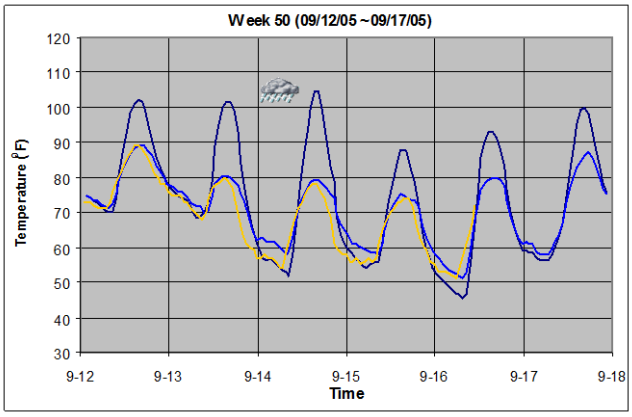
Week 50 (09/12/05 ~09/17/05)
Temperature (°F)
120
110
100
90
80
70
60
50
40
30
9-12
9-13
9-14
9-15
9-16
9-17
9-18
Time

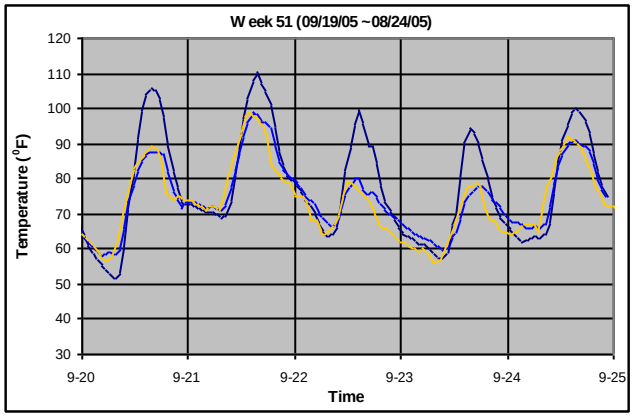
Week 51 (09/19/05 ~08/24/05)
Temperature (°F)
120
110
100
90
80
70
60
50
40
30
9-20
9-21
9-22
9-23
9-24
9-25
Time

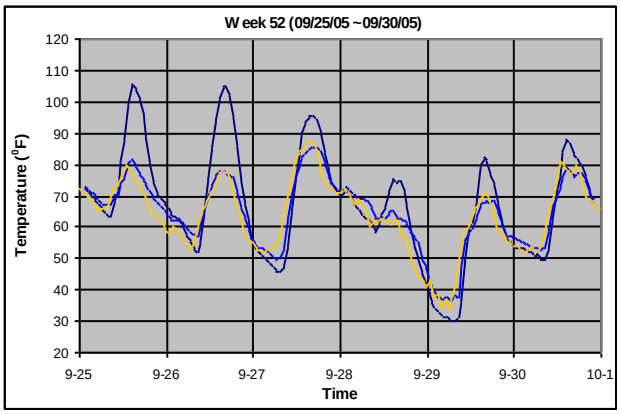
Week 52 (09/25/05 ~09/30/05)
Temperature (°F)
120
110
100
90
80
70
60
50
40
30
20
9-25
9-26
9-27
9-28
9-29
9-30
10-1
Time

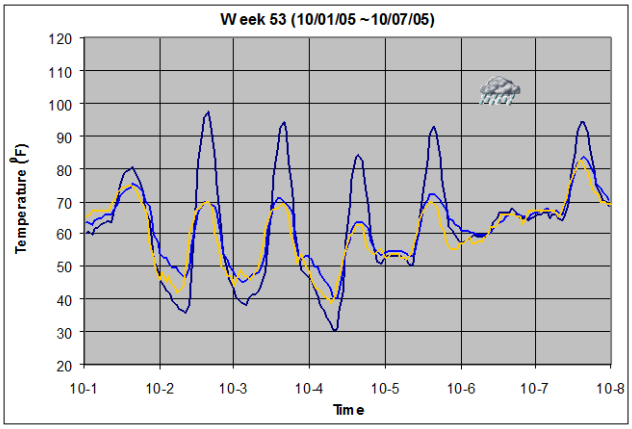
Week 53 (10/01/05 ~10/07/05)
Temperature (°F)
120
110
100
90
80
70
60
50
40
30
20
10-1
10-2
10-3
10-4
10-5
10-6
10-7
10-8
Time

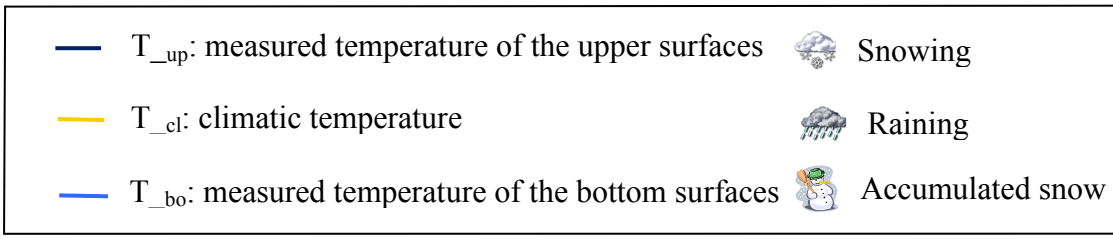
T_up: measured temperature of the upper surfaces
T_cl: climatic temperature
T_bo: measured temperature of the bottom surfaces
Snowing
Raining
Accumulated snow

Appendix II: Temperature Load and Deflections

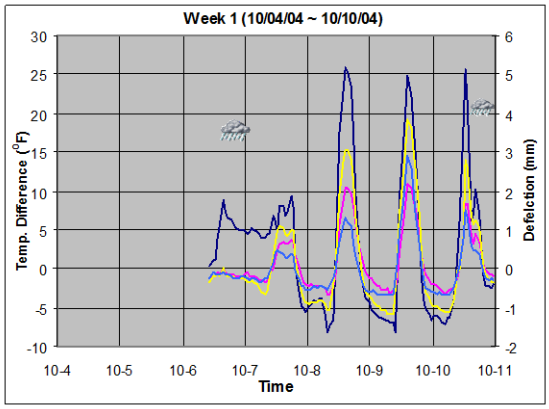

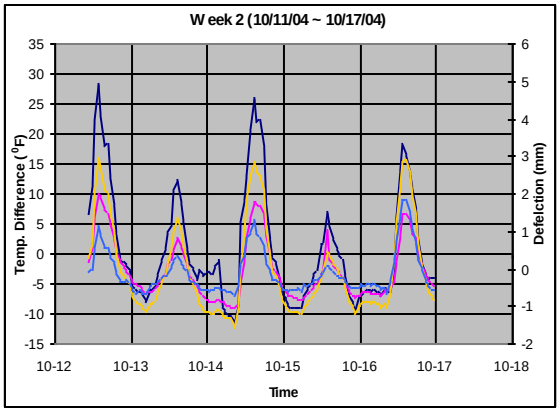

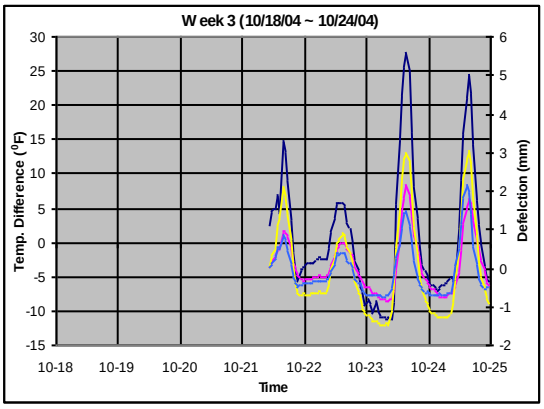

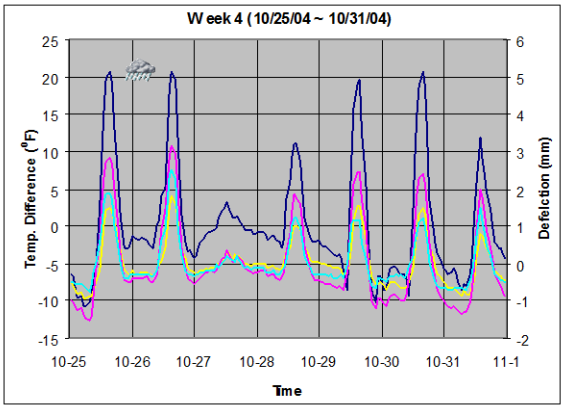

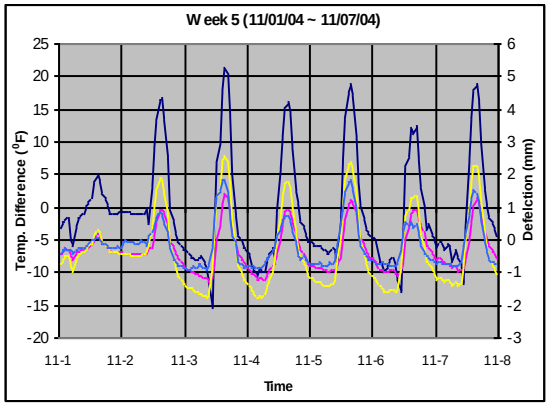

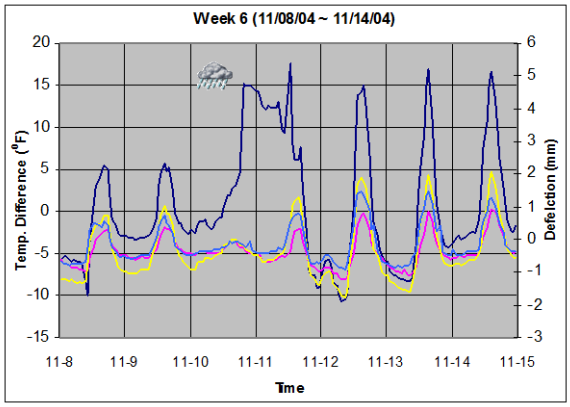

dT: temperature difference between the upper and bottom surfaces

D_{center}: deflection of the center panel

D_{south}: deflection of the south panel

D_{north}: deflection of the north panel

Snowing

Raining

Accumulated snow

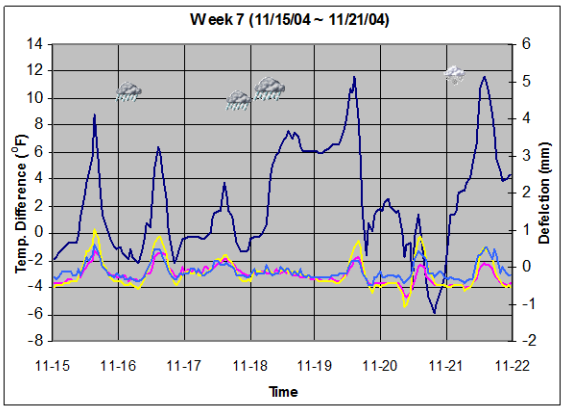

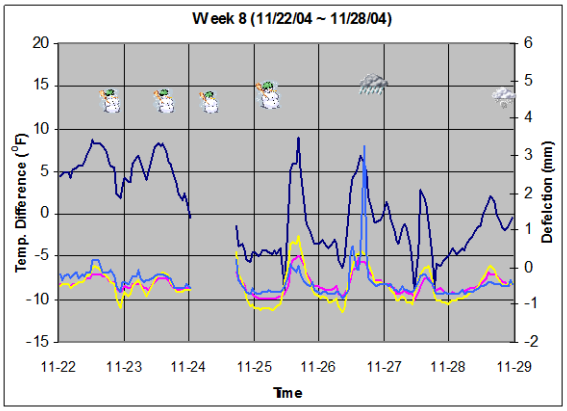

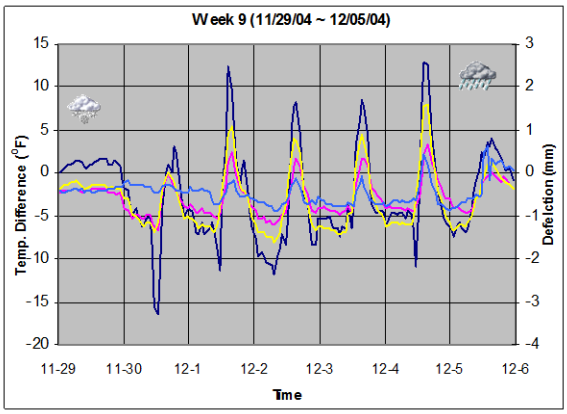

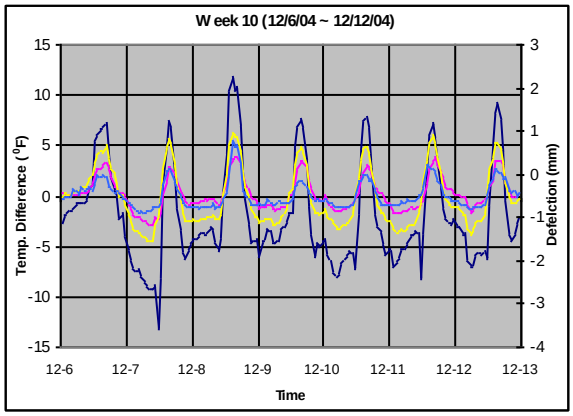

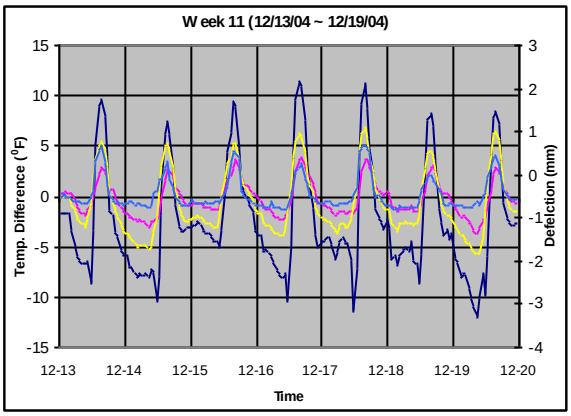

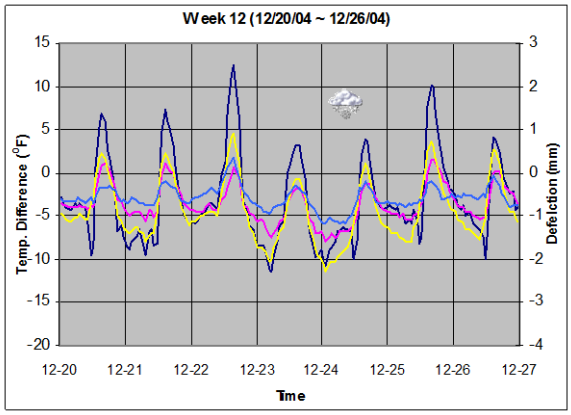

dT: temperature difference between the upper and bottom surfaces

$D_{\_center}$: deflection of the center panel

$D_{\_south}$: deflection of the south panel

$D_{\_north}$: deflection of the north panel

Snowing

Raining

Accumulated sonw

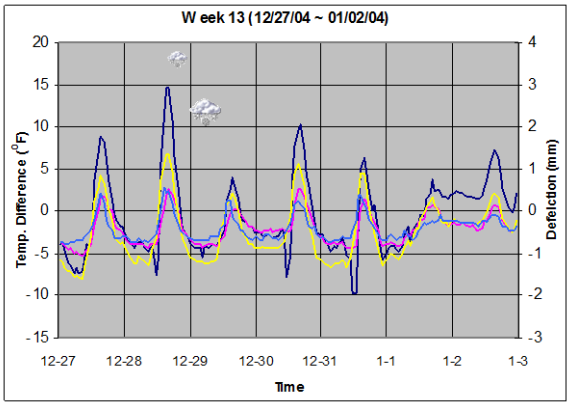
W eek 13 (12/27/04 ~ 01/02/04)
Temp. Difference (°F)
Defelction (mm)
Time
12-27
12-28
12-29
12-30
12-31
1-1
1-2
1-3

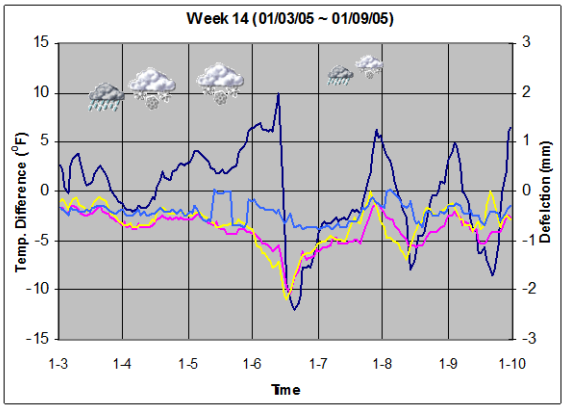
Week 14 (01/03/05 ~ 01/09/05)
Temp. Difference (°F)
Defelction (mm)
Time
1-3
1-4
1-5
1-6
1-7
1-8
1-9
1-10

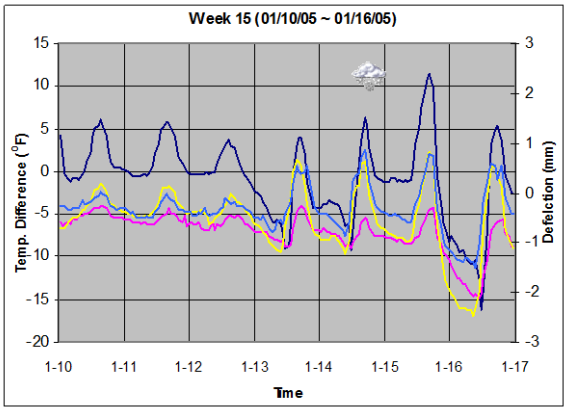
Week 15 (01/10/05 ~ 01/16/05)
Temp. Difference (°F)
Defelction (mm)
Time
1-10
1-11
1-12
1-13
1-14
1-15
1-16
1-17

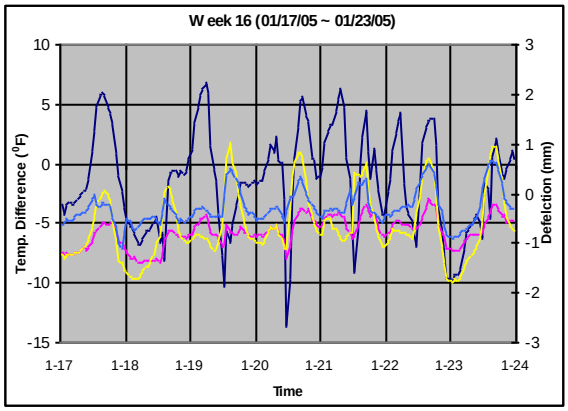
W eek 16 (01/17/05 ~ 01/23/05)
Temp. Difference (°F)
Defelction (mm)
Time
1-17
1-18
1-19
1-20
1-21
1-22
1-23
1-24

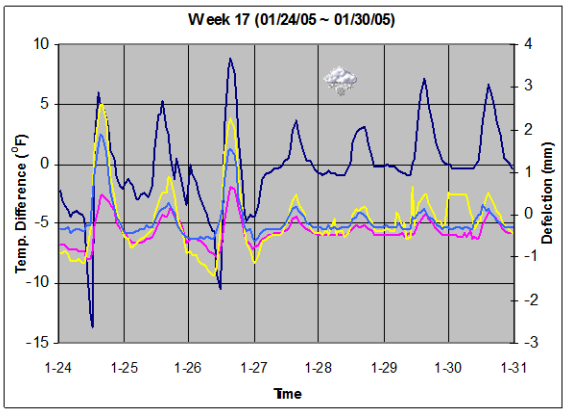
Week 17 (01/24/05 ~ 01/30/05)
Temp. Difference (°F)
Defelction (mm)
Time
1-24
1-25
1-26
1-27
1-28
1-29
1-30
1-31

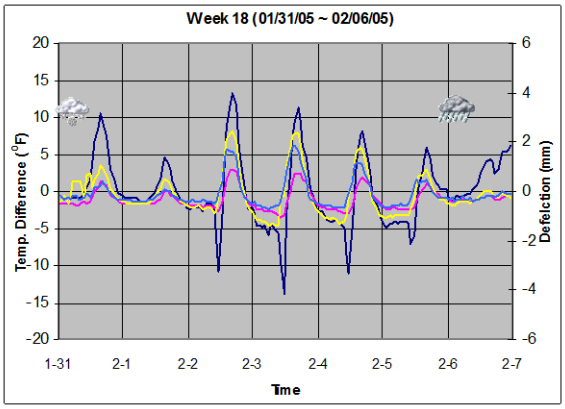
Week 18 (01/31/05 ~ 02/06/05)
Temp. Difference (°F)
Defelction (mm)
Time
1-31
2-1
2-2
2-3
2-4
2-5
2-6
2-7

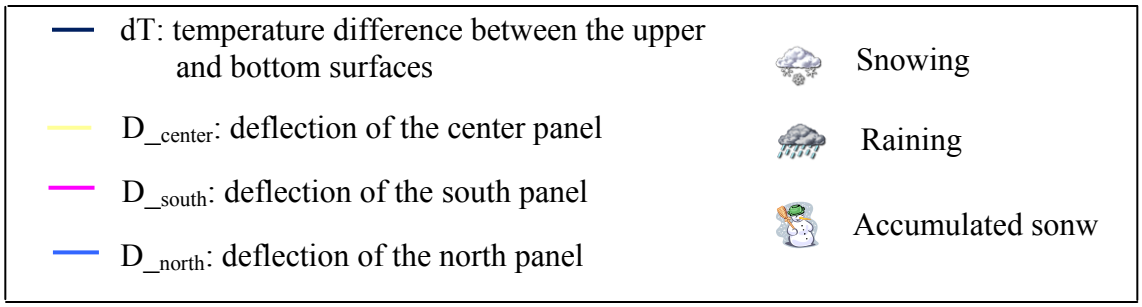
dT: temperature difference between the upper and bottom surfaces
D_center: deflection of the center panel
D_south: deflection of the south panel
D_north: deflection of the north panel
Snowing
Raining
Accumulated sonw

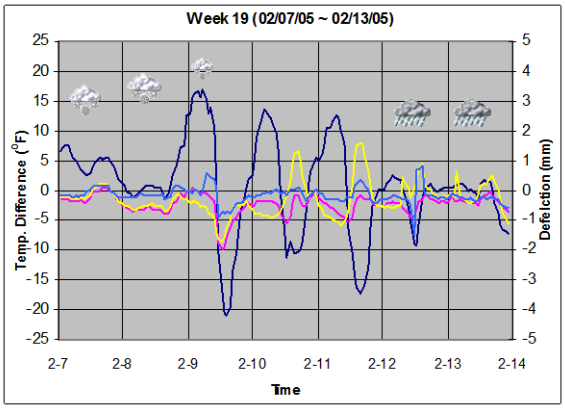

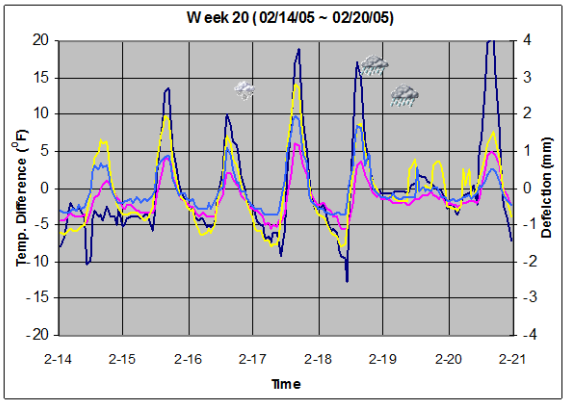

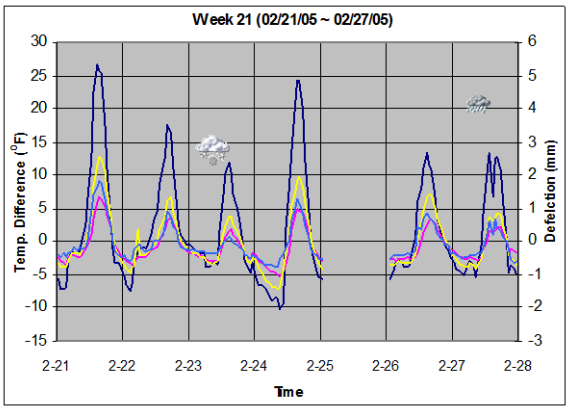

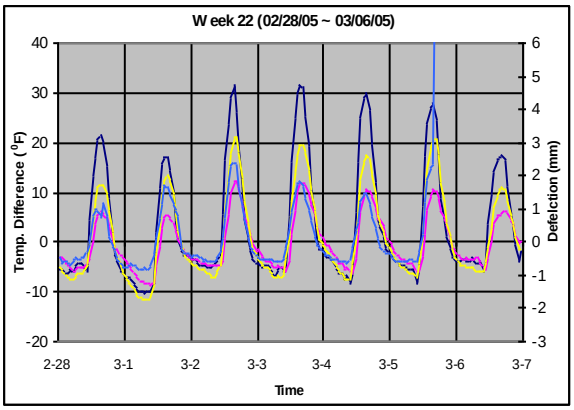

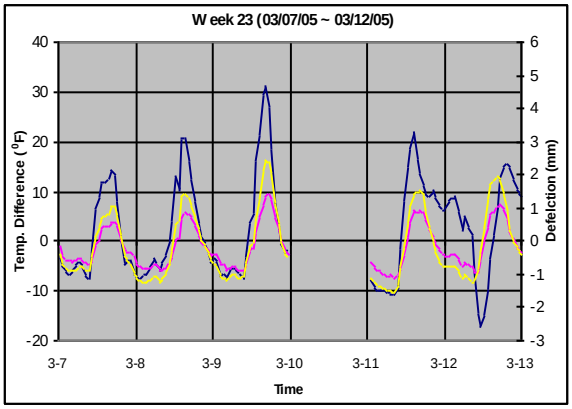

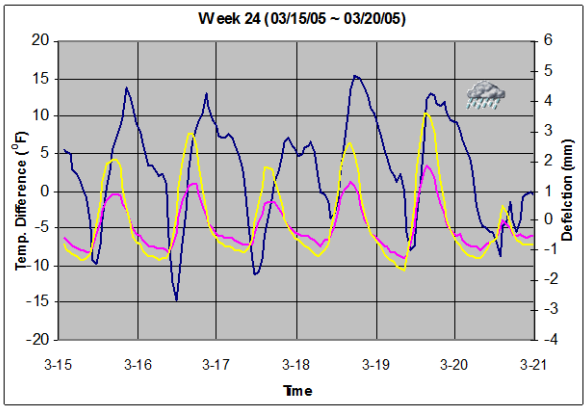

dT: temperature difference between the upper and bottom surfaces

$D_{\_center}$: deflection of the center panel

$D_{\_south}$: deflection of the south panel

$D_{\_north}$: deflection of the north panel

Snowing

Raining

Accumulated sonw

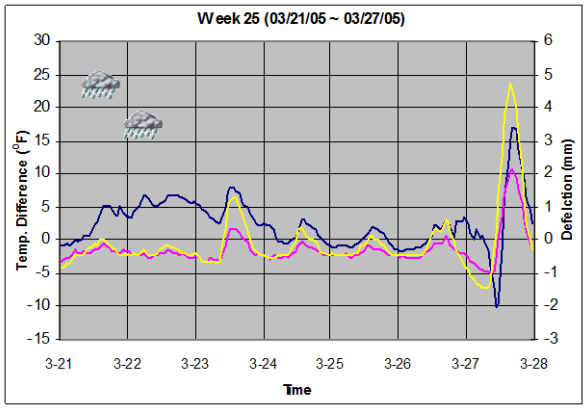

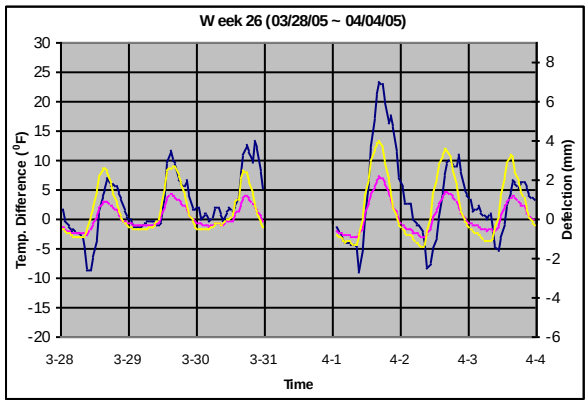

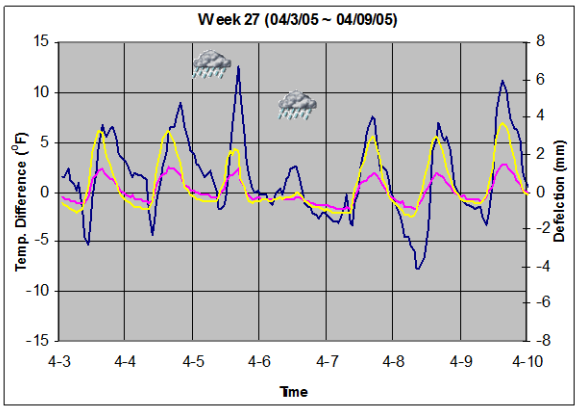

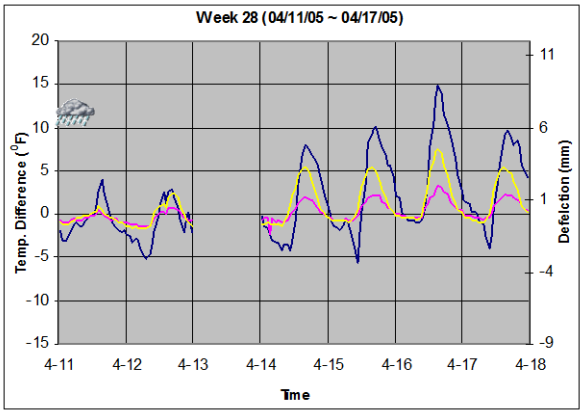

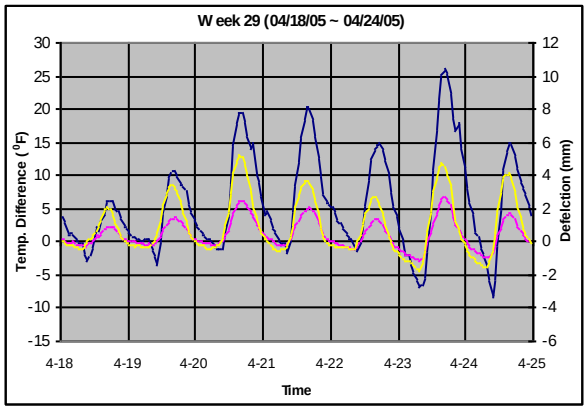

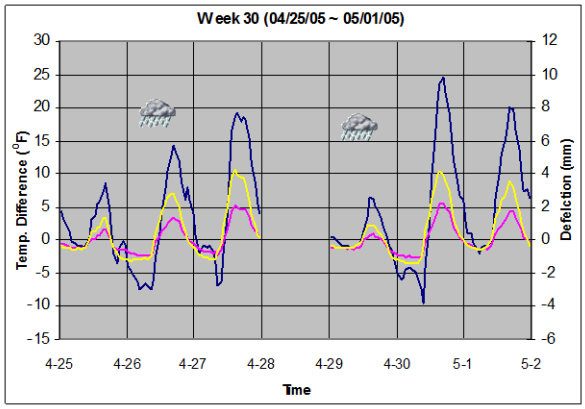

dT: temperature difference between the upper and bottom surfaces

$D_{\_center}$: deflection of the center panel

$D_{\_south}$: deflection of the south panel

$D_{\_north}$: deflection of the north panel

Snowing

Raining

Accumulated sonw

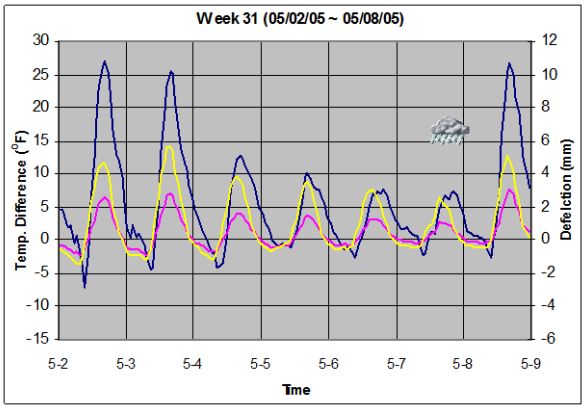
Week 31 (05/02/05 ~ 05/08/05)
Temp. Difference (°F)
Defelction (mm)
Time
5-2
5-3
5-4
5-5
5-6
5-7
5-8
5-9

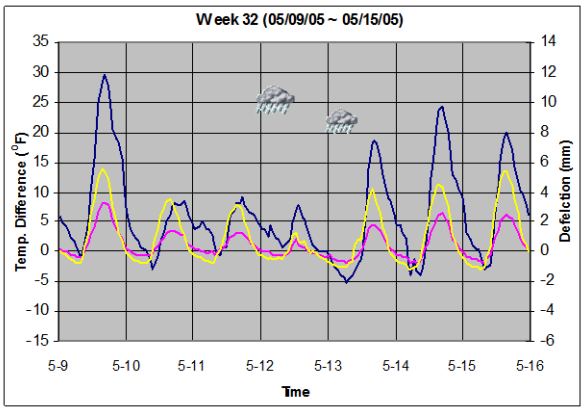
Week 32 (05/09/05 ~ 05/15/05)
Temp. Difference (°F)
Defelction (mm)
Time
5-9
5-10
5-11
5-12
5-13
5-14
5-15
5-16

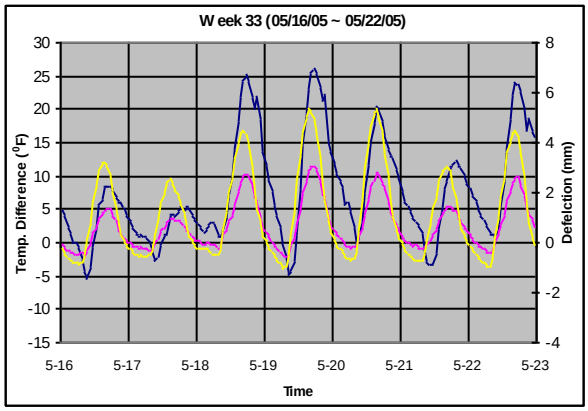
Week 33 (05/16/05 ~ 05/22/05)
Temp. Difference (°F)
Defelction (mm)
Time
5-16
5-17
5-18
5-19
5-20
5-21
5-22
5-23

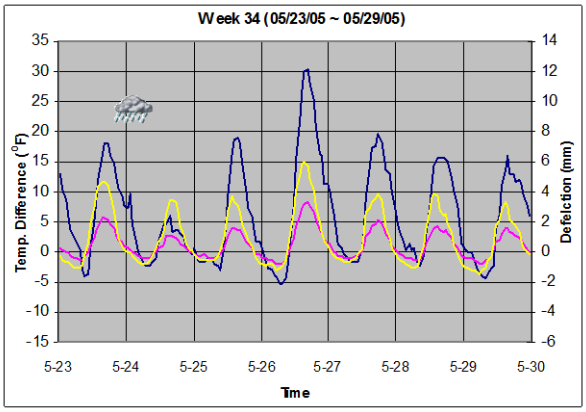
Week 34 (05/23/05 ~ 05/29/05)
Temp. Difference (°F)
Defelction (mm)
Time
5-23
5-24
5-25
5-26
5-27
5-28
5-29
5-30

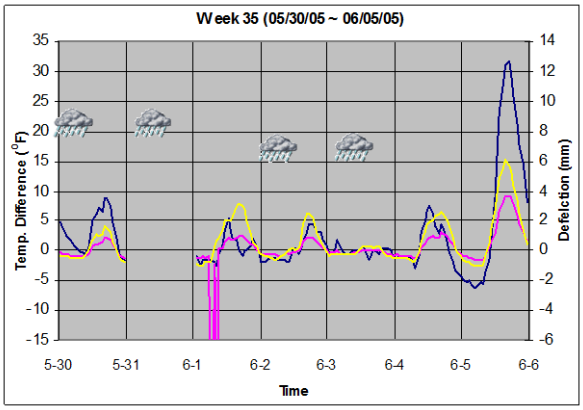
Week 35 (05/30/05 ~ 06/05/05)
Temp. Difference (°F)
Defelction (mm)
Time
5-30
5-31
6-1
6-2
6-3
6-4
6-5
6-6

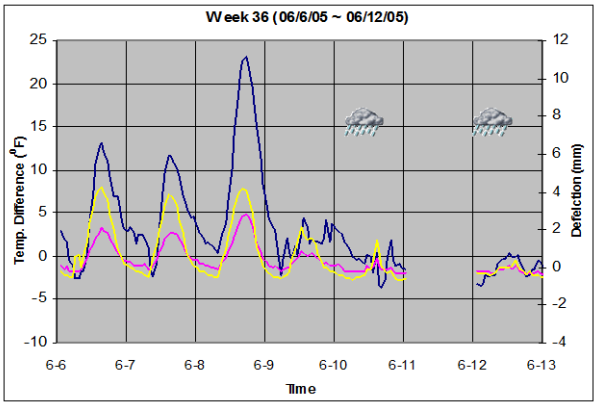
Week 36 (06/6/05 ~ 06/12/05)
Temp. Difference (°F)
Defelction (mm)
Time
6-6
6-7
6-8
6-9
6-10
6-11
6-12
6-13

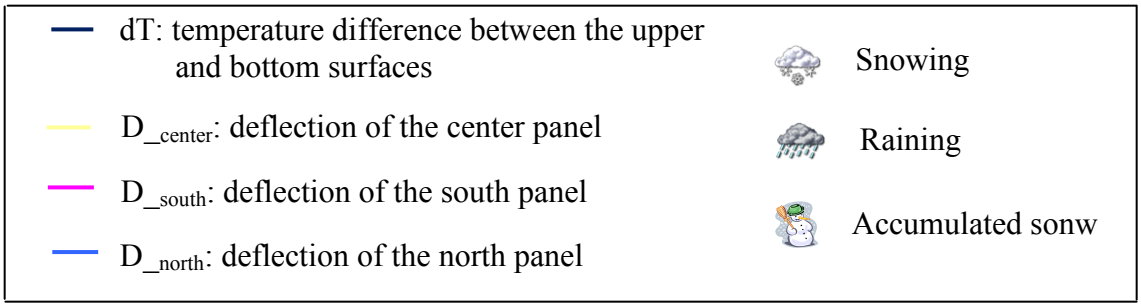
dT: temperature difference between the upper and bottom surfaces
D_center: deflection of the center panel
D_south: deflection of the south panel
D_north: deflection of the north panel
Snowing
Raining
Accumulated sonw

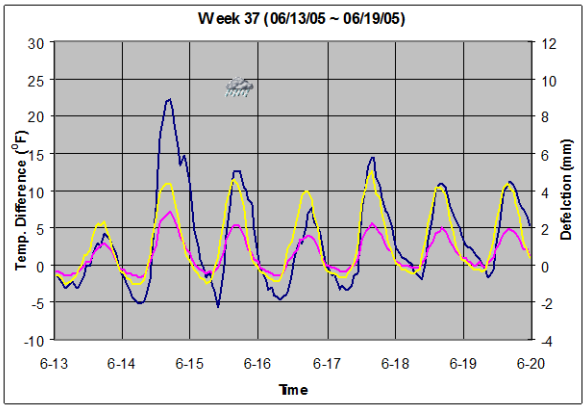
Week 37 (06/13/05 ~ 06/19/05)
Temp. Difference (°F)
Defelction (mm)
Time
6-13
6-14
6-15
6-16
6-17
6-18
6-19
6-20

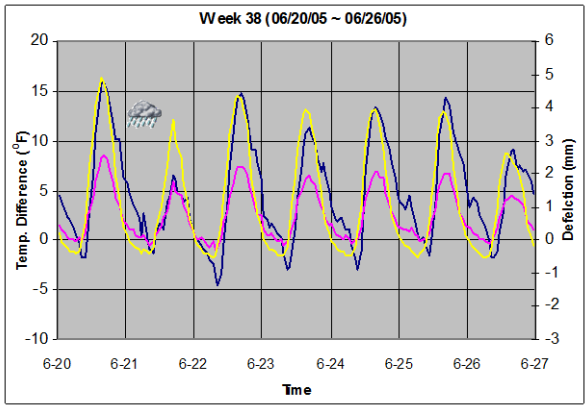
Week 38 (06/20/05 ~ 06/26/05)
Temp. Difference (°F)
Defelction (mm)
Time
6-20
6-21
6-22
6-23
6-24
6-25
6-26
6-27

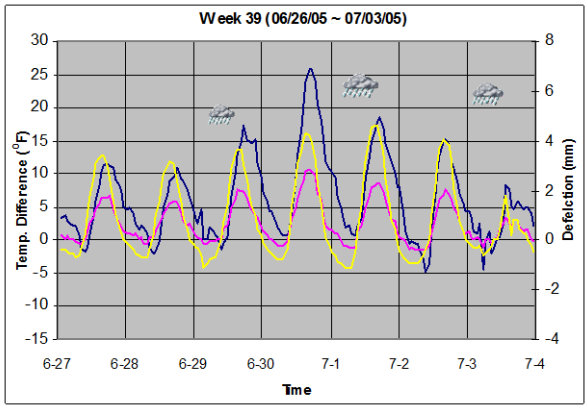
Week 39 (06/26/05 ~ 07/03/05)
Temp. Difference (°F)
Defelction (mm)
Time
6-27
6-28
6-29
6-30
7-1
7-2
7-3
7-4

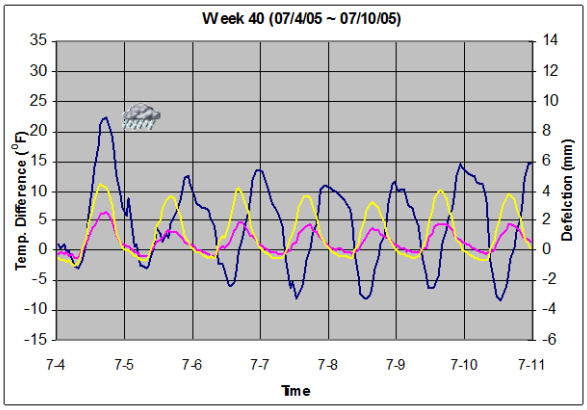
Week 40 (07/4/05 ~ 07/10/05)
Temp. Difference (°F)
Defelction (mm)
Time
7-4
7-5
7-6
7-7
7-8
7-9
7-10
7-11

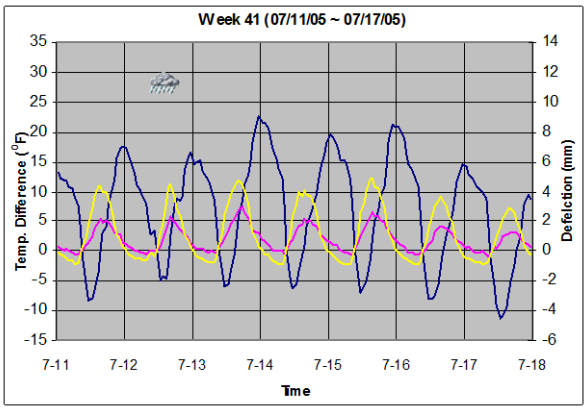
Week 41 (07/11/05 ~ 07/17/05)
Temp. Difference (°F)
Defelction (mm)
Time
7-11
7-12
7-13
7-14
7-15
7-16
7-17
7-18

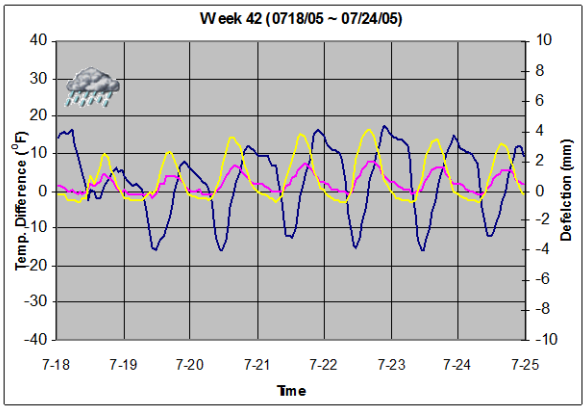
Week 42 (0718/05 ~ 07/24/05)
Temp. Difference (°F)
Defelction (mm)
Time
7-18
7-19
7-20
7-21
7-22
7-23
7-24
7-25

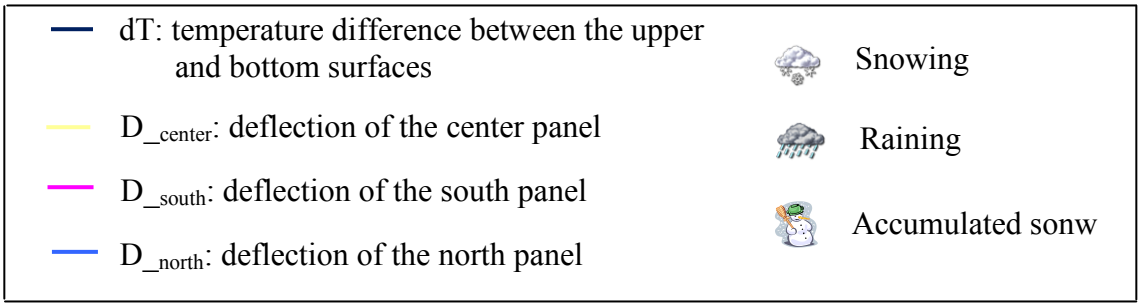
dT: temperature difference between the upper and bottom surfaces
D_center: deflection of the center panel
D_south: deflection of the south panel
D_north: deflection of the north panel
Snowing
Raining
Accumulated sonw

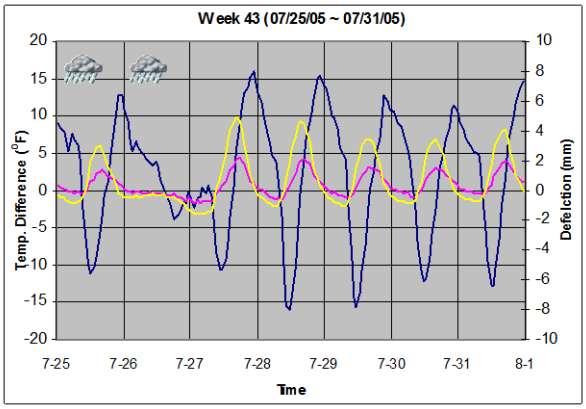

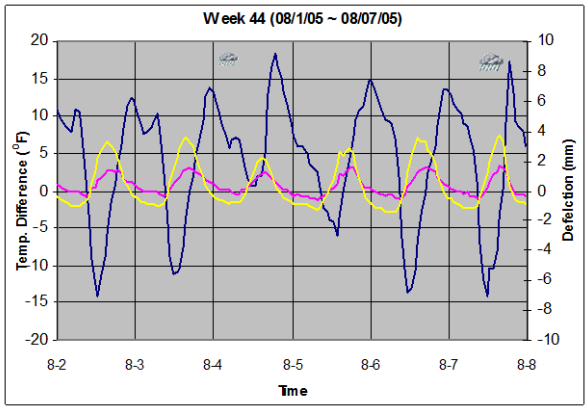

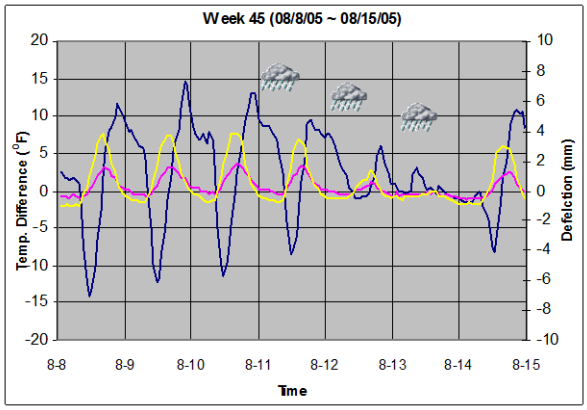

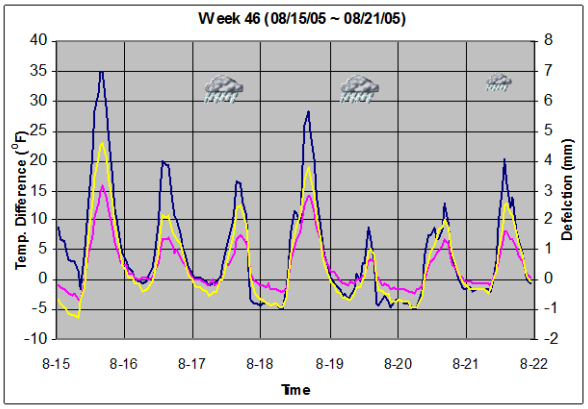

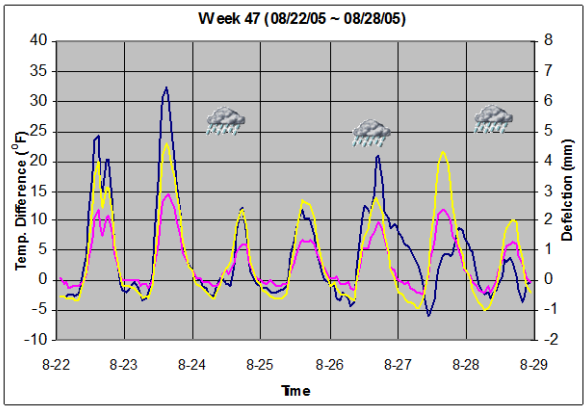

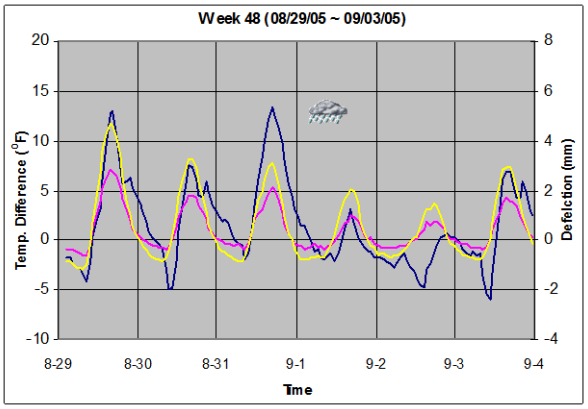

dT: temperature difference between the upper and bottom surfaces

D_{center}: deflection of the center panel

D_{south}: deflection of the south panel

D_{north}: deflection of the north panel

Snowing

Raining

Accumulated sonw

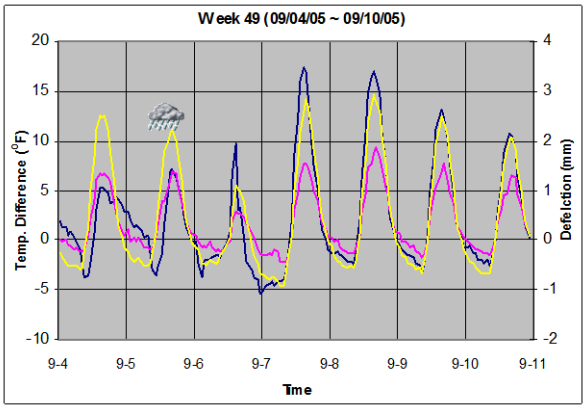

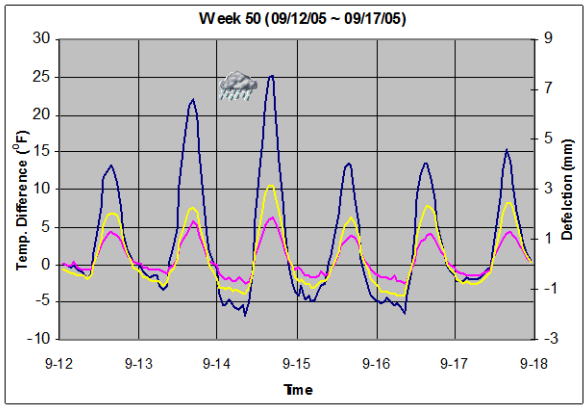

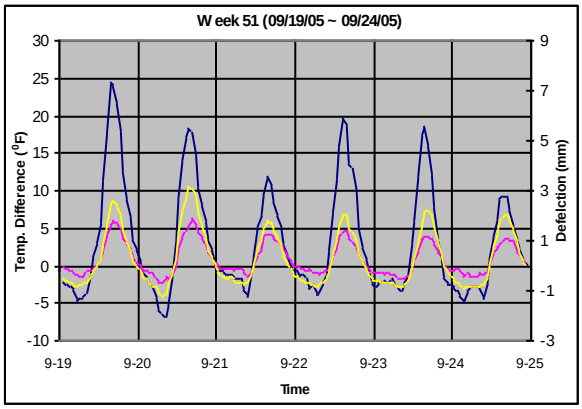

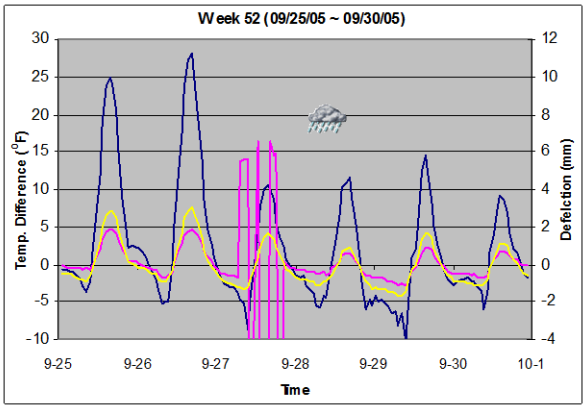

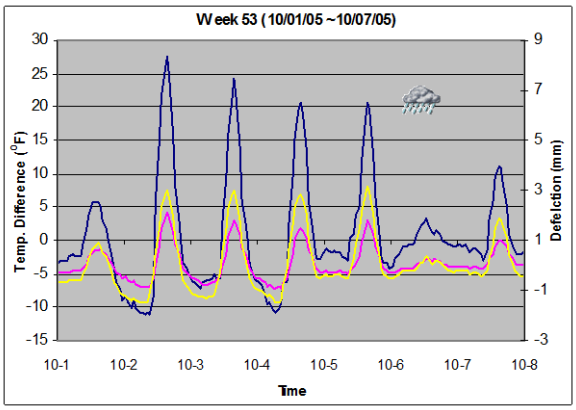

dT: temperature difference between the upper and bottom surfaces

D_{center}: deflection of the center panel

D_{south}: deflection of the south panel

D_{north}: deflection of the north panel

Snowing

Raining

Accumulated sonw

Appendix III: Relations of Bridge Deflection and Thermal Loads

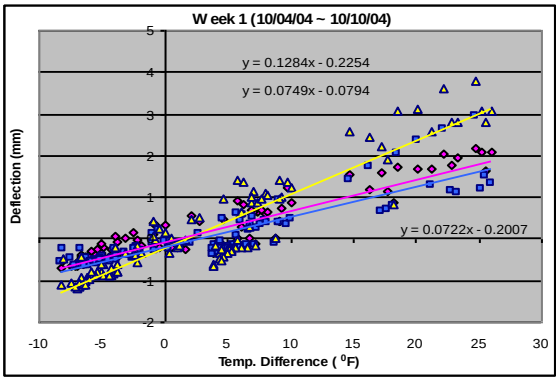

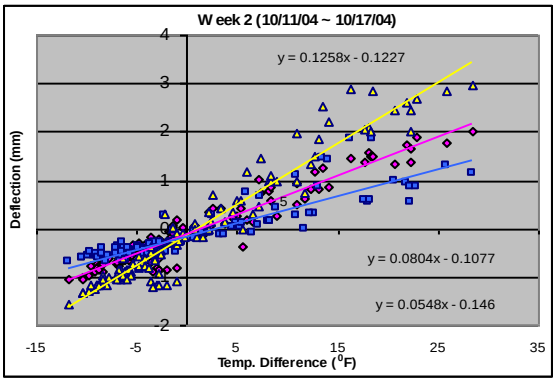

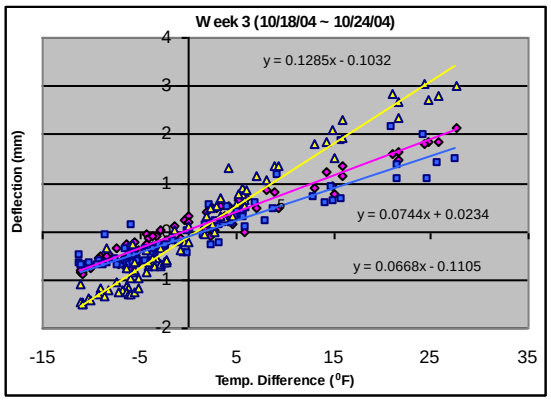

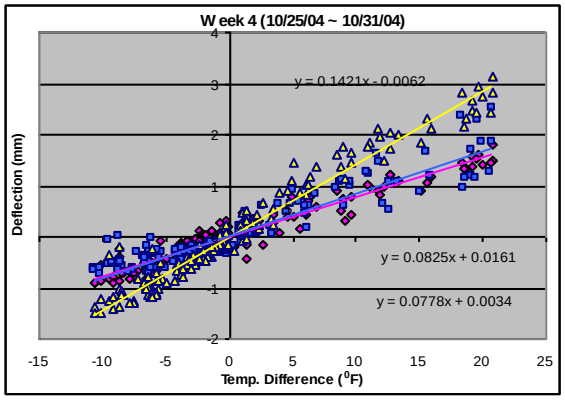

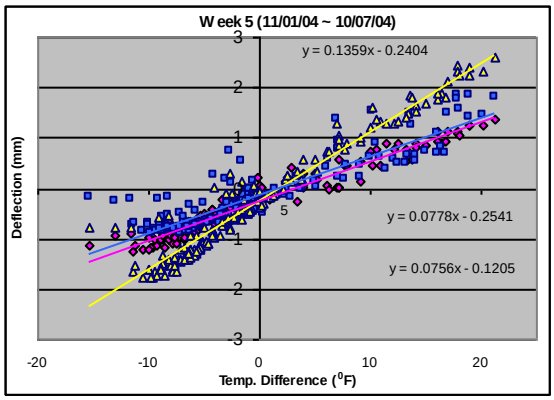

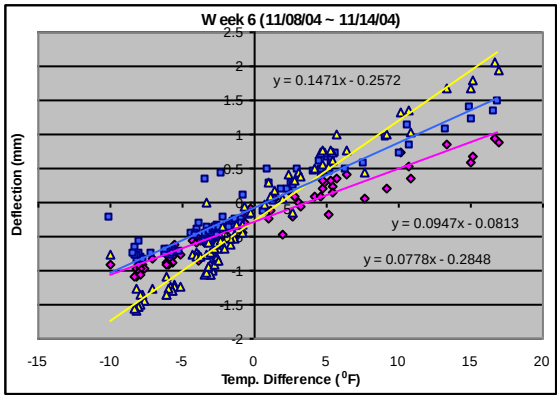

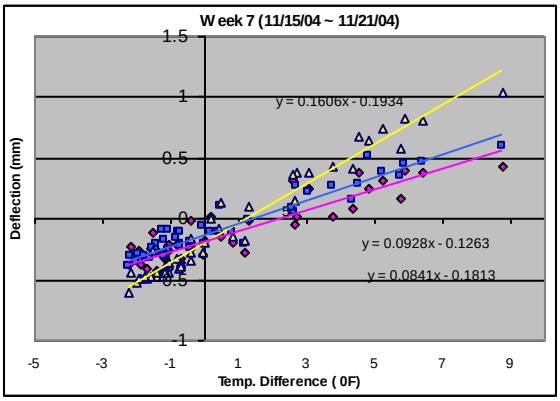
W eek 7 (11/15/04 ~ 11/21/04)
y = 0.1606x - 0.1934
y = 0.0928x - 0.1263
y = 0.0841x - 0.1813
Deflection (mm)
Temp. Difference (0F)

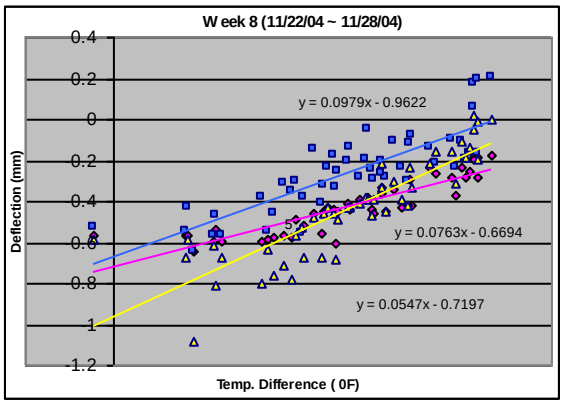
W eek 8 (11/22/04 ~ 11/28/04)
y = 0.0979x - 0.9622
y = 0.0763x - 0.6694
y = 0.0547x - 0.7197
Deflection (mm)
Temp. Difference (0F)

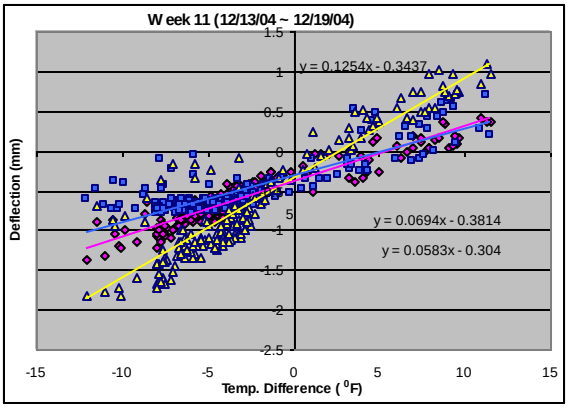
W eek 11 (12/13/04 ~ 12/19/04)
y = 0.1254x - 0.3437
y = 0.0694x - 0.3814
y = 0.0583x - 0.304
Deflection (mm)
Temp. Difference (0F)

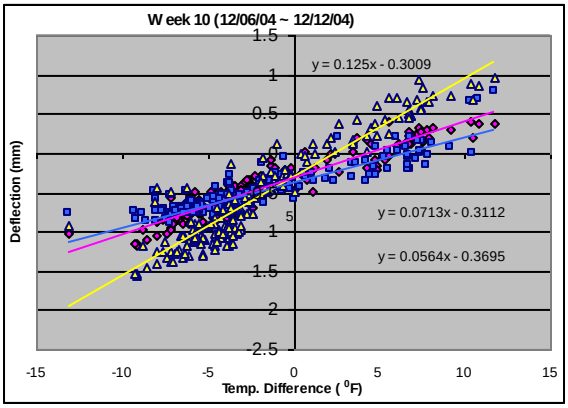
W eek 10 (12/06/04 ~ 12/12/04)
y = 0.125x - 0.3009
y = 0.0713x - 0.3112
y = 0.0564x - 0.3695
Deflection (mm)
Temp. Difference (0F)

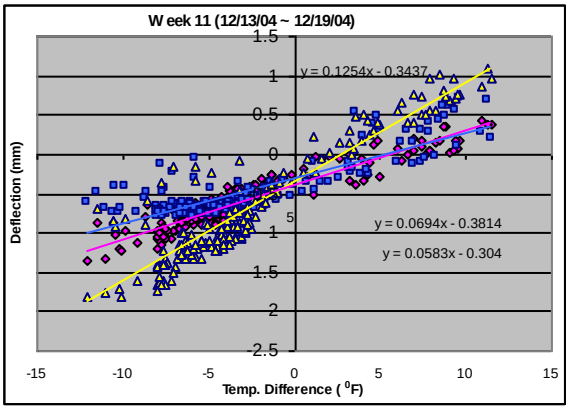
W eek 11 (12/13/04 ~ 12/19/04)
y = 0.1254x - 0.3437
y = 0.0694x - 0.3814
y = 0.0583x - 0.304
Deflection (mm)
Temp. Difference (0F)

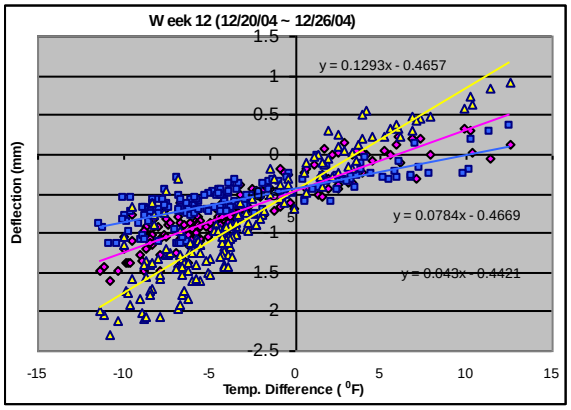
W eek 12 (12/20/04 ~ 12/26/04)
y = 0.1293x - 0.4657
y = 0.0784x - 0.4669
y = 0.043x - 0.4421
Deflection (mm)
Temp. Difference (0F)

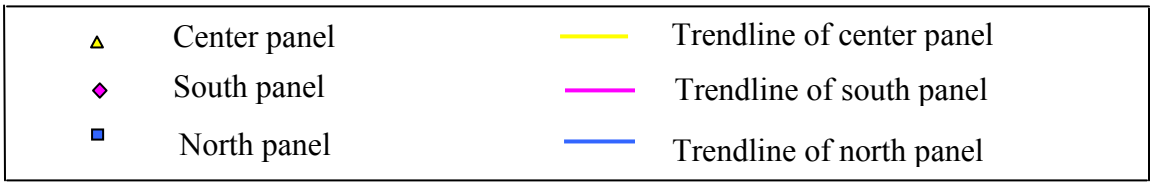
Center panel
South panel
North panel
Trendline of center panel
Trendline of south panel
Trendline of north panel

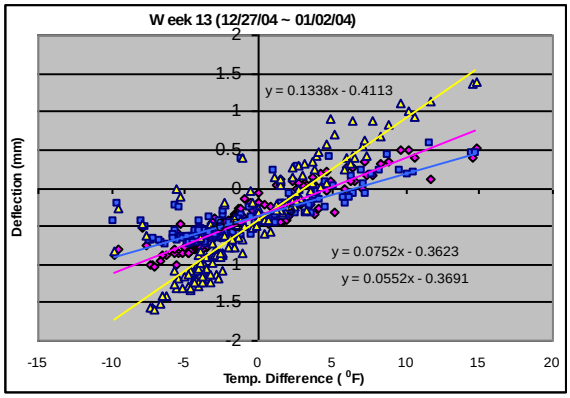
W eek 13 (12/27/04 ~ 01/02/04)
y = 0.1338x - 0.4113
y = 0.0752x - 0.3623
y = 0.0552x - 0.3691
Deflection (mm)
Temp. Difference (°F)

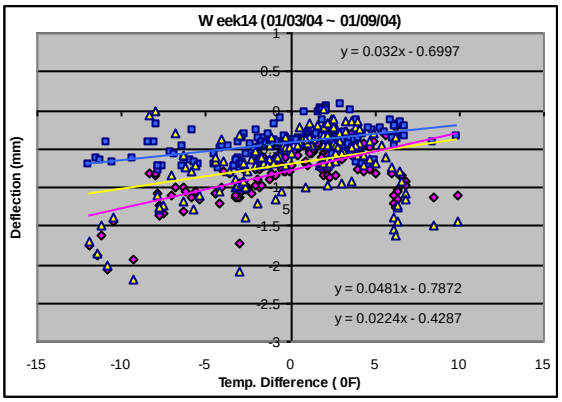
W eek14 (01/03/04 ~ 01/09/04)
y = 0.032x - 0.6997
y = 0.0481x - 0.7872
y = 0.0224x - 0.4287
Deflection (mm)
Temp. Difference (0F)

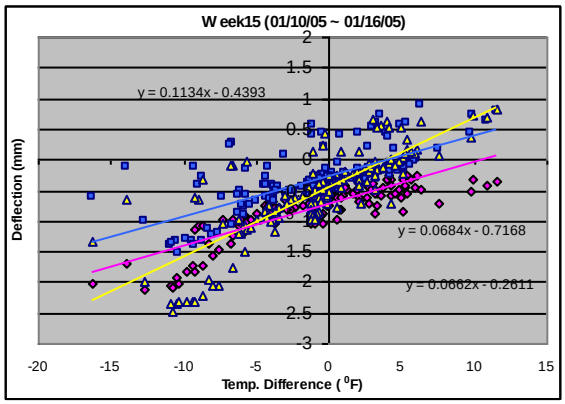
W eek15 (01/10/05 ~ 01/16/05)
y = 0.1134x - 0.4393
y = 0.0684x - 0.7168
y = 0.0662x - 0.2611
Deflection (mm)
Temp. Difference (°F)

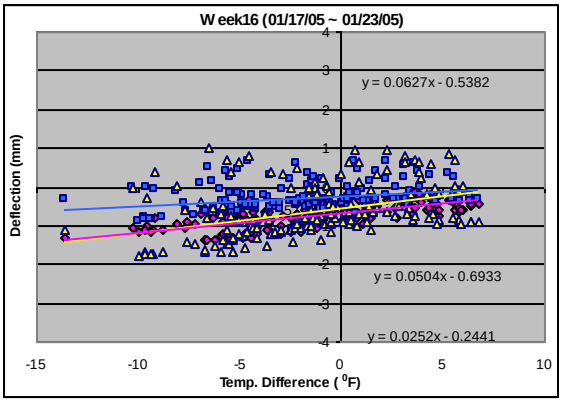
W eek16 (01/17/05 ~ 01/23/05)
y = 0.0627x - 0.5382
y = 0.0504x - 0.6933
y = 0.0252x - 0.2441
Deflection (mm)
Temp. Difference (°F)

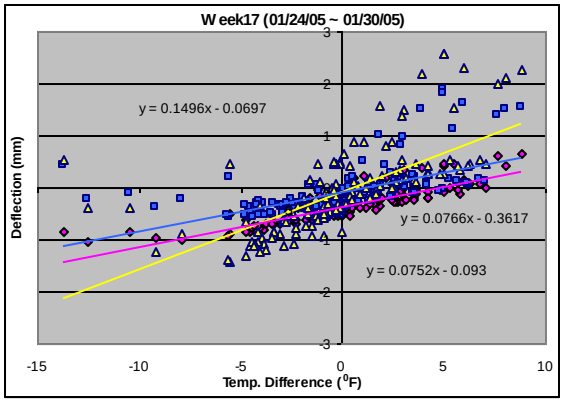
W eek17 (01/24/05 ~ 01/30/05)
y = 0.1496x - 0.0697
y = 0.0766x - 0.3617
y = 0.0752x - 0.093
Deflection (mm)
Temp. Difference (°F)

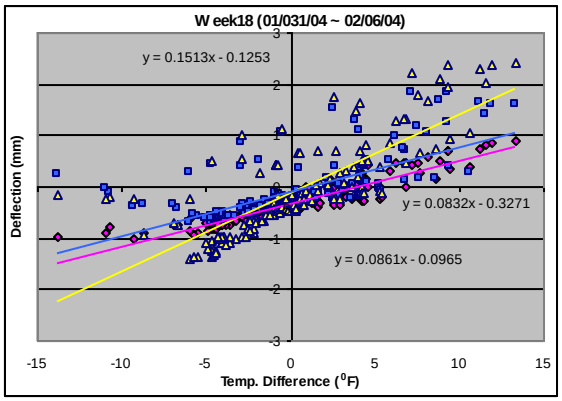
W eek18 (01/031/04 ~ 02/06/04)
y = 0.1513x - 0.1253
y = 0.0832x - 0.3271
y = 0.0861x - 0.0965
Deflection (mm)
Temp. Difference (°F)

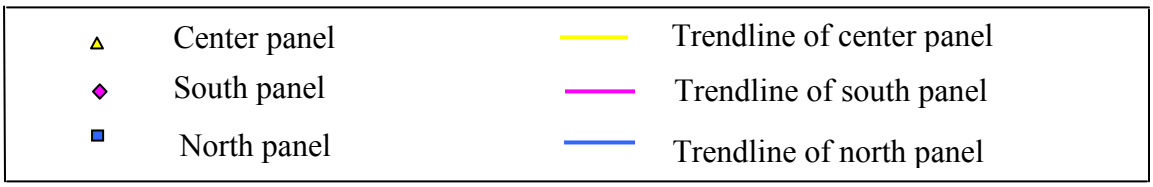
Center panel
South panel
North panel
Trendline of center panel
Trendline of south panel
Trendline of north panel

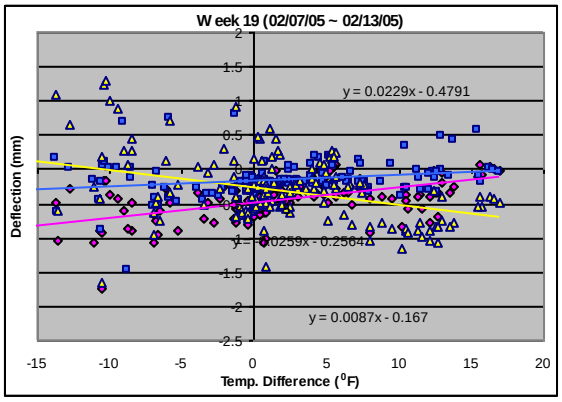
W eek 19 (02/07/05 ~ 02/13/05)
y = 0.0229x - 0.4791
y = 0.0259x - 0.2504
y = 0.0087x - 0.167
Deflection (mm)
Temp. Difference (0F)

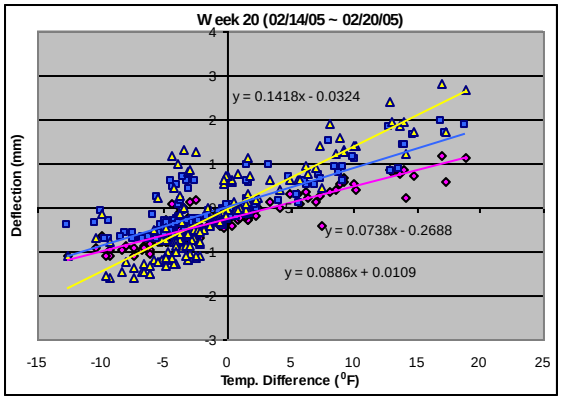
W eek 20 (02/14/05 ~ 02/20/05)
y = 0.1418x - 0.0324
y = 0.0738x - 0.2688
y = 0.0886x + 0.0109
Deflection (mm)
Temp. Difference (0F)

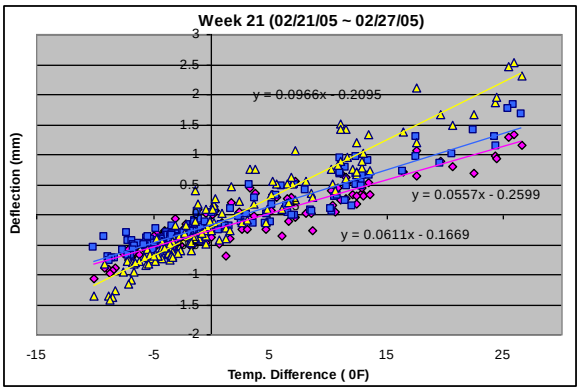
Week 21 (02/21/05 ~ 02/27/05)
y = 0.0966x - 0.2095
y = 0.0557x - 0.2599
y = 0.0611x - 0.1669
Deflection (mm)
Temp. Difference (0F)

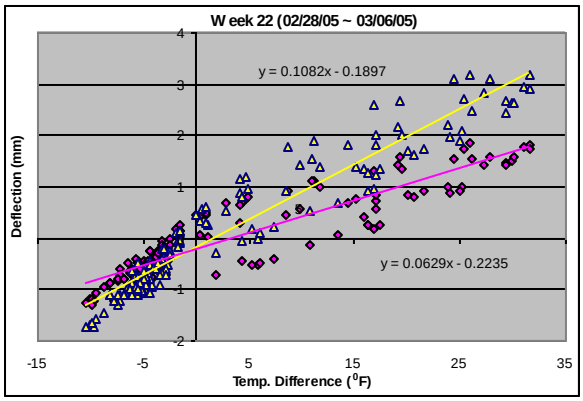
W eek 22 (02/28/05 ~ 03/06/05)
y = 0.1082x - 0.1897
y = 0.0629x - 0.2235
Deflection (mm)
Temp. Difference (0F)

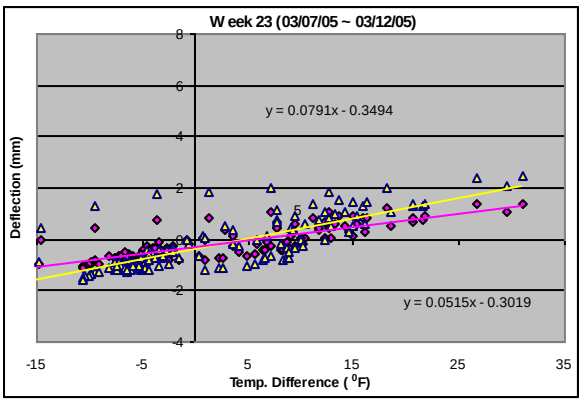
W eek 23 (03/07/05 ~ 03/12/05)
y = 0.0791x - 0.3494
y = 0.0515x - 0.3019
Deflection (mm)
Temp. Difference (0F)

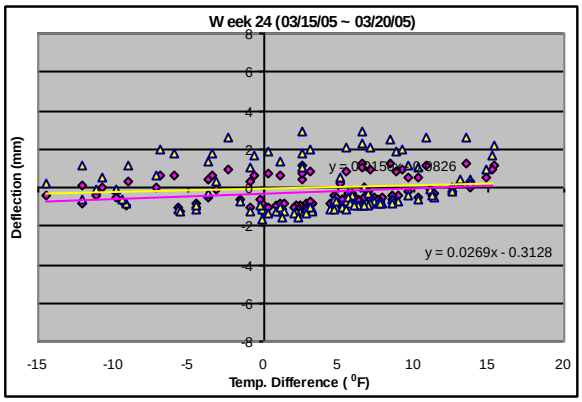
W eek 24 (03/15/05 ~ 03/20/05)
y = 0.0269x - 0.3128
Deflection (mm)
Temp. Difference (0F)


Center panel
South panel
North panel
Trendline of center panel
Trendline of south panel
Trendline of north panel

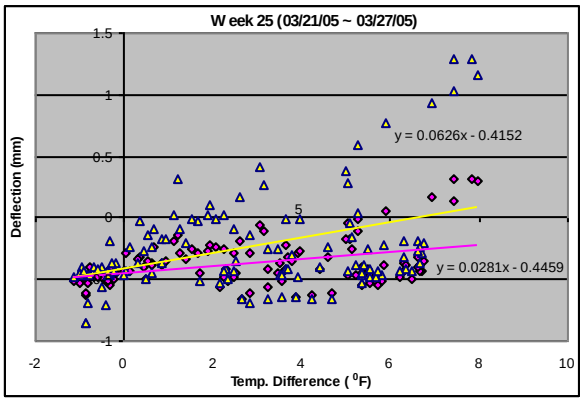
W eek 25 (03/21/05 ~ 03/27/05)
y = 0.0626x - 0.4152
y = 0.0281x - 0.4459
Deflection (mm)
Temp. Difference (0F)

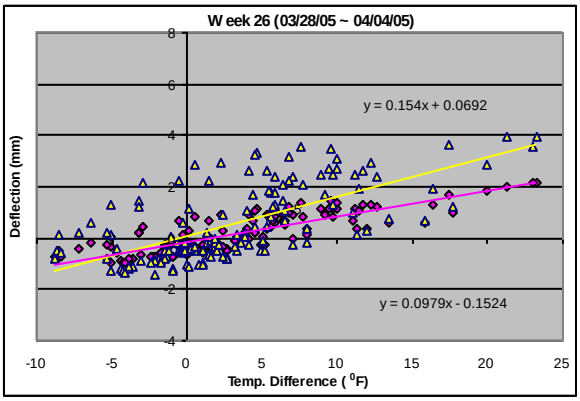
W eek 26 (03/28/05 ~ 04/04/05)
y = 0.154x + 0.0692
y = 0.0979x - 0.1524
Deflection (mm)
Temp. Difference (0F)

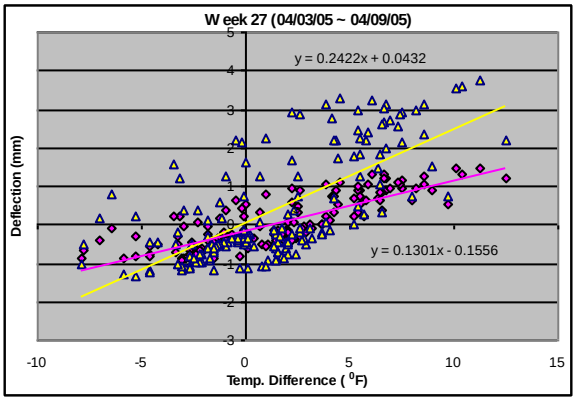
W eek 27 (04/03/05 ~ 04/09/05)
y = 0.2422x + 0.0432
y = 0.1301x - 0.1556
Deflection (mm)
Temp. Difference (0F)

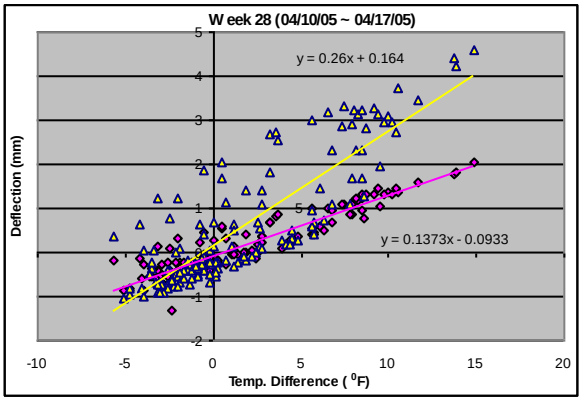
W eek 28 (04/10/05 ~ 04/17/05)
y = 0.26x + 0.164
y = 0.1373x - 0.0933
Deflection (mm)
Temp. Difference (0F)

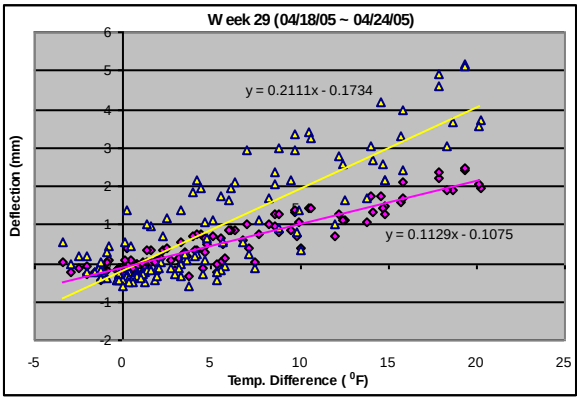
W eek 29 (04/18/05 ~ 04/24/05)
y = 0.2111x - 0.1734
y = 0.1129x - 0.1075
Deflection (mm)
Temp. Difference (0F)

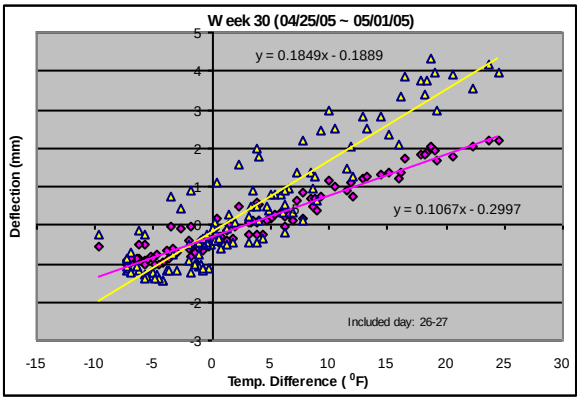
W eek 30 (04/25/05 ~ 05/01/05)
y = 0.1849x - 0.1889
y = 0.1067x - 0.2997
Included day: 26-27
Deflection (mm)
Temp. Difference (0F)

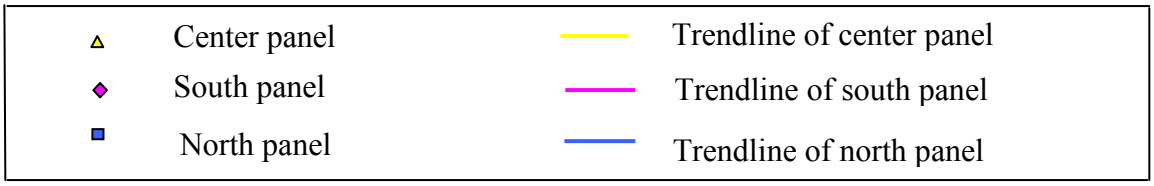
Center panel
South panel
North panel
Trendline of center panel
Trendline of south panel
Trendline of north panel

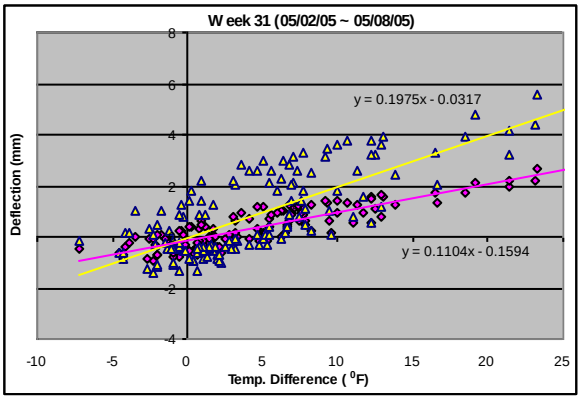
W eek 31 (05/02/05 ~ 05/08/05)
y = 0.1975x - 0.0317
y = 0.1104x - 0.1594
Deflection (mm)
Temp. Difference (°F)

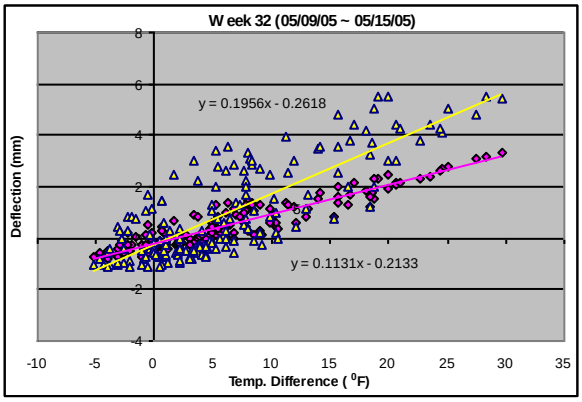
W eek 32 (05/09/05 ~ 05/15/05)
y = 0.1956x - 0.2618
y = 0.1131x - 0.2133
Deflection (mm)
Temp. Difference (°F)

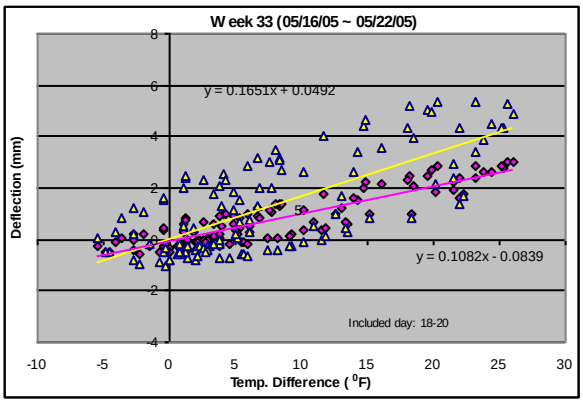
W eek 33 (05/16/05 ~ 05/22/05)
y = 0.1651x + 0.0492
y = 0.1082x - 0.0839
Included day: 18-20
Deflection (mm)
Temp. Difference (°F)

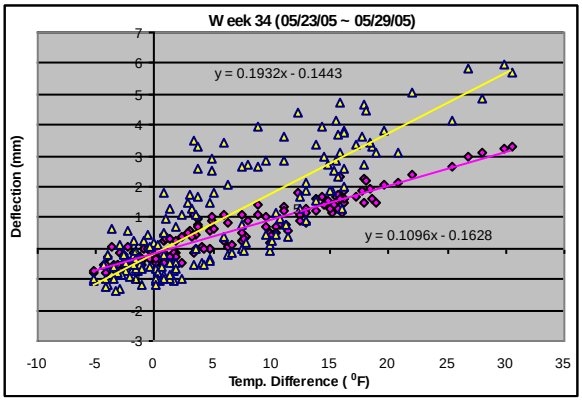
W eek 34 (05/23/05 ~ 05/29/05)
y = 0.1932x - 0.1443
y = 0.1096x - 0.1628
Deflection (mm)
Temp. Difference (°F)

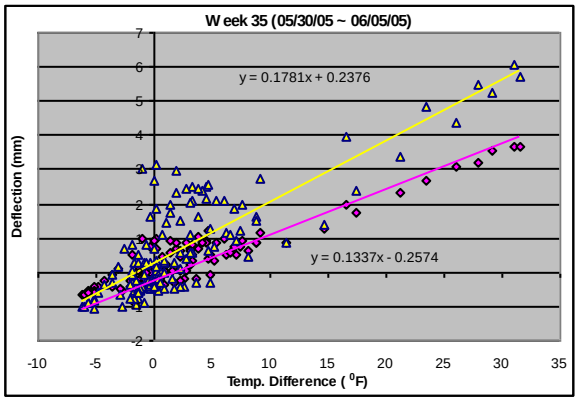
W eek 35 (05/30/05 ~ 06/05/05)
y = 0.1781x + 0.2376
y = 0.1337x - 0.2574
Deflection (mm)
Temp. Difference (°F)

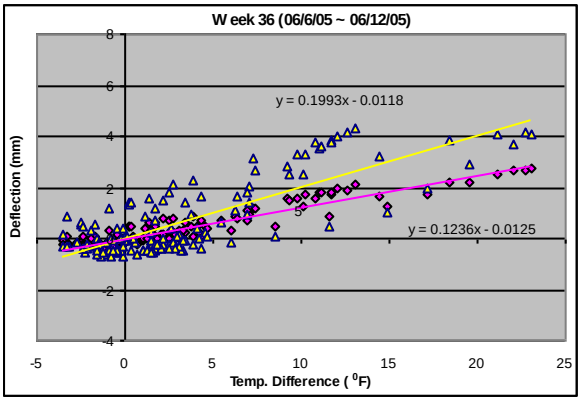
W eek 36 (06/6/05 ~ 06/12/05)
y = 0.1993x - 0.0118
y = 0.1236x - 0.0125
Deflection (mm)
Temp. Difference (°F)

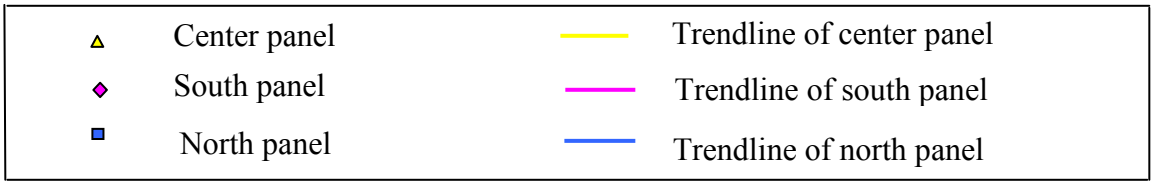
Center panel
South panel
North panel
Trendline of center panel
Trendline of south panel
Trendline of north panel

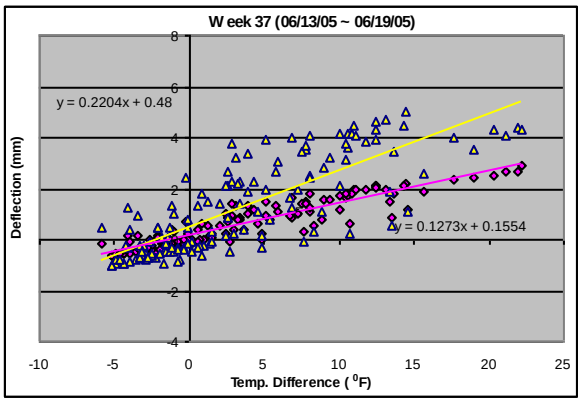
W eek 37 (06/13/05 ~ 06/19/05)
y = 0.2204x + 0.48
y = 0.1273x + 0.1554
Deflection (mm)
Temp. Difference (0F)

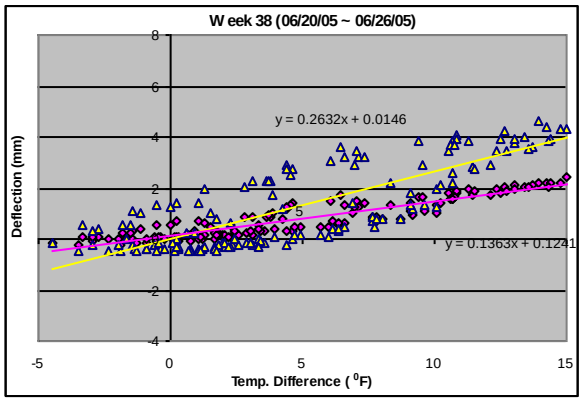
W eek 38 (06/20/05 ~ 06/26/05)
y = 0.2632x + 0.0146
y = 0.1363x + 0.1241
Deflection (mm)
Temp. Difference (0F)

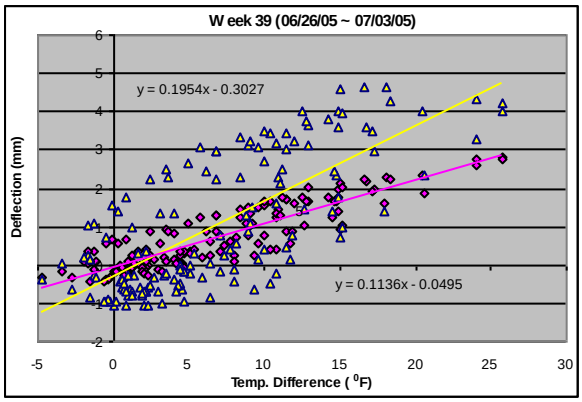
W eek 39 (06/26/05 ~ 07/03/05)
y = 0.1954x - 0.3027
y = 0.1136x - 0.0495
Deflection (mm)
Temp. Difference (0F)

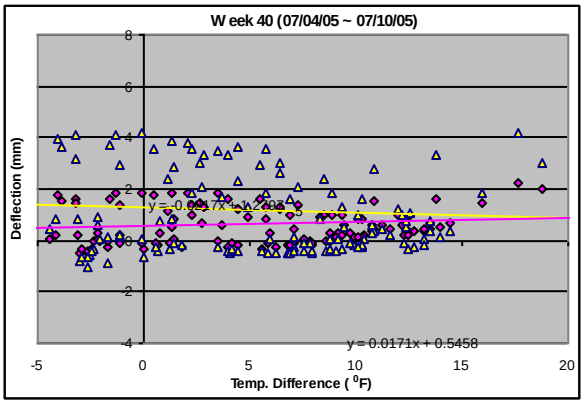
W eek 40 (07/04/05 ~ 07/10/05)
y = 0.0171x + 0.5458
Deflection (mm)
Temp. Difference (0F)

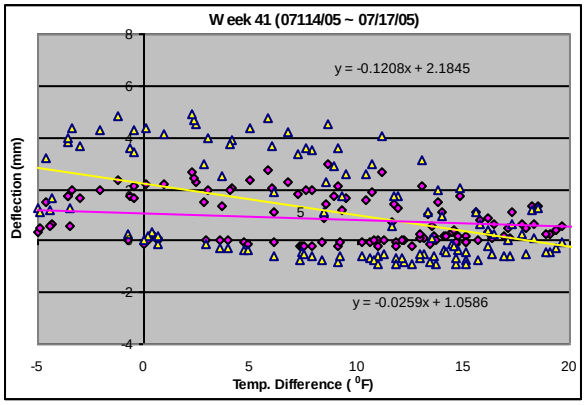
W eek 41 (07114/05 ~ 07/17/05)
y = -0.1208x + 2.1845
y = -0.0259x + 1.0586
Deflection (mm)
Temp. Difference (0F)

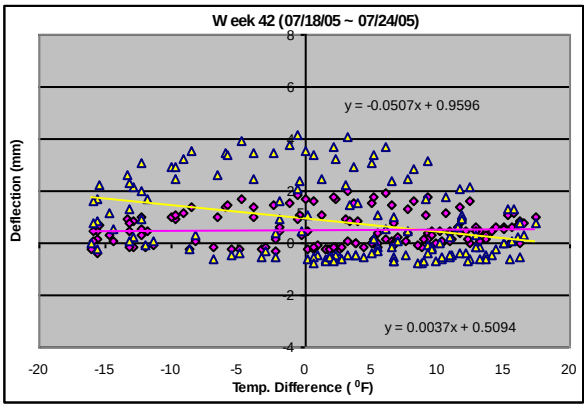
W eek 42 (07/18/05 ~ 07/24/05)
y = -0.0507x + 0.9596
y = 0.0037x + 0.5094
Deflection (mm)
Temp. Difference (0F)


Center panel
South panel
North panel
Trendline of center panel
Trendline of south panel
Trendline of north panel

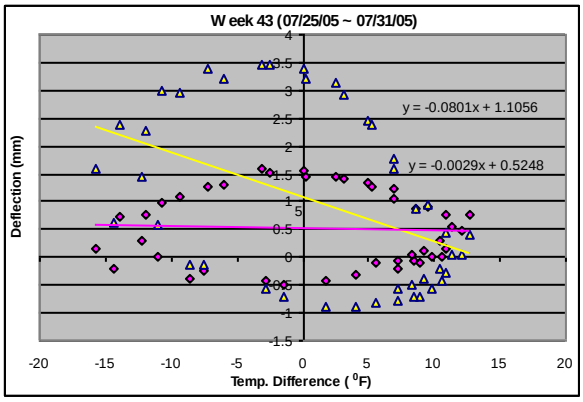
W eek 43 (07/25/05 ~ 07/31/05)
y = -0.0801x + 1.1056
y = -0.0029x + 0.5248
Deflection (mm)
Temp. Difference (0F)

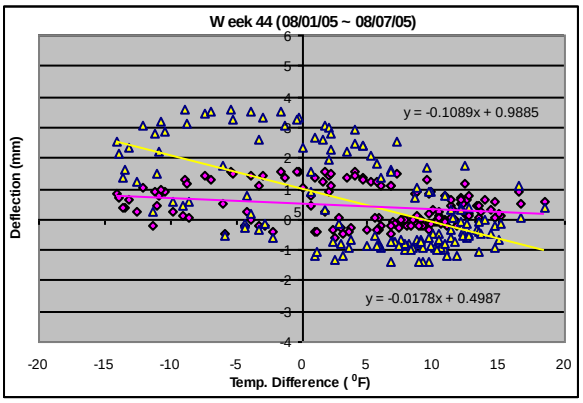
W eek 44 (08/01/05 ~ 08/07/05)
y = -0.1089x + 0.9885
y = -0.0178x + 0.4987
Deflection (mm)
Temp. Difference (0F)

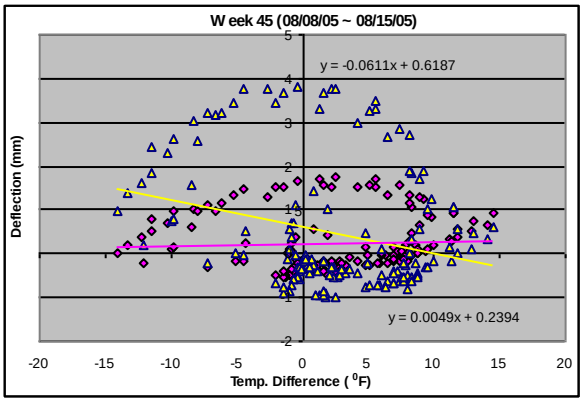
W eek 45 (08/08/05 ~ 08/15/05)
y = -0.0611x + 0.6187
y = 0.0049x + 0.2394
Deflection (mm)
Temp. Difference (0F)

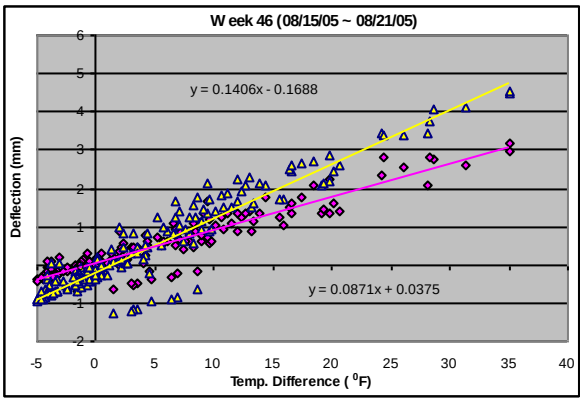
W eek 46 (08/15/05 ~ 08/21/05)
y = 0.1406x - 0.1688
y = 0.0871x + 0.0375
Deflection (mm)
Temp. Difference (0F)

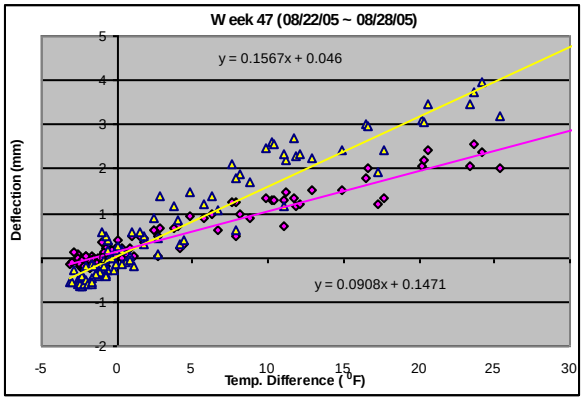
W eek 47 (08/22/05 ~ 08/28/05)
y = 0.1567x + 0.046
y = 0.0908x + 0.1471
Deflection (mm)
Temp. Difference (0F)

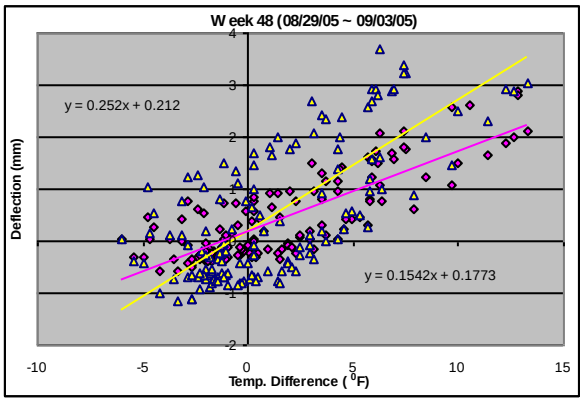
W eek 48 (08/29/05 ~ 09/03/05)
y = 0.252x + 0.212
y = 0.1542x + 0.1773
Deflection (mm)
Temp. Difference (0F)


Center panel
South panel
North panel
Trendline of center panel
Trendline of south panel
Trendline of north panel

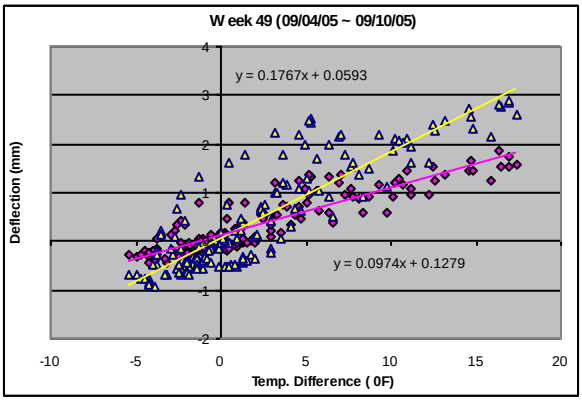
W eek 49 (09/04/05 ~ 09/10/05)
y = 0.1767x + 0.0593
y = 0.0974x + 0.1279
Deflection (mm)
Temp. Difference (0F)

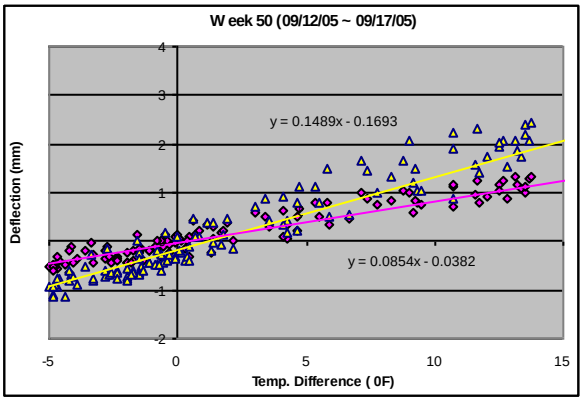
W eek 50 (09/12/05 ~ 09/17/05)
y = 0.1489x - 0.1693
y = 0.0854x - 0.0382
Deflection (mm)
Temp. Difference (0F)

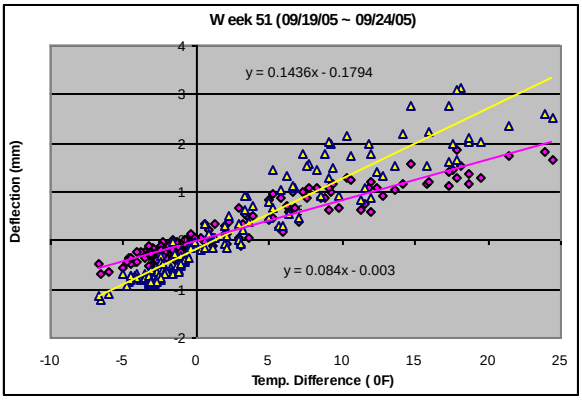
W eek 51 (09/19/05 ~ 09/24/05)
y = 0.1436x - 0.1794
y = 0.084x - 0.003
Deflection (mm)
Temp. Difference (0F)

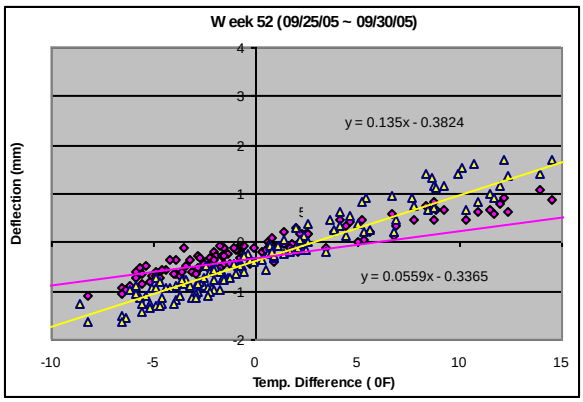
W eek 52 (09/25/05 ~ 09/30/05)
y = 0.135x - 0.3824
y = 0.0559x - 0.3365
Deflection (mm)
Temp. Difference (0F)

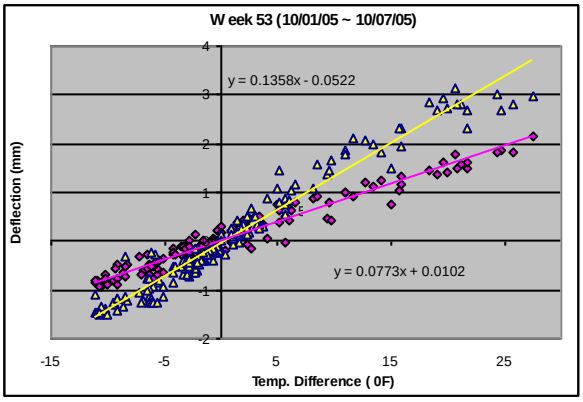
W eek 53 (10/01/05 ~ 10/07/05)
y = 0.1358x - 0.0522
y = 0.0773x + 0.0102
Deflection (mm)
Temp. Difference (0F)

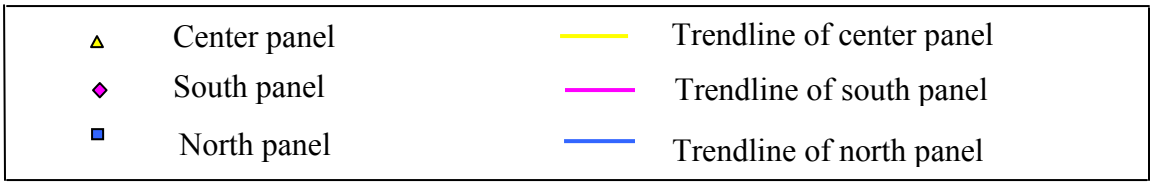
Center panel
South panel
North panel
Trendline of center panel
Trendline of south panel
Trendline of north panel

Modified figures

(Described by daily extreme deflections and temperatures are selected)

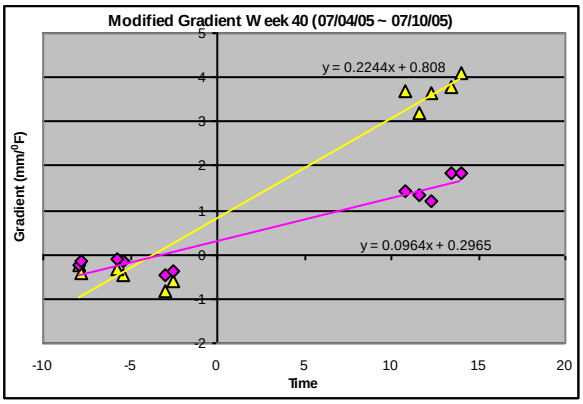

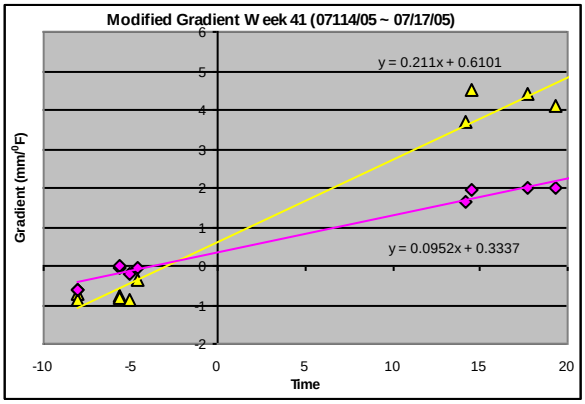

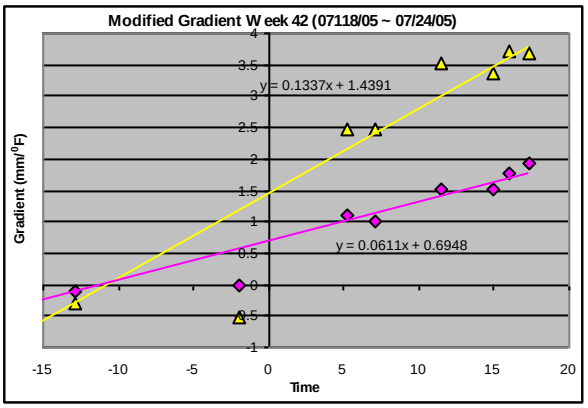

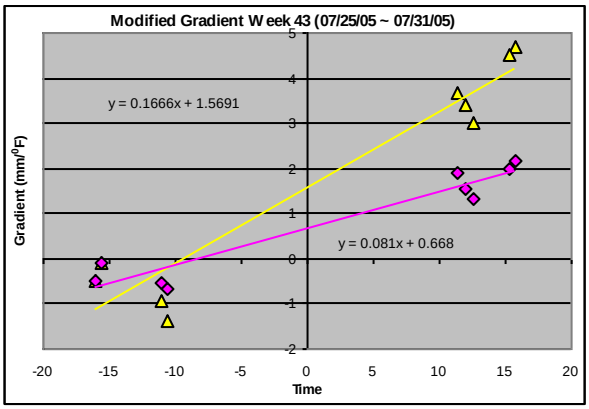

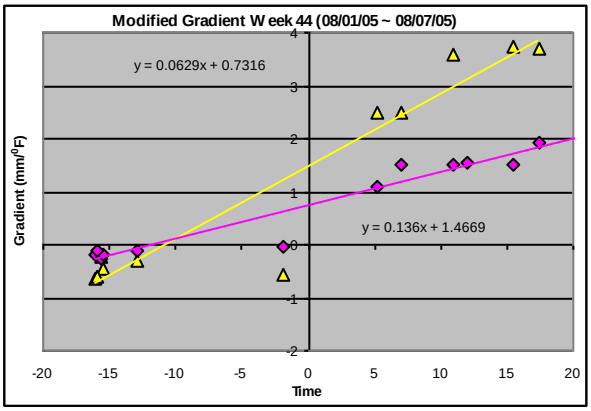

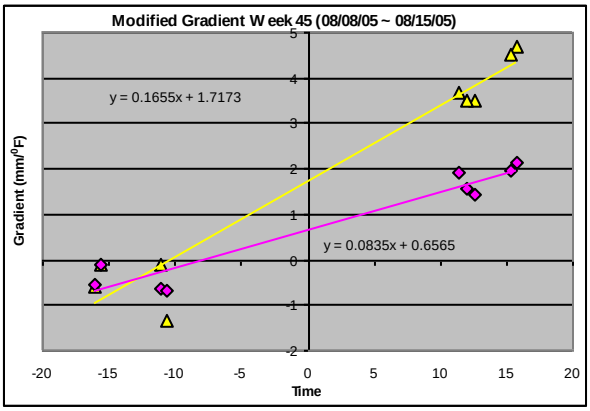

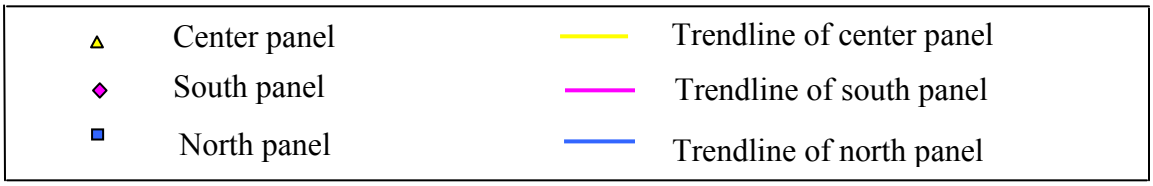

AD ASTRA PER ASPERA

Kansas

Department of Transportation